電解重合導電高分子を利用したリチウム二次電池の研究

A Study on Lithium Secondary Batteries Using Electropolymerized Conductive Polymers

(01550634)

平成元年度科学研究費補助金（一般研究C）研究成果報告

平成3年3月

研究代表者　　逢坂　哲彌

(早稲田大学理工学部応用化学科)

はしがき

電子機器の高密度化，コードレス化が進むなかで，その電源の高エネルギー，高出力，小型電池のニーズが高まっている。また，クリーンなエネルギー源としての電気自動車用電源，さらには小規模のエネルギー貯蔵装置，ロードコンディショナーとしての二次電池の可能性が検討され始めている。このような状況下で，高密度電池材料の一つとして導電性高分子が注目され，π電子共役系高分子が主に導電性を発現する材料として取り上げられている。この中で，特に電解重合法で作製できるポリピロール，ポリアニリン，ポリアズレンを取り上げ，リチウム二次電池のカソード材料として利用し得る可能性を検討した。この新型リチウム二次電池は，エネルギー密度が高く，かつ軽量フレキシブルな電池としての可能性をもつため，この目的に沿って導電性高分子を電解重合により作製し，評価を行った。

ポリアニリンに関しては，非プロトン性溶媒であるプロピレンカーボネート中で電気化学的に活性な膜を重合できることを明らかにした。さらにポリアニリン重合の条件を明らかにするために重合溶媒の誘電率，粘度，ドナー数を変化させ重合した結果，活性なポリアニリンの重合には溶媒の誘電率，及びドナー数が大きな影響を与えていることが明らかとなった。またこれらポリアニリンを正極とし，様々な電解液溶媒を用いたリチウム電池を構成して充放電の特性を評価したところ，電解液の溶媒粘度及び誘電率による影響が大きく現れ，特にプロピレンカーボネート－ジメトキシエタン混合溶媒は従来のプロピレンカーボネート単独溶媒より，大電流で充放電が可能となった。

ポリピロールに関しては，膜のモルフォロジー制御のため複合材料としてNBR（ニトリルブタジエンラバー）をコートした電極上で重合を行った。NBRの分子構造，ガラス転移点，また重合支持塩を変えてポリピロールを重合し，生成したポリピロール膜の基礎特性及び電池特性を評価した。作製条件の最適化を行うことにより従来のポリピロールの2～3倍の大電流まで充放電可能なポリピロールカソードを合成することが可能となった。

さらに，複合膜の可能性を検討し，ポリアズレン－ポリピロール共重合膜の作製を行い，安価なピロールによりコストの低減化，アズレンにより充電電圧及びエネルギー密度の向上が可能な複合膜が得られた。この複合膜の電気化学的特性をインピーダンス法にて評価したところ，アズレン50～75mol%以上において膜内アニオン拡散速度及び膜容量の増加がみられ，電池特性ともよい一致を示すことが明らかになり，膜の基礎特性と電池特性との相関性を示唆することができた。

次に，ポリアニリン膜の機械的強度が劣ることに対し，膜強度の強いポリピロール膜との積層化を行うことによる膜強度の改善を行った。さらに，重合条件による下地層のポリピロールの電気化学的性質が積層膜の充放電容量に影響を与え，ラフネスが高くドープ率に優れたポリピロール下地を用いた複合膜が良好な充放電特性を示すことを明らかにした。

本報告書は，平成元年および平成２年度文部省科学研究費補助金（一般研究Ｃ）の援助によって行われた研究の成果を述べたものである。

本研究の大部分は，すでに学会等において論文もしくは口頭発表で発表されているが，本報告書によりその全体像を把握され，関連分野の研究の資として頂ければ幸いである。

研究組織

研究代表者　：　逢坂　哲彌　（　早稲田大学理工学部教授　）

研究分担者　：　中村　節子　（　日本女子大学家政学部教授　）

研究経費

平成元年度	１，４００千円
平成２年度	９００千円
計	２，３００千円

（1） 学会誌等

1. Effect of Acrylonitrile Composition in NBR on Enhanced Anion Doping-Undoping Process of NBR-Guided-Grown-Polypyrrole Film Electrode.
T.Osaka, K.Naoi, M.Maeda, S.Nakamura, J.Electrochem. Soc., 136, No.5, 1385 (1989).
2. ＮＢＲ／ポリピロール複合膜を用いたリチウム二次電池の特性：電解重合時の支持塩による影響.
前田美知子, 中村節子, 上山健一, 逢坂哲彌, 電気化学, 57, No.6, 568 (1989).
3. Electrochemical Study on Electropolymerized Polyazulene Film.
T.Osaka, K.Ueyama, Denki Kagaku, 57, No.6, 572 (1989).
4. Preparation of MIM (Metal-Insulator-Metal) Non-linear Device Using Electropolymerized Poly-N-methylpyrrole.
T.Osaka, K.Ueyama, K.Ouchi, Chem. Lett., No.9, 1543 (1989).
5. Electrochemical Study on Charge-Discharge Performance of Lithium/Polyazulene Battery.
K.Naoi, K.Ueyama, T.Osaka, J.Electrochem.Soc.,136, No.9, 2444 (1989).
6. Lithium Secondary Batteries:Role of Polymer Cathode Morphology.
K.Naoi, B.B.Owens, M.Maeda, T.Osaka, Proc.of Sym.on Matl.and Processes for Lithium Batteries, Electrochem. Soc., 89-4, 269 (1989).
7. Impedance Analysis of Ionic Transport in Polypyrrole-Polyazulene Copolymer and Its Charge-Discharge Characteristics.
K.Naoi, K.Ueyama, T.Osaka, W.H.Smyrl, J.Electrochem. Soc., 137, No.2, 494 (1990).
8. 機能材料としての導電性高分子薄膜の合成と評価
逢坂哲彌, 電気化学, 58, No.3, 218 (1990).
9. Electroactive Polyaniline Film Deposited from Nonaqueous Organic 2: Effect of Acid Concentration in Solution.
T.Osaka, T.Nakajima, K.Naoi, B.B.Owens, J.Electrochem. Soc., 137 No.7, 2139 (1990).

10. Rechargeable Lithium/Polymer Cathode Batteries.
T.Osaka, T.Nakajima, K.Shiota, B.B.Owens, Proc. of Symp. on Rechargeable Lithium Batteries, Electrochem. Soc., 90-5, 170 (1990).
11. An Application of Polypyrrole Films Electropolymerized in NaOH Aqueous Solution to Non-Linear MIM Devices.
T.Osaka, K.Ouchi, T.Fukuda, Chem. Lett., No.9, 1535 (1990).
12. Rechargeable Lithium/Polymer Batteries: Application of Electropolymerized Polymer Films to Lithium Batteries.
T.Osaka, Workshop Proc. Rechargeable Lithium Polymer Batteries by EPRI and US DOE, RP2415-22, C4 (1990).

（2） 口頭発表

1. 電解重合有機薄膜を用いた非線型素子の作製.
   逢坂哲彌，上山健一，大内潔，大野好弘，松島文明，
   日本化学会第58春季年会講演 予稿集 I，P.418， 京都，(1989.4.3.)
2. 電気化学的手法を利用した機能性薄膜の合成とエレクトロニクス材料への応用.
   逢坂哲彌，電気化学協会第56回大会講演要旨集，P.134， 横浜，(1989.4.7.)
3. 非水溶媒中で重合したポリアニリン膜の重合時電流密度依存.
   逢坂哲彌，上山健一、中島俊貴，塩田晃，電気化学協会
   第56回大会講演要旨集， P.213， 横浜，(1989.4.9)
4. Application of Polypyrrole-Polyazulene Copolymer to Cathode of Rechargeable Lithium Battery.
   T.Osaka, K.Naoi, K.Ueyama, T.Nakajima, W.H.Smyrl, The 40th Meeting of the International Society of Electrochemistry, Extended Abstracts, Vol.1, P.549, Kyoto, (1989.9.21.)
5. ポリアニリン/ ポリピロール積層膜のリチウム二次電池への応用.
   逢坂哲彌，中島俊貴，塩田晃，河野智恵，第30回電池討論会講演要旨集，
   P.57，名古屋，(1989.9.27.)
6. Rechargeable Lithium/Polymer Cathode Batteries.
   T.Osaka, T.Nakajima, K.Shiota, B.B.Owens, 176th Meeting of Electrochem. Soc. Extended Abstracts Vol.89-2, P.89, Florida, (1989.10.18.)
7. 電解重合ポリ－Ｎ－メチルピロールを用いたＭＩＭ素子.
   逢坂哲彌，大内潔，福田俊広，1989年電気化学秋季大会講演要旨集，
   P.91，東京，(1989.10.22.)
8. 非水溶媒からの電気化学的に活性なポリアニリンの合成と電池材料への応用.
   中島俊貴，逢坂哲彌，表面技術協会第81回講演大会講演要旨集，P.242
   横浜 (1990.3.27.)
9. ポリアニリン／ポリピロール積層膜の交流インピーダンス法による解析.
   逢坂哲彌，中島俊貴，塩田晃，柳沢暁，1990年日本化学会
   第59春季年会講演予稿集I，P.236，横浜，(1990.4.3.)
10. 電解重合ポリピロールを用いたＭＩＭ素子のスイッチング特性.
    逢坂哲彌，大内潔，福田俊広，1990年電気化学協会第57回大会講演予稿集，
    P.151， 京都，(1990.4.5.)

11. 電池への導電性ポリマーの応用とその展開.
逢坂哲彌, 電気化学協会電気化学セミナー「電池の新しい展開」, 東京, (1990.9.20.)
12. 非水溶媒より作製した電解重合ポリアニリン膜の交流インピーダンスよる二次電池カソード材料としての評価.
逢坂哲彌, 塩田晃, 門間聰之, 1990年電気化学協会電気化学秋季大会講演要旨集, P.146,千葉, (1990.9.30.)
13. 電気化学的活性高分子膜の溶媒交換における活性変化.
逢坂哲彌, 塩田晃, 門間聰之, 西村賢, 1990年電気化学協会電気化学秋季大会講演要旨集, P.67, 千葉,(1990.9.30.)
14. Application of Electropolymerized Polymer Films to Lithium Batteries.
T.Osaka, Workshop on Rechargeable Lithium Polymer Batteries, Kirkland, Washington, USA (Oct.11.1990).
15. 電解重合PPy/PSS複合膜の重合条件最適化及びリチウム二次電池への適用.
逢坂哲彌, 塩田晃, 門間聰之, 西村賢, 第31回電池討論会講演要旨集, P.27, 大阪, (1990.11.12).
16. PC系電解液中でのLi電析形態及び充放電特性の検討.
逢坂哲彌, 塩田晃, 門間聰之, 木村聡文, 大崎隆久, 高見則雄, 第31回電池討論会講演要旨集, P.267,大阪, (1990.11.14).
17. ポリマーバッテリー.
逢坂哲彌, ハイテクケミカル交流フォーラム「小型高容量電池の今後の展望」, 日本能率協会, 東京, (1990.12.11).

（3）　出版物

1. 電気化学法－基礎測定マニュアル－：〔共著〕講談社サイエンティフィク，1989.4.
2. 電気化学法－応用測定マニュアル－：〔共編及び共著〕講談社サイエンティフィク，1990.1.
3. 電池便覧：〔執筆〕ポリマー電池，電池便覧編集委員会編，丸善，1990.8.

Reprinted from JOURNAL OF THE ELECTROCHEMICAL SOCIETY
Vol. 136, No. 5, May 1989
Printed in U.S.A.

Effect of Acrylonitrile Composition in NBR on Enhanced Anion Doping-Undoping Process of NBR-Guided-Grown-Polypyrrole Film Electrode

Tetsuya Osaka* and Katsuhiko Naoi

Department of Applied Chemistry, School of Science and Engineering, Waseda University, 3-4-1 Okubo, Shinjuku-ku, Tokyo 169, Japan

Michiko Maeda and Sadako Nakamura

Department of Chemistry, Japan Women's University, 2-8-1 Mejirodai, Bunkyo-ku, Tokyo 112, Japan

ABSTRACT

The anion doping-undoping process of NBR (nitrile butadiene rubber)-guided-grown-polypyrrole (PPy/NBR) film electrode was investigated by varying the precoated NBR film thickness and the acrylonitrile content in the NBR host polymer. The electrode kinetics and the morphology orientation of the PPy/NBR film were found to depend greatly on the nature of the precoated NBR film. Compared to a normally polymerized PPy film, a PPy/NBR film formed particularly with ClO_4^- anion showed an enhanced switching reversibility and an acceleration of the dopant movement within the polymer layer. Impedance analysis revealed that the PPy/NBR films show a clear change in their overall electrode process, from a charge transfer limiting process to a diffusion limiting process according to an increase in the precoated NBR thickness and also to a decrease in the acrylonitrile content of the NBR film. The perpendicularly formed morphology is easily formed when using NBR with less acrylonitrile. The rechargeable lithium battery with a PPy/NBR cathode shows a better charging-discharging performance than a PPy/NBR cathode formed with a lower AN content NBR.

A remarkable enhancement of the diffusion rate of anions at an oriented-grown PPy (polypyrrole) film formed with a guide of insulating NBR (nitrile butadiene rubber) film was the result of our investigations (1, 2). A similar procedure for controlling the morphology of conductive polymer was attempted by Penner and Martin (3, 4) using polypyrrole and nuclepore membrane. The preparation procedure for such a PPy film has already been reported in previous papers (1, 2). First, a NBR film is coated on a Pt substrate and immersed in an acetonitrile solution containing pyrrole monomer and electrolyte. After the PPy is electropolymerized along the etched tubular channels built up in the NBR film, the precoated NBR film is completely rinsed and extracted with an organic solvent. By virtue of the flexible and insulating nature of the NBR film, the morphology of the PPy film can be modified especially in the perpendicular direction, where the precoated NBR film performs the role of a guide polymer, regulating the polymer growth in a direction normal to the Pt substrate. Such a polypyrrole electrode of a regulated morphology is designated as a PPy/NBR electrode in the text. It is noteworthy that the PPy film prepared by such a method satisfies the optimum conditions of an effective battery material (5, 6). Therefore, it is interesting to investigate the PPy/NBR film further in the basic research of the plastic battery.

Of particular interest is the control of the degree of morphology orientation and the rate of anion doping-undoping process of the PPy/NBR film. In our previous work (1, 2), we used constant acrylonitrile composition of NBR, 22% acrylonitrile (AN) content. However, the morphology of polypyrrole formed with a guide of NBR film might be changed with varying acrylonitrile content of NBR, because the NBR film of lower AN becomes flexible. In this paper, we attempt to understand the mechanism of electropolymerization in nonconducting NBR films and also control the orientation of the guest polymer morphology by varying the acrylonitrile composition of NBR for electropolymerization.

Experimental

Chemicals and solutions.—Reagent grade acetonitrile and lithium perchlorate ($LiClO_4$) were used without further purification. Reagent grade propylene carbonate (PC) was used after purification by percolating through activated alumina. The water in the PC was removed with molecular sieves. A solution of acetonitrile, containing 0.2 mol

* Electrochemical Society Active Member.

dm^{-3} pyrrole monomer and 0.2 mol dm^{-3} $LiClO_4$ electrolyte salt, was used for the preparation of the polypyrrole (PPy) film. Electrochemical analysis was made in the acetonitrile solution containing 1.0 mol dm^{-3} of electrolyte. Charging-discharging tests were conducted in 1.0 mol dm^{-3} $LiClO_4$/PC solution at various current densities. NBRs with various compositions of acrylonitrile were used with the products Nipol DN-005(AN content 44%), Nipol DN-200 (AN 33%), Nipol DN-402 (AN 22%) and Nipol 401LL (AN 18%) of Nippon Zeon Company, Limited. The formation procedure of the polypyrrole through the NBR films was the same as in the previous work (1, 2) except for varying electropolymerization charge and NBR thickness.

Film preparation.—Conducting PPy films used in this work were invariably prepared by the potentiostatic electro-oxidation method. A normal PPy film was grown directly on a Pt substrate at 0.8V *vs.* Ag/Ag^+ (0.01 mol dm^{-3} $AgNO_3$) by passing 1 C cm^{-2} of charge. For the preparation of NBR-guided grown PPy film (PPy/NBR), this procedure is the same as that described in the previous paper (1, 2). The surface and cross-sectional morphologies of the PPy/NBR (5 μm in thickness) films formed by the passage of 5 C cm^{-2} were inspected by a scanning electron microscope (SEM).

Electrochemical measurements.—For the electrochemical measurements, the cell was assembled with a PPy-coated Pt working electrode, a stainless-plate (large surface area) counterelectrode, and Ag/Ag^+ reference electrode. Cyclic voltammograms were obtained for a normal PPy and a PPy/NBR electrodes formed with various types of NBR films in an Ar gas atmosphere. The electrode impedance was measured at some doping potentials in a frequency range from 1 Hz to 100 kHz by the FFT impedance method. The battery was assembled in a dry box in an Ar gas atmosphere, employing a Li/Ni-mesh anode and PPy/NBR/Pt cathode. Discharge of the cell was terminated when the cell voltage reached 2.0V.

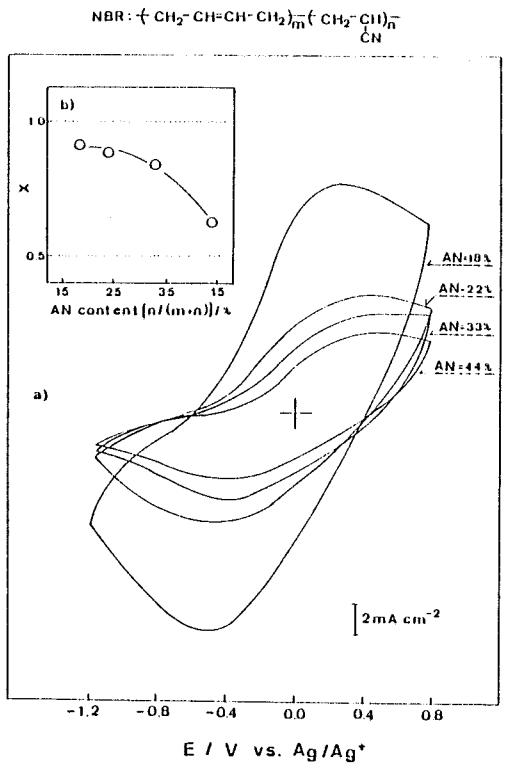

Fig. 1. (a) Typical cyclic voltammograms for PPy (1 C cm^{-2})/NBR (5 μm) film electrodes with varying acrylonitrile content of pre-coated NBR polymers in 1.0 mol dm^{-3} $LiClO_4$ at 50 mV s^{-1}. (b) Dependence of acrylonitrile content of NBR films on x value of $i_p = Av^x$.

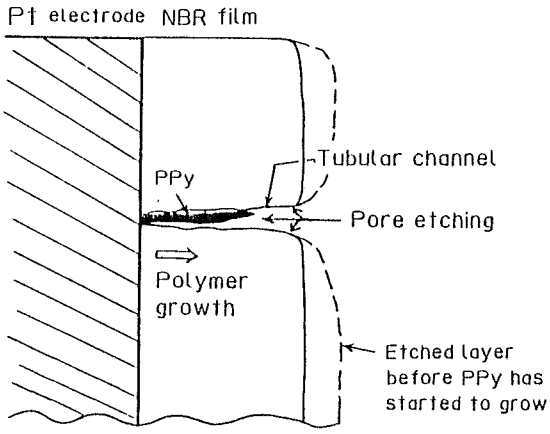

Fig. 2. Schematic model of the tubular channel formation in NBR film and the polymer growth through them.

Results and Discussion

Figure 1a shows a typical effect of the acrylonitrile content in a NBR film on the cyclic voltammograms for the PPy (1 C cm^{-2})/NBR (5 μm) films in 1.0 mol dm^{-3} $LiClO_4$/acetonitrile at 5 mV s^{-1}. The values of "m" and "n" correspond to the composition of butadiene and AN in NBR. As the AN content of NBR decreases, the potential separation becomes narrower, indicating that the reversibility of the anion doping-undoping process of PPy/NBR electrodes becomes more complete.

Figure 1b shows the dependence of the AN content in the NBR polymer on the rate-determining stage of the electrode process of the PPy/NBR films. When the curves of the peak current (i_p) on the scan rate (v) show the linear relationship ($i_p = Av^x$), the x value can be determined from the slope of these lines. The dashed lines at $x = 0.5$ ($i_p \propto \sqrt{v}$) and $x = 1.0$ ($i_p \propto v$) can be assigned to the diffusion-controlled and reaction-controlled processes, respectively. As the AN content of NBR increases, the x value shows a gradual decrease and finally reaches a value near *ca.* 0.5. This means that the electrode process changes from the reaction-controlled process to the diffusion-controlled process, as the AN content of the NBR film decreases. In order to consider how this oriented morphology is constructed, the growth model of the PPy/NBR film is illustrated in Fig. 2. This model corresponds to the initial stage of the PPy growth through the etched tubular channels formed in the NBR film. Just after the NBR/Pt electrode is immersed in

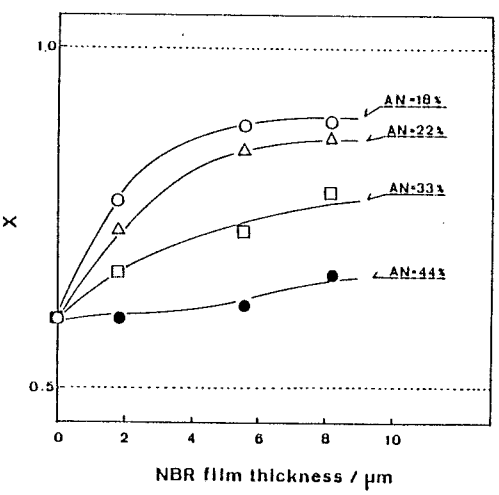

Fig. 3. Dependence of NBR thickness on rate-determining stage occurred at PPy/NBR electrodes formed with various kind of NBR polymer.

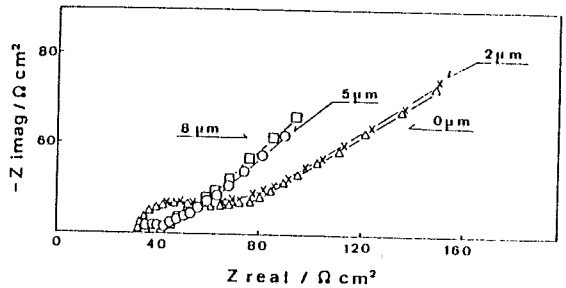

Fig. 4. Typical Cole-Cole plots for PPy/NBR (AN = 22%) films formed at four different NBR thicknesses (0, 2, 5, 8 μm).

the acetonitrile solution, the ($LiClO_4$ + pyrrole)/acetonitrile solution begins to etch fine tubular channels in the NBR film to establish the conduction paths from the solution side to the substrate. When the pore reaches the surface of the substrate, a PPy film begins to grow along these channels. The degree of morphology modification and the diameter of fibrils must be determined by the relative balance of the rates of polymer growth and tubular channel formation due to pre-etching. The potential at electropolymerization is fixed at 0.8V in the present work, and only the acrylonitrile content in the NBR host polymer is varied. Thus, the rate of pore etching is in relation to the solubility of NBR in acetonitrile. The NBR with a large amount of butadiene component may be easier to etch and also may become more flexible. Thus, the easier etching feature and the stress caused by the PPy growth may be modified to a much larger extent to form the columnar growth of PPy in the NBR film, when the AN content in NBR decreases.

Figure 3 shows the effect of the NBR thickness on the scan rate dependence of peak currents in voltammograms. All of the curves grow up to NBR = 5 μm in thickness and saturate over *ca.* 5 μm thick. As the NBR becomes thicker, the diffusion rate of anions is gradually enhanced to reach a certain limiting value at more than 5 μm in thickness. Therefore, in these preparation conditions, the 5 μm thickness is the critical point in forming an optimum oriented morphology. The doping-undoping kinetics of PPy/NBR films are further analyzed from the electrode impedance with the FFT impedance method by varying the NBR thickness as shown in Fig. 4.

Figure 4 shows typical Cole-Cole plots for PPy/NBR films (formed with $LiClO_4$/acetonitrile solution by passing 1 C cm^{-2}). Generally, as the NBR becomes thicker, the absolute values of the total impedance decrease. Judging from the impedance behavior at low frequencies, the electrode process changes from the charge-transfer controlled process to the diffusion-controlled process by thickening the precoated NBR film. In other words, the diffusion rate of anions within films is greatly enhanced. The impedance behavior for a PPy/NBR film formed with a NBR film thicker than 5 μm is essentially the same as that of the PPy/NBR (5 μm) film; *i.e.*, 5 μm is the critical thickness value for the largest diffusion rate enhancement for anions.

To check the time scale relevant to the anion diffusion within the polymer film, the impedance results were analyzed with the so-called Bode plots. Figure 5 shows typical Bode plots for PPy/NBR films formed with various kinds of PPy/NBR (5 μm) films. The frequency range in which mass transfer (indicated by the slope of 0.5) occurs shows a noticeable change upon varying the AN content. As the AN content decreases, the corresponding frequency value at which the 0.5 gradient line starts becomes higher. This indicates an enhancement in the diffusion rate of the dopant within the PPy/NBR film with a decrease in the AN content. This enhancement can be explained by the fact that the guest polymer film grows easily to form a perpendicular orientation with an increase in the flexibility of the NBR film caused by the decrease in the AN content.

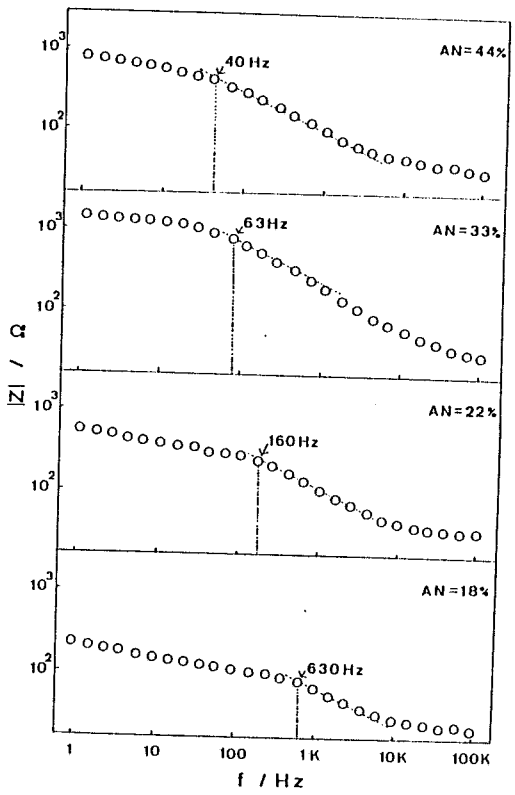

Fig. 5. Typical Bode plots for PPy (1 C cm^{-2})/NBR (5 μm) films with varying acrylonitrile content of NBR.

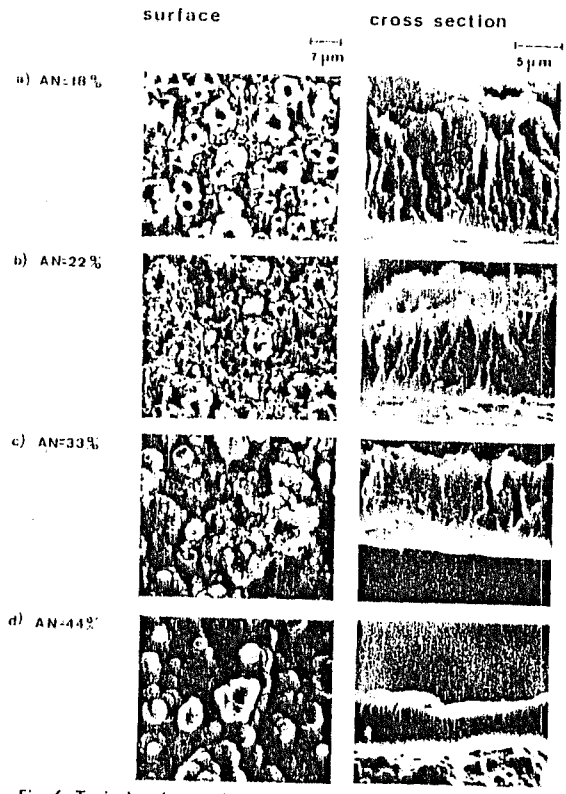

Fig. 6. Typical surface and cross-sectional SEM micrographs of PPy (5 C Cm^{-2})/NBR (5 μm) films formed with various kinds of NBR polymer.

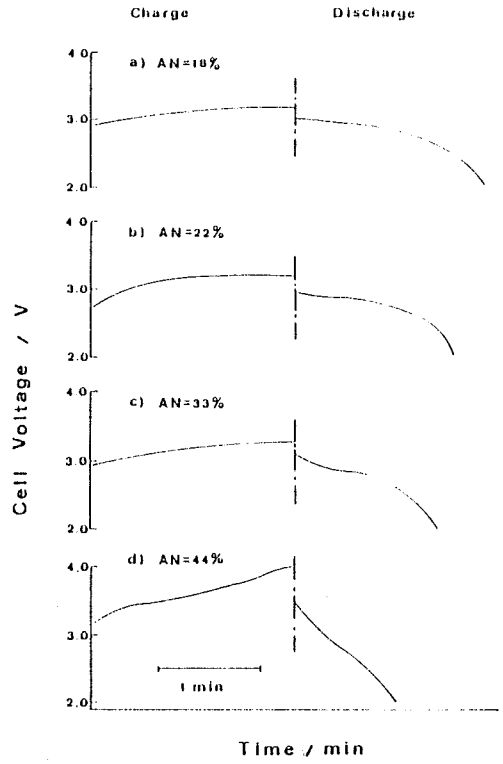

Fig. 7. Charging-discharging curves for Li/$LiClO_4$-PC/PPy (3 C cm^{-2})/NBR (5 μm) batteries assembled with NBR/PPy cathode with various acrylonitrile content of NBR. The depth of charge was 60 mC cm^{-2}.

The surface and the cross-sectional morphology of these films are shown in the SEM micrographs (see Fig. 6). When PPy is formed with a guide of NBR having a higher AN content, the surface of the PPy film becomes smooth. On the other hand, when using an NBR film of a lower AN content as the host polymer, the surface of the resulting film becomes rougher. The cross-sectional micrographs show such a relationship between AN content and morphology more exactly. As the AN content decreases, the columnar channel morphology becomes clearer. The columnar morphology results in the faster polymer growth due to the weaker attraction force between the NBR molecules.

On the basis of the SEM observations and electrochemical properties of these PPy/NBR films, we examined the charging-discharging properties of Li/$LiClO_4$-PC/(PPy/NBR) batteries. A Li/$LiClO_4$-PC/(PPy/NBR) battery was assembled with a PPy/NBR cathode and an Li anode pressed on a Ni-expanded mesh, where the PPy/NBR films were formed by passing a charge (3 C cm^{-2}) at a constant potential of 0.8V. Figure 7 shows typical charging-discharging curves for Li batteries assembled with the PPy cathode prepared at several AN contents of NBR. The current density of charging-discharging is 0.5 mA cm^{-2}. The Li battery with a PPy film formed with a low AN content shows a better charging-discharging performance than that with a PPy film formed with a high AN content.

Figure 8 shows the coulombic efficiency of Li/$LiClO_4$-PC/(PPy/NBR) batteries at various current densities. As is evident from the figure, an Li battery with a PPy film with a low AN content of NBR shows a better coulombic efficiency than that with a PPy film formed with a high AN content. The experimental results indicate clearly that the improvement of the battery properties in its current density depend upon decreasing the AN content of NBR. This can be attributed to the different diffusion rates of anions within these electrodes. These experimental facts on the performance characteristics of the Li/$LiClO_4$-PC/(PPy/NBR) battery as a function of the AN content of NBR support the previous results of the electrochemical properties of the PPy/NBR films in Fig. 1-5.

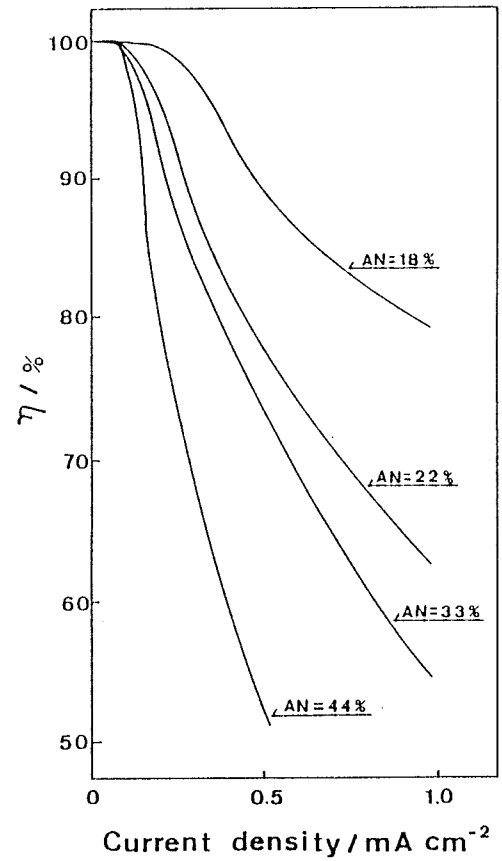

Fig. 8. Dependence of current density on coulombic yield (η) for Li/$LiClO_4$-PC/PPy (3 C cm^{-2})/NBR (5 μm) batteries with various acrylonitrile content of NBR. The depth of charge was 60 mC cm^{-2}.

Conclusion

The electrochemical properties of PPy/NBR electrodes by varying the AN content of NBR can be interpreted by the different diffusion rates of the doping-anion diffusion. As the AN content of NBR decreases, the NBR film becomes flexible, and thus, the diffusion rate of the dopants within the grown PPy/NBR film becomes faster. The growth of polypyrrole is considered to be more perpendicularly oriented with a guide of the NBR having an NBR film of less acrylonitrile content.

Acknowledgment

The authors wish to thank Professor Masako Osumi, Japan Women's University, for assisting in the SEM measurements. A part of this work was supported financially by a grant for Scientific Research from the Japanese Ministry of Education and the General Sekiyu Research and Development Encouragement and Assistance Foundation.

Manuscript submitted June 22, 1988; revised manuscript received Sept. 26, 1988.

Waseda University assisted in meeting the publication costs of this article.

REFERENCES

1. K. Naoi and T. Osaka, *Denki Kagaku*, 54, 808 (1986).
2. K. Naoi and T. Osaka, *This Journal*, 134, 2479 (1987).
3. R. M. Penner and C. R. Martin, *ibid.*, 133, 310 (1986).
4. R. M. Penner and C. R. Martin, *ibid.*, 133, 2206 (1986).
5. K. Naoi, A. Ishijima, and T. Osaka, *J. Electroanal. Chem.*, 217, 203 (1987).
6. T. Osaka and K. Naoi, *Shokubai (Catalyst)* 29, 130 (1987).

NBR/ポリピロール複合膜を用いたリチウム二次電池の特性：電解重合時の支持塩による影響

前田美知子，中村　節子*，上山　健一†，逢坂　哲彌†

Characteristics of Secondary Lithium Batteries using an NBR/Polypyrrole Cathode: Effect of Anions at Polymerization

Michiko MAEDA, Sadako NAKAMURA*, Ken-ichi UEYAMA† and Tetsuya OSAKA†

Received January 31, 1989 ; Accepted April 17, 1989

1　緒言

導電性高分子の中で 膜が比較的安定であるものとして、 最近ではポリピロール（PPy）[1,2]、ポリアニリン[3,4]が注目されているが、モノマーとして多環化合物のポリアズレン[5,6]も検討されている。これらの導電性高分子の中でリチウム二次電池用正極材料の可能性を考えるとドーピングレベルが最も高く、充放電容量が大きくなるポリアニリンが、その利点により注目され、一部実用化されるようになった[7]。またポリピロールはポリアニリンに比べドーピングレベルが低く、充放電容量が小さくなるが、その膜強度の高さから魅力ある材料であり、電池正極として試作されている[8]。そこで我々はこのポリピロール膜に注目し、特に重合時のアニオンにより膜特性が大きく依存することを利用して、電気化学的特性が優れた最もドーピング・脱ドーピングしやすい膜を検討した。その結果、 PF_6^-アニオン存在下で良好な膜が得られることを報告し、さらにこの膜がリチウム二次電池正極としても優れた特性を示すことを明らかにした[9,10]。 ポリピロール膜をより容易なアニオン拡散を可能とする方法として、著者らはさらに絶縁性NBR(ニトリルブタジエンラバー)をホストポリマーとして用いてポリピロール複合膜を電解重合により作製し、柱状に配向した粗な構造のポリピロール膜を成長させる方法を試みた[11,12]。ナフィオン等をホストポリマーとした同様な研究例はいくつか報告されている[13-19]。 我々は既にこのようなポリピロール膜(NBRは洗浄除去しポリピロールのみを残す)においてアニオン拡散速度が向上する事を電気化学的測定で確認し、さらにこの複合膜をリチウム二次電池正極として高い充放電速度で使用できることを見いだしている[13,14]。このようなNBR/ポリピロール膜の正極特性はNBRの物性(特に、剛性)に大きく依存し、ブタジエンとアクリロニトリル(AN)の比においてアクリロニトリルが低下すると膜の柔らかさが増し、その結果、より速いポリピロールの成長速度により垂直配向性に優れたポリピロール膜が得られる[20]。 そのため膜内アニオンの可逆性のよい膜ができ、電池正極に利用するに適するものが得られている。 そこで本研究ではこのアクリロニトリルの含量が低い NBR(AN=22%)をホストとし、さらにポリピロール重合時の支持塩効果を検討し、良好なリチウム二次電池正極特性の可能性を見いだすことを目的としている。

2　実験

2．1　複合膜作製

電解酸化重合は ステンレス板を 対極として、 面積0.196cm^2の白金電極上に、 0.8V vs. Ag/Ag^+(0.01mol $dm^{-3}AgNO_3$)の定電位で行い，重合通電量は1C cm^{-2}とした。0.2mol dm^{-3}ピロールモノマーと0.2mol dm^{-3}支持塩を含むPC(プロピレンカーボネート)溶液を重合液として用いた。 支持塩には$LiCF_3SO_3$、$LiPF_6$、$LiBF_4$、$LiClO_4$の4種類をとりあげた。この電解重合時に各支持電解質アニオンがポリマー内にとり込まれるが電気化学および電池測定には、このアニオンを十分脱ドープした後用いた。PCは活性アルミナで精製後、モレキュラーシーブで水分を除去して用いた。試薬はすべて特級を用い、溶液はAr脱気を行った後使用した。ポリピロール膜(Pt/PPy膜)の作製は白金電極上に直接ポリピロール膜を成長させた。NBRを介して重合するポリピロール膜(Pt/NBR/PPy膜)の作製は NBR をあらかじめ白金電極上に種々の膜厚(0~6μm)に被覆し、ピロールを重合した後NBR膜はアセトンにより洗浄除去し、成長したポリピロール膜だけを残した。

また重合膜の断面の状態を走査型電子顕微鏡(SEM)により観察した。この時、膜を電極面からはがしやすくするために重合通電量は5C cm^{-2}とした。

日本女子大学化学科(〒112 東京都文京区目白台2-8-1)
Department of Chemistry, Japan Women's University (2-8-1 Mejirodai, Bunkyo-ku, Tokyo 112)

*早稲田大学理工学部応用化学科(〒169 東京都新宿区大久保3-4-1) Department of Applied Chemistry, School of Science and Engineering, Waseda University (3-4-1 Okubo, Shinjuku-ku, Tokyo 169)

Key words: Polypyrrole, Doping process, NBR, Rechargeable Li battery

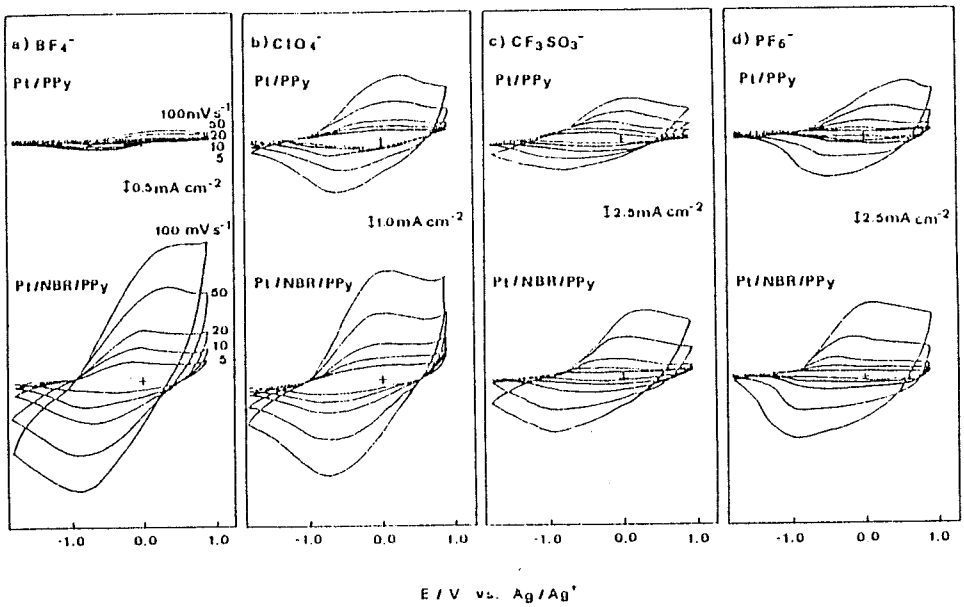

Fig.1 Cyclic voltammograms for Pt/PPy(1.0C cm^{-2}) and Pt/NBR(4μm)/PPy(1.0C cm^{-2}) film electrodes in 1.0mol dm^{-3} $LiClO_4$/PC at various scan rates. PPy films were formed with (a)BF_4^-, (b)ClO_4^-, (c)$CF_3SO_3^-$ and (d)PF_6^- anions.

2．2　電気化学的測定

電気化学的測定はサイクリックボルタンメトリー(走査速度5~100mV s^{-1})を用いて行い、試料極にPt/PPy膜あるいはPt/NBR/PPy膜を、対極にステンレス板、参照電極にはAg/Ag$^+$を用いた。電解液には1.0mol dm^{-3} $LiClO_4$を含むPC溶液を用いた。

2．3　電池充放電試験

充放電挙動の検討には正極にはPt/PPy(1C cm^{-2})膜あるいはPt/NBR(4μm)/PPy(1C cm^{-2})膜電極、負極にはニッケルエキスパンドメタルに圧着したリチウム電極、電解液には1.0mol dm^{-3} $LiClO_4$/PC溶液を用い、定電流充放電で行い、放電終止電圧は2.0Vとした。また測定はリチウム、電解液を充分に用いた簡単なガラスセルにて行い、全ての測定はAr通気下で行った。

3　結果と考察

3．1　種々の支持塩を用いて作製したPt/PPy膜およびPt/NBR/PPy膜の電気化学的挙動

4種類の支持塩を用いて作製したPt/PPy膜およびPt/NBR/PPy膜の代表的なサイクリックボルタモグラムをFig.1に示した。アノード、カソード電流は各々ポリピロール膜の酸化還元反応に伴うClO_4^-アニオンのドーピング・脱ドーピング反応に対応する。どの支持塩の場合にもNBR被覆により電流応答が増加し膜の特性が向上する事がわかるが、電解重合時の支持塩による膜特性の序列；PF_6^->$CF_3SO_3^-$>ClO_4^->BF_4^-はNBRを被覆しても逆転することはなく、NBRによる複合化は膜内アニオン拡散速度を大幅に向上させる効果をもっている。特に、NBRを被覆しない場合にClO_4^-アニオンのドープ・脱ドープ反応が優れた応答電流を示す$LiPF_6$の場合、NBR被覆による膜作製によりさらに応答電流が増加しており、アニオンのドーピング・脱ドーピング反応の応答速度、ドープ量をより向上させることが明らかである。一方$LiBF_4$に関してはNBRを被覆しないで重合した場合、電流応答が非常に小さく正極材料に用いる事は不適当であるが、NBRを被覆して重合した膜は応答電流が増大しておりNBR被覆による膜作製が効果をもつことが認められる。

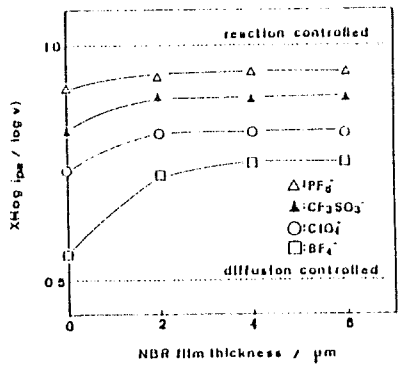

Fig.2 Change in the rate-determining step of the electrode process at Pt/NBR/PPy film upon thickening the pre-coated NBR films.

次にこれらの膜中での拡散挙動を調べるため、NBRの膜厚を段階的(0~6μm)に変化させてPt/NBR/PPy膜を作製しサイクリックボルタモグラムを測定した。このボルタモグラム中のアノードピーク電流値(i_{pa})と走査速度(v)とを両対数プロットすると直線関係を得る事ができ、その傾きxとNBRの膜厚の関係を示したのがFig.2である。図においてx=0.5($i_{pa}\propto\sqrt{v}$)およびx=1.0($i_{pa}\propto v$)の点線はそれぞれ電極反応が拡散律速および反応律速の場合に対応する。各支持塩ともNBRを介して重合する事によりxの値は増加し、電極反応が拡散律速から反応律速へと移

行している事がわかる。これはNBRを用いる事により膜が粗な構造になり膜内でのアニオン拡散が速くなるためと考えられる。ここで注目すべきことはNBRを介して重合しても支持塩によるx値の序列は同様であり、NBRは物理的に膜形態を粗にし、膜内アニオン拡散速度を向上させる事が予想される。また図よりNBRの膜厚が約4 μmでxの値がほぼ飽和していることから、1C cm^{-2}のポリピロールを重合する場合にはNBRを最低4 μm被覆する必要があることがわかる。

ここで電解重合時の支持塩によるポリピロール膜の形態の違いをSEMにより観察したものがFig.3である。これらの膜はNBRを介して重合後、NBRを溶かし出してポリピロール膜だけを残しているが、どの支持塩の場合にもNBRを介して重合すると膜の構造が粗になり、ポリピロールが柱状に生成している。特に、BF_4^-の場合、NBR被

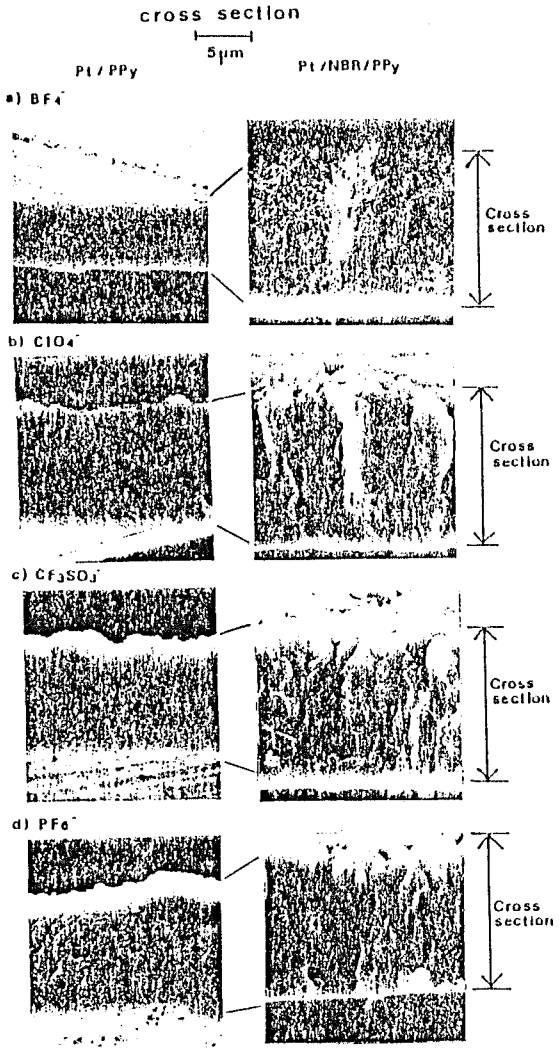

Fig.3 Typical cross sectional micrographs of Pt/PPy and Pt/NBR/PPy films formed at 0.8V from various kinds of electrolytes.

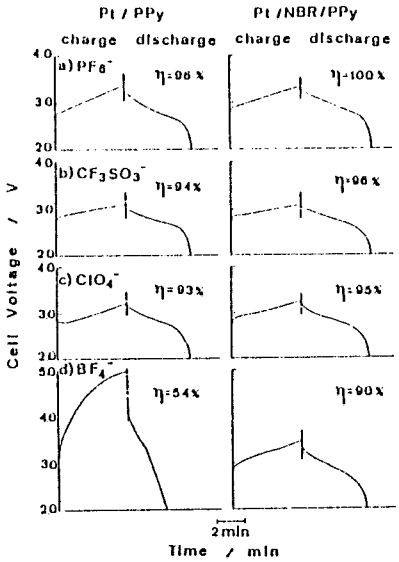

Fig.4 Charging-discharging curves for Li/$LiClO_4$/PPy batteries assembled with PPy cathodes pre-pared in the presence of various electrolytes anions (BF_4^-, ClO_4^-, $CF_3SO_3^-$ and PF_6^-) Current density; 0.2 mA cm^{-2}, end point of charging ; 60mC cm^{-2}

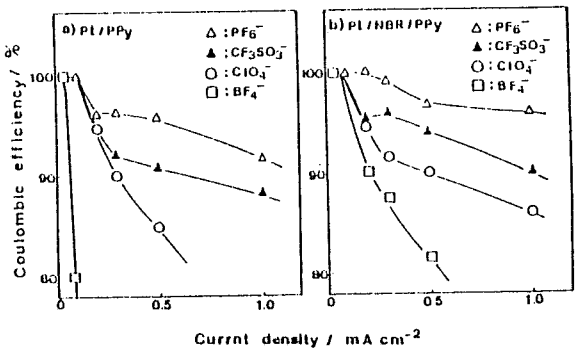

Fig.5 Coulombic efficiencies of (a)Li/$LiClO_4$/(Pt/PPy(1.0C cm^{-2})) and (b) Li/$LiClO_4$/(Pt/NBR/PPy(1.0C cm^{-2})) batteries at various current densities.

覆による膜厚の増加が顕著に認められ、緻密な膜が粗な状態になり膜厚方向にイオン拡散が容易になることが推察される。

3．2 電池充放電試験

Fig.4 は各 PPy膜を正極とするリチウム二次電池の代表的な充放電曲線を示している。どの支持塩の場合にもNBRを介して得られた膜の方が高い充放電効率を示している。この現象はBF_4^-の場合特に顕著であるが、これはFig.3のSEM観察から明らかのように、Pt/NBR/PPy膜の膜構造の急激な変化のため、膜のアニオンの拡散速度が上昇したことに対応すると考えられる。

次に種々の電流密度における充放電のクーロン効率を示したものがFig.5である。どの支持塩に関してもNBRを介して重合する事によって高いクーロン効率を示す電流密度域が拡がり、膜の充放電特性が向上している。特

に、Pt/PPy膜でも優れた特性を示すPF_6^-の場合、NBRを被覆する事によりさらに充放電速度を向上させている。

充電電気量に対するクーロン効率の変化をFig.6に示す。全ての充放電試験は電流密度0.2mA cm^{-2}で行っている。いずれの膜の場合にも充電電気量を上げていくと、クーロン効率が低下するが、どの充電電気量におけるクーロン効率も Pt/NBR/PPy膜の方が Pt/PPy膜に比べて高い。この場合にも NBR被覆効果はどの支持塩に関しても見られる。NBR被覆効果は電流密度に対しては著しいが、ドーピング量に対してはそれ程急激には改善されていない。これは NBRを介するという物理的方法は、膜内アニオン拡散を効果的に行えるようにするが、実効表面積を増大させるという点では、即ち活性サイト数の増加にはある程度の限界があることを示しているのであろう。

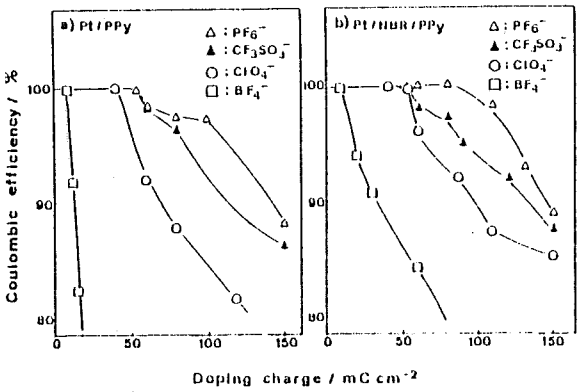

Fig.6 Coulombic efficiencies of (a)Li/$LiClO_4$/(Pt/PPy(1.0C cm^{-2})) and (b) Li/$LiClO_4$/(Pt/NBR/PPy(1.0C cm^{-2})) batteries at various doping charges.

4 結論

NBRを介して電解重合し、その後 NBRを溶解して得たポリピロール膜は粗な柱状構造をもち、NBRを利用しないポリピロールの支持塩効果 ($PF_6^- > CF_3SO_3^- > ClO_4^- > BF_4^-$)に従って特性が向上し、リチウム二次電池正極として優れた特性を示す。これは膜内アニオンの移動速度が有効に上昇し、充放電速度の向上につながるためである。従って、NBR/ポリピロール膜法は膜内アニオン拡散を著しく速くし、電池の高電流密度充放電における特性を大きく改善する効果をもつことが明らかとなった。

本研究の一部は、日本女子大学大橋廣記念奨学金で行った。付記して、感謝する。

文献

1) A.F.Diaz, K.K.Kanazawa and G.P.Gardini, J.C.S. Chem.Commun., 635(1979).
2) A.F.Diaz and J.I.Castillo, J.C.S.Chem.Commun., 397(1980).
3) A.F.Diaz and J.A.Logan, J.Electroanal.Chem., 111, 111(1980).
4) A.G.MacDiarmid, J.C.Chiang, M.Halpern, W.S. Huang, J.R.Krawczyk, R.J.Mammone, S.L.Mu, N.L. Somasiri and W.Wu, Poly. Prepr., 25,248(1984).
5) J.Bargon, S.Mohmand and R.J.Waltman, Mol. Cryst.Liq.Cryst., 93,279(1984).
6) R.J.Waltman, A.F.Diaz and J.Bargon, J. Electrochem.Soc., 131,1452(1984).
7) 小川雅男、布施正、喜多敏夫、川越隆博、松永孜、第27回電池討論会講演要旨集、3A06L(1986).
8) H.Mustedt, G.Kohler, H.Mohwald, D.Naegele, R.Bitthin, G.Ely and E.Meissner, Syn.Met., 18, 259(1987).
9) T.Osaka, K.Naoi, H.Sakai and S.Ogano, J.Electrochem. Soc., 134, 285(1987).
10) T.Osaka, K.Naoi and S.Ogano, J.Electrochem. Soc., 135, 1071(1988).
11) K.Naoi and T.Osaka, Denki Kagaku, 54, 808 (1986).
12) 逢坂哲彌、直井勝彦、触媒、29,130(1987).
13) K.Naoi and T.Osaka, J.Electrochem.Soc., 134, 2479(1987).
14) K.Naoi, A.Ishijima and T.Osaka, J.Electroanal. Chem., 217, 203(1987).
15) O.Niwa and T.Tamura, J.C.S.Chem.Commun.,817 (1984).
16) R.M.Penner and C.R.Martin, J.Electrochem.Soc., 133, 310(1986).
17) R.M.Penner and C.R.Martin, J.Electrochem.Soc., 133, 2206(1986).
18) T.Hirai, S.Kuwabata and H.Yoneyama, J. Electrochem.Soc., 135,1132(1988).
19) X.Bi and Q.Pei, Syn.Met., 22,145(1987).
20) T.Osaka, M.Maeda, K.Naoi and S.Nakamura, J.Electrochem. Soc., 136,1385(1989).

Abstract

Electrochemical anion doping-undoping process of NBR-guided-grown-polypyrrole(Pt/NBR/PPy) film electrodes was investigated by varying polymerization anions, i.e., $LiBF_4$, $LiClO_4$, $LiCF_3SO_3$ and $LiPF_6$ in order to apply the films to the cathode rechargeable Li battery. Compared with an ordinary polypyrrole(Pt/PPy) film grown directly on the Pt substrate, the Pt/NBR/PPy films enhance the movement of a dopant. As in a case of Pt/PPy films, the mobility of a dopant(ClO_4^- anion) in Pt/NBR/PPy films changes with a kind of anions in electropolymerizing solutions in a manner of $PF_6^- > CF_3SO_3^- > ClO_4^- > BF_4^-$. From the charging-discharging behavior of Li/$LiClO_4$/(Pt/NBR/PPy) batteries, a highly enhanced coulombic efficency is also obtained, and the Pt/NBR/PPy film electropolymerized in a $LiPF_6$ solution shows the best charging-discharging characteristics.

Electrochemical Study on Electropolymerized Polyazulene Film

Tetsuya OSAKA* and Ken-ichi UEYAMA

Received January 26, 1989 ; Accepted April 17, 1989

Anion doping-undoping process at an electrochemically prepared polyazulene(PAz) film was investigated as a function of polymerization charge by using cyclic voltammetry and ac impedance method. From cyclic voltammetric results, the anion doping-undoping process at PAz electrode was found to be highly reversible, when formed with less than ca. 2 C cm^{-2} of charge, while the charge capacity became saturated over 5 C cm^{-2}. From the resistive component(R_r) derived from impedance spectra by postulating a modified Randles circuit, the reversibility of doping-undoping process is discussed. The resistive component showed a clear hysteresis against the direction of scanning potential, and the degree of its hysteresis, which varied with the formation charge, corresponded well to the cyclic voltammetric results. Moreover, the degree of R_r hysteresis as a function of doping-undoping potential was found to be an effective scale of reversibility of kinetic reaction at PAz electrode.

INTRODUCTION

Many workers have investigated lithium cell systems using conductive polymer materials(1-19). At present, attentions have focused on chemically stable electrodeposited heterocyclic polymers. Recently electrochemical properties of polycyclic hydrocarbons such as polyazulene(PAz) and polypyrene have begun to be elucidated by some workers (16, 17, 20, 21). In general, polymeric films prepared by electro-oxidative polymerization of polycyclic hydrocarbons give lower electrical conductivity than, for example, polyaniline and polypyrrole. Among variety of polycyclic heterocarbon polymers, PAz electrode exhibits highly reversible and reproducible electrochemical doping-undoping process (16, 17). We have already shown that an electrodeposited PAz film could be an excellent cathode material in rechargeable lithium battery in view of showing high and flat voltage output (21). However, the charge capacity of Li /$LiClO_4$/PAz battery showed the saturation if the formation charge(Q_f) of PAz exceeded 5 C cm^{-2} due possibly to kinetic problems (21). It has already been found in polypyrrole electrodes that film thickness influence greatly the rate of doping-undoping reaction and also battery performance(15). In this study, kinetics of PAz will be investigated in detail as a function of polymerization charge(i.e., film thickness) with focusing to apply this cathode material to rechargeable lithium battery.

Department of Applied Chemistry, School of Science and Engineering, Waseda University, 3-4-1 Okubo, Shinjuku-ku, Tokyo 169, Japan
Key Words: Polyazulene, Conductive Polymer, Lithium Battery

EXPERIMENTAL

Reagent grade $LiClO_4$ and propylene carbonate(PC) were used as the electrolyte salt and the solvent, respectively. PC was purified by percolating through activated alumina (24). Water in PC was removed by adding molecular sieves to it and letting it stand for a few days until use. A Pt plate(0.283 cm^2) and a Pt wire were used as substrate for PAz deposition and counter electrode, respectively. All potentials were referred to Li/Li^+ electrode. PAz film was polymerized galvanostatically at 0.3 mA cm^{-2} in 0.1 mol dm^{-3} $LiClO_4$/PC containing 0.01 mol dm^{-3} azulene monomer. Deposited amount of PAz was controlled by monitoring electrolysis charges passed during electropolymerization. From a scanning electron microscope (SEM) observation, film thickness of PAz became ca.30 μm at 5 C cm^{-2} and had tendency to be saturated with increasing electrolysis charge, so it became almost the same between 5-10 C cm^{-2}. Electrochemical measurements such as cyclic voltammetry and impedance method were performed in 1.0 mol dm^{-3} $LiClO_4$/PC in argon gas atmosphere. In order to avoid aging effects, electrode impedance of PAz film was measured in very short duration of time (several seconds) for frequencies ranging from 10 Hz to 2.5 kHz with use of the FFT impedance method(25). Impedance results were analyzed based on modified Randles circuit as shown in Fig. 5 using digital simulation technique.

RESULTS AND DISCUSSION

Figure 1 a) shows typical cyclic voltammograms of PAz electrodes formed with various amount of charges, viz. 1, 3, 5 and 10 C cm^{-2}. In these voltammograms, anodic and cathodic currents are mainly involved in anion doping and undoping processes, respectively. The doping-undoping process occurs synchronously with the oxidation and reduction of PAz film. PAz electrodes prepared with the polymerization charges less than 10 C cm^{-2} show quite reproducible voltammograms between 2.0 V and 4.2 V, indicating that the oxidative decomposition does not occur within this potential range. Since all these voltammograms were obtained at a low scan rate of 5 mV s^{-1}, the over-all electrode process should be controlled by electron exchange at reaction sites within the PAz films. Hence, the amount of charges consumed in anodization and cathodization must reflect the effective number of active sites. Relationship between anodization charges(Q_a) estimated from these cyclic voltammograms and film formation charges(Q_f) is shown in Fig. 1 b). The Q_a values obtained for PAz films which were prepared with 5 and 10 C cm^{-2} do not differ appreciably with each other, suggest-

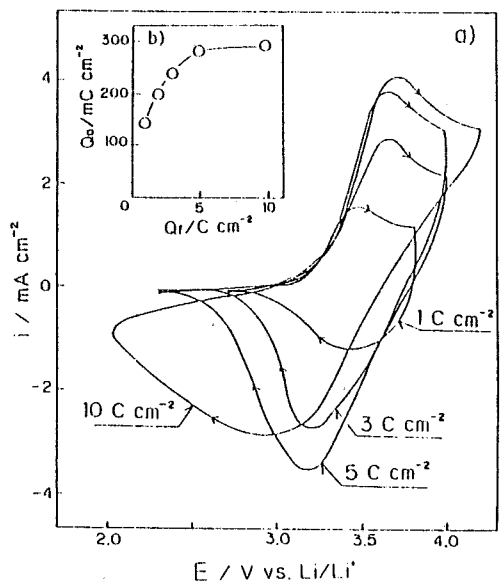

Fig. 1 a)Typical cyclic voltammograms for polyazulene electrodes of various formation charges obtained at 5 mV s^{-1} b)Formation charge(Q_f) dependence of anodization charge(Q_a) estimated from voltammograms in a).

ing that diffusion of dopant anions in the thicker PAz films is limited and the charge capacity of PAz film becomes almost saturated for the polymerization charge grater than ca. 5 C cm^{-2}.

In order to analyze the kinetic process at the PAz electrode in detail as a function of formation charge, the dependence of anodic peak currents(i_{pa}) in cyclic voltammograms on the scan rate(v) was analyzed in terms of a simple relationship of $i_{pa} = A\ v^x$. Figure 2 shows the x values against the formation charges(Q_f). The x value was determined in the scanning rate range between 2-20 mV s^{-1}. The dashed lines at x=0.5 and x=1.0 correspond to the diffusion-controlled and reaction-controlled processes, respectively. The x value shows gradual decrease at around 2-3 C cm^{-2}, and finally reaches a certain saturated value of ca. 0.5, as the Q_f value becomes larger than 5 C cm^{-2}. This means that the electrode process changes from the reaction-controlled to the diffusion-controlled process, as the film becomes thicker. It is worthwhile noting that an appreciable retardation of dopant diffusion is observed between 2 and 5 C cm^{-2}. It is concluded from kinetic point of view that thin PAz films formed with less than 2 C cm^{-2} are kinetically advantageous.

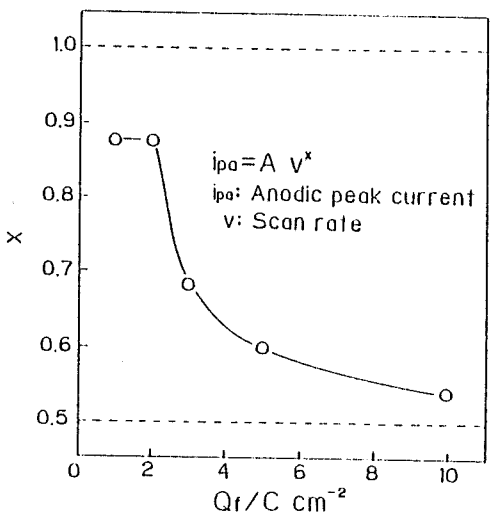

Fig. 2 Film formation charge(Q_f) dependence of x value estimated from log i_{pa} - log v plots.

In order to ascertain the influence of polymerization charge on the surface morphology, PAz films were inspected by SEM. Figure 3 shows surface SEM micrographs of the PAz films formed with electrolysis charges of 1, 2, 3, 10 C cm^{-2} . A number of small grains are observed for the 1 and 2 C cm^{-2} PAz films. The nucleation seems to occur preferentially on Pt substrate rather than the continuous film formation for the first 1 or 2 C cm^{-2} of electrolysis. As the film grows thicker than 3 C cm^{-2}, the surface becomes somewhat smooth, indicating that the small grains of PAz grow. As far as the SEM micrographs are concerned, the cyclic voltammetric results shown in Fig. 1 are intimately correlated with the surface morphology.

Figure 4 shows typical Cole-Cole plots at various applied potentials for PAz electrodes formed with 1, 5 and 10 C cm^{-2}. Each PAz film shows similar dependence upon applying potential. Namely, the semi-circle becomes smaller with an increase in

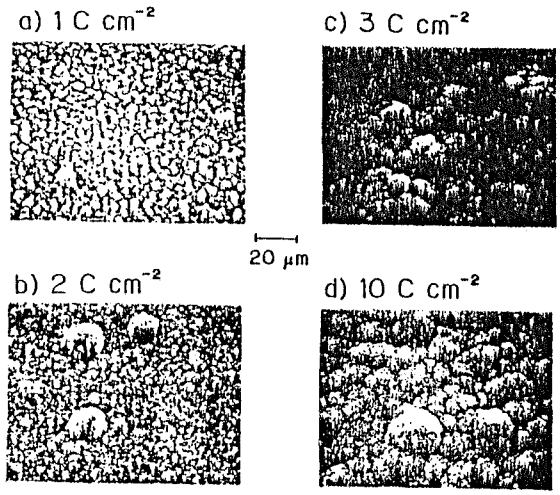

Fig. 3 Surface SEM micrographs of polyazulene films prepared at various formation charge.

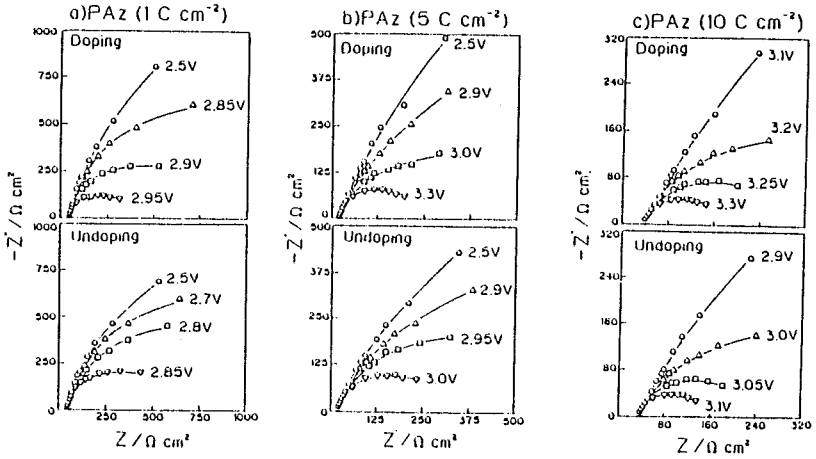

Fig. 4 Cole-Cole plots for polyazulene films of various formation charge as a function of doping and/or undoping potential.

anodic potential and also bigger again with a drop in anodic potential. The impedance behavior can be reasonably interpreted by postulating a modified Randles equivalent circuit as shown in Fig. 5. This model has already been adopted successfully to the analysis of polyacetylene(22, 23) and polyaniline(24). The circuit elements of R_s, C_p, R_r, $Z_w(=\sigma\,\omega^{-1/2})$ and a/ω correspond to the solution resistance, the parallel capacitance, the faradaic and/or film resistance, the Warburg diffusion impedance and the impedance component owing to its surface roughness, respectively. Among these components only the R_r value shows drastic change. The other components do not change appreciably, irrespective of PAz formation charge, and these values are in the following ranges; R_s = 20-30 Ω cm^2, C_p= 15-20 μF cm^2, σ= 100-200 Ω cm^2 s$^{-0.5}$, a = 2 × 10^5 Ω cm^2 s^{-1}.

As the R_r value is useful as one of sensitive scales to check the doping-undoping process, a relationship between R_r and potential was obtained and shown in Fig.6 as a function of formation charge. It was previously reported for PAz films prepared with 1 C cm^{-2} that the sensitive changes in R_r values reflected both the polymer layer resistance and doping-undoping kinetics (22, 23). According to Fig.6 the R_r values show drastic decrease of three orders of magnitude in an initial doping stage. At higher potentials, the R_r values vary within a reasonable range of faradaic impedance due to kinetic process. Although all the PAz electrodes show similar R_r-potential dependences, the

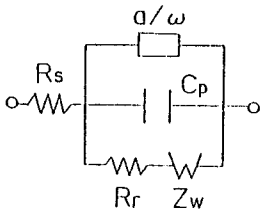

Fig. 5 Modified Randles circuit model assumed for the doping-undoping process at polyazulene films.

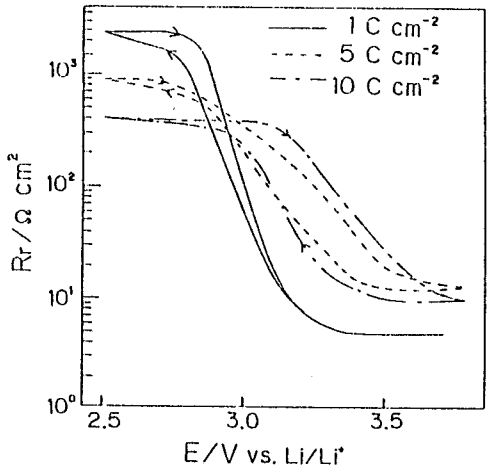

Fig. 6 Potential dependence of R_r component for polyazulene films formed by passing 1, 5 and 10 C cm^{-2}.

degree of hysteresis in the R_r-potential relations becomes more pronounced with a rise in formation charge and becomes almost the same between PAz films prepared with 5 and 10 C cm^{-2} though at a film prepared with 1 C cm^{-2} the hysteresis is small. This may indicate that the total electrode process becomes almost saturated at 5 C cm^{-2} of formation charge. Another important finding is that the change in R_r value during the redox reaction of PAz film itself becomes less marked as the PAz film becomes thicker. The R_r values range from ca. 5 to ca. 3000 Ω cm^2 for 1 C cm^{-2} film, from ca. 10 to ca. 1000 Ω cm^2 for 5 C cm^{-2}, and from ca. 10 to ca. 400 Ω cm^2 for 10 C cm^{-2}, respectively. The R_r value at 2.5 V, decreased with increasing formation charge, suggests that the electrical conductivity of PAz at undoped state becomes higher with an increase in polymerization charge. This fact can be explained as follows; as the thickness of PAz film increases, the dopant anions that are confined deeply inside the polymer layer can not be reversibly undoped within the time scale of measurement of FFT impedance method (10 Hz - 2.5 kHz). On the contrary, there is no essential change between the R_r values at around 3.5 V, although films prepared with 1 C cm^{-2} show a little smaller R_r than those prepared with 5 and 10 C cm^{-2}. This fact may suggest that the faradaic resistance due to electron exchange process is unchanged by increasing the film formation charge of PAz electrode.

In conclusion, the present study has revealed that the PAz film should be prepared with less than 5 C cm^{-2} of charge, when one wants to use it as a cathode material in a rechargeable lithium battery.

ACKNOWLEDGMENT

The authors are indebted to Dr. Katsuhiko Naoi for his valuable discussion. A part of this work was financially supported from the General Sekiyu Res. Dev. Encouragement Assistance Foundation.

REFERENCE

1. A. F. Diaz and J. A. Logan, J. Electroanal. Chem., 111, 111 (1980).
2. A. G. MacDiarmid, S-L Mu, N. L. D. Somasiri and W. Wu, Mol. Cryst. Liq. Cryst., 121, 187 (1985).
3. K. Abe, F. Goto, K. Okabayashi, T. Yoshida and H. Morimoto, The 27th Battery Symposium of Japan in Osaka, p.201 (1986).
4. M. Ogawa, T. Fuse, T. Kita, T. Kawagoe and T. Matsunaga, The 27th Battery Symposium of Japan in Osaka, p.197 (1986).
5. A. Kitani, M. Kaya and K. Sasaki, J. Electrochem. Soc., 133, 1069 (1986).
6. G. C. Farrington, B. Scrosati, D. Frydrych and J. DeNuzzio, J. Electrochem. Soc., 131, 7 (1984).
7. E. M. Genies and C. Tsintavis, J. Electroanal. Chem., 195, 109 (1986).
8. S. H. Glarum and J. H. Marshall, J. Electrochem. Soc., 134, 142 (1987).
9. H. Sakai, K. Naoi, T. Hirabayashi and T. Osaka, Denki Kagaku, 54, 516 (1986).
10. T. Osaka, S. Ogano, K. Naoi, J. Electrochem. Soc., 135, 539(1988).
11. A. F. Diaz, J. L. Castillo, J. A. Logan, and W. Y. Lee, J. Electroanal. Chem., 129, 115 (1981).
12. E. M. Genies and J. M. Pernaut, J. Electroanal. Chem., 191, 111 (1985).
13. A. Mohammadi, O. Inganaes and I. Lundstroem, J. Electrochem. Soc., 133, 947 (1986).
14. H. Sakai, K. Naoi, T. Hirabayashi and T. Osaka, Denki Kagaku, 54, 75 (1986); T. Osaka, K. Naoi,

H. Sakai and S. Ogano, J.Electrochem. Soc., 134, 285 (1987).
15. T. Osaka, K. Naoi, S. Ogano and S. Nakamura, Chem. Lett., 1986, 1687; T. Osaka, K. Naoi, S. Ogano and S. Nakamura, J. Electrochem. Soc., 134, 2096 (1987).
16. J. Bargon, S. Mohmand and R. J. Waltman, Mol. Cryst. Liq. Cryst., 93, 279 (1983).
17. R. J. Waltman, A. F. Diaz and J. Bargon, J. Electrochem. Soc., 131, 1452 (1984).
18. T. Osaka, K. Naoi and S. Ogano, J. Electrochem. Soc., 135, 1071 (1988).
19. T. Nagamoto and O. Omoto, J. Electrochem. Soc., 135, 2144 (1988).
20. G. Tourillon and F. Garnier, J. Electroanal. Chem., 135, 173 (1982).
21. T. Osaka, K. Naoi and T. Hirabayashi, J. Electrochem. Soc., 134, 2645 (1987).
22. T.Osaka and T.Kitai, Bull. Chem. Soc. Jpn, 57, 759 (1984).
23. T.Osaka and T.Kitai, Bull. Chem. Soc. Jpn, 57, 3386 (1984).
24. H. Sakai, K. Naoi, T. Hirabayasi and T. Osaka, Denki Kagaku, 54, 516 (1986).
25. T. Osaka and k. Naoi, Bull. Chem. Soc. Jpn., 55, 36 (1982).

CHEMISTRY LETTERS, pp. 1513 1514, 1989.

Preparation of MIM(Metal-Insulator-Metal) Non-linear Device Using Electropolymerized Poly-N-methylpyrrole

Tetsuya OSAKA,* Ken'ichi UEYAMA, and Kiyoshi OUCHI
Department of Applied Chemistry, School of Science and Engineering,
Waseda University, 3-4-1 Okubo, Shinjuku-ku, Tokyo 169

The MIM cell of ITO(indium tin oxide)/polymer/ITO type was prepared by sandwiching electrochemically polymerized poly-N-methylpyrrole(PMPy) film for the insulator between sputtered ITO layers of the cell. When using undoped polymer layer, the two-terminal device shows non-linear and symmetric current-voltage(I-V) curve, where the current changes 5 orders between the voltage of 0 V and ±15 V, respectively.

It has reported that the use of MIM switching devices allows for larger and/or high resolution liquid crystal (LC) displays.[1] Devices are fabricated in industrial process by thin film techniques, where tantalum oxide (Ta_2O_5) layer, as an insulator of MIM, is usually formed by partially anodizing a sputtered tantalum layer. The application of organic insulating layers has already been tried to a Schottky diode (metal/polymer),[2] an organic heterojunction (polymer/polymer),[3] a FET,[4] a microelectrochemical diode,[5] a MIM device using a LB(Langmuir-Blodgett) film,[6] and so on. However, the MIM device using electropolymerized insulating layer has not been realized. In this letter, we attempt the electropolymerized polymer film for the insulator of the MIM cell, since the technique of electropolymerization has the merit of forming insulating thin films easily and also simplifying the preparation of MIM cells. Therefore, it can be accelerated by this switching device that larger area LC display is industrially realized. A schematic representation of the MIM device experiments is shown in Fig. 1. The holes for the deposited polymer layer with various areas, 100, 300, 500, 700, 1000 μm in diameter were prepared by photolithographic technique on the 0.4 μm thick ITO layer. The PMPy(poly-N-methylpyrrole) film was galvanostatically polymerized on the ITO electrode in propylene carbonate (PC) solution containing 0.2 mol dm^{-3} N-methylpyrrole and 0.2 mol dm^{-3} $LiClO_4$ under the condition of drawing as low current density as possible. The PMPy film was electrochemically undoped at -1.2 V vs. Ag/Ag^+ for 5 minutes to become the insulating state. After the PMPy film was rinsed in acetone and dried in vacuum condition, the 600 Å

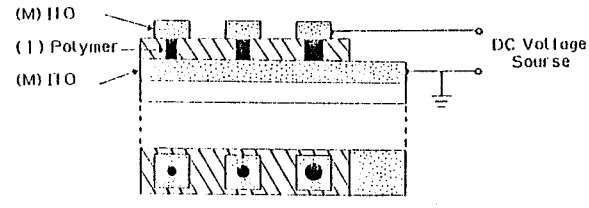

Fig. 1. Schematic representation for the MIM device experiments.

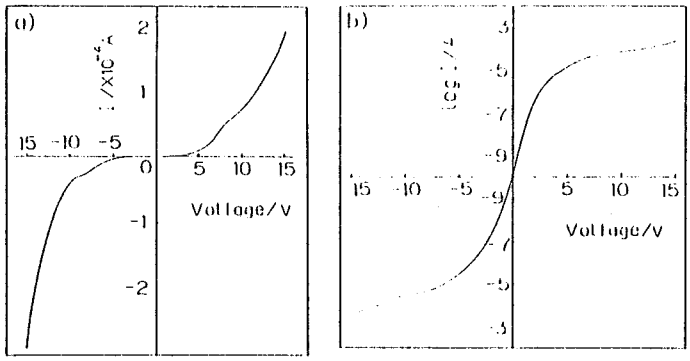

Fig. 2. I-V(a) and logI-V(b) characteristics of ITO/PMPy(undoped)/ITO cell.

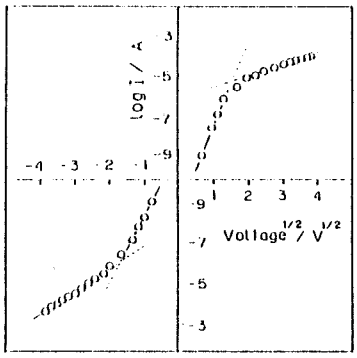

Fig. 3. LogI-$V^{1/2}$ characteristics of ITO/PMPy undoped)/ITO cell.

thick ITO was sputtered on it and patterned by etching.

Figure 2 shows the representative current-voltage (I-V) characteristics of the ITO/PMPy/ITO cell. The current is shown in I(a) and logI(b) units. The diameter and thickness of the PMPy film are 300 μm and 1 μm, respectively. The current increases steeply from ±3 V and it shows symmetrical shape in Fig. 2(a). It is demonstrated that the current gives 5 orders changes from 10^{-9} to 10^{-4} amperes symmetrically between 0 V and ±15 V in Fig. 2(b). The excellent reproducibility was given in the region between ±15 V. While in cases of the larger area than 500 μm in diameter or the thinner than 1 μm in thickness, the high reproducibility and such current changes were not obtained for the PMPy film usage in this MIM system.

Figure 3 shows the logI-$V^{1/2}$ plots, giving the straight lines but the slopes clearly change at ca. ±4 V region. At the higher electric field region, the conduction mechanism might be the Poole-Frenkel effect through the bulky PMPy film,[7] and at the lower field region another mechanism should be considered.

Consequently, the high potential of the MIM device using electropolymerized layer at undoped state is demonstrated by the symmetrical non-linear I-V response. This suggests another application of functional organic thin films.

References

1) D. R. Baraff, J. R. Long, B. K. MacLaurin, C. J. Miner, and R. W. Streater, Conf. Record. of 1980 Biennial Display Research Conf., IEEE, p.107 (1980).
2) H. Koezuka and S. Etoh, J. Appl. Phys., 54, 2511 (1983).
3) H. Koezuka, K. Hyodo, and A. G. MacDiarmid, J. Appl. Phys., 58, 1279 (1985).
4) A. Tsumura, H. Koezuka, S. Tsunoda, and T.Ando, Chem. Lett., 1986, 863.
5) G. P. Kittlesen, H. S. White, and M. S. Wrigrton, J. Am. Chem. Soc., 107, 7373 (1985).
6) K. Sakai, H. Matsuda, H. Kawada, K. Eguchi, and T. Nakagiri, Appl. Phys. Lett., 53, 1274 (1988).
7) J. G. Simmons, Phys. Rev., 166, 912 (1968).

(Received May 26, 1989)

Reprinted from JOURNAL OF THE ELECTROCHEMICAL SOCIETY
Vol. 136, No. 9, September 1989
Printed in U.S.A.

Electrochemical Study on Charge-Discharge Performance of Lithium/Polyazulene Battery

Katsuhiko Naoi,*,[1] Kenichi Ueyama, and Tetsuya Osaka*

Department of Applied Chemistry, School of Science and Engineering, Waseda University, 3-4-1 Okubo, Shinjuku-ku, Tokyo 169, Japan

ABSTRACT

Electrodeposited polyazulene (PAz) films show high electroactivity and fast redox switching behavior when polymerized under suitable conditions. Such PAz films are more electroactive than electrodeposited polypyrrole or polyaniline and were successfully applied in a rechargeable lithium battery. We determined suitable polymerization conditions so as to obtain an electroactive PAz film possessing the highest charge-storing ability and fastest electrode processes. Specifically, the electrochemical kinetics (anion doping-undoping process) of PAz films was investigated by varying the polymerizing current density and formation charge. Charge capacity showed a maximum value when polymerized at 1.4 mA cm^{-2} by passage of 5C cm^{-2}. Cyclic voltammograms coupled with scanning electrons microscope observation of PAz films evidenced that a highly electroactive PAz film can be prepared at 1.4 mA cm^{-2}. The charge-discharge property and cyclability of Li/$LiClO_4$/PAz batteries were studied. Li/$LiClO_4$/PAz batteries showed fairly high and flat discharge voltage (*ca.* 3.2V), while maintaining 100% coulombic efficiency when charging by ca. 45% of doping level (per unit cathode weight). The Li/$LiClO_4$/PAz battery performed best when PAz film was formed at 1.4 mA cm^{-2} by passage of 5C cm^{-2}.

Several years have passed since the investigation of advanced lithium cell systems using conducting polymer materials started (1-15). Polymer materials seem to be most effectively used as cathodes in rechargeable lithium cell systems as an alternative of conventional metal oxides such as NiOOH, PbO_2, or MnO_2. Polyacetylene was the first target of investigation. However, this material is quite unstable in an ambient atmosphere and is now considered to be far from practical. Instead of this material, attention has focused on electrodeposited heterocyclic polymers such as polyaniline (1-9) and polypyrrole (10-16) which are mechanically more stable, and show higher electroactivity than polyacetylene. Series of research works (15-18) has revealed that good quality and highly electroactive films are also derived from benzenoid or aromatic hydrocarbons. Among these polymers, polyazulene (PAz) was found to have the highest electrochemical activity, and the free-standing film conducts electrically in the range: 10^{-2} to 10^{0}S cm^{-2} (15). Earliest papers on PAz film reported a possible application as an electrochromic material and also the mechanism of doping process (15-17).

Regarding applicability as a battery material, we have already examined and pointed out that electrodeposited PAz films could be a possible cathode material in rechargeable plastic batteries (18).

Like polypyrrole already investigated by us (13, 14), electrochemical properties (doping charge, switching reversibility) of PAz film can also be enhanced by choosing suitable electropolymerization conditions. Polymerization factors, potential (13), current (3), electrolyte anion (13, 14), and formation charge (14) have been shown to greatly influence electrode kinetics of the resulting film and its morphology. In this regard, a great deal of experimental work has evidenced this fact and shown a strong correlation between charge-discharge performance of Li/$LiClO_4$/PAz battery and morphology of PAz films. However, the effect of these factors on the suitability as a battery material has not fully been clarified so far.

An important part of this work was to determine suitable current density and formation charge and to optimize the electrochemical property of PAz film to provide a cathode material in rechargeable lithium batteries (18).

Experimental

Chemicals and solutions.—The highest grade products of $LiClO_4$ (Mitsuwa Chemical) and azulene monomer were used as obtained without further purification. Propylene carbonate (PC) used as a solvent was purified by percolation through activated alumina. Water in PC was removed by letting PC stand over molecular sieves for a few days. Electropolymerization of azulene was conducted in a PC solution deaerated by pure argon gas.

Film preparation.—PAz films were prepared by galvanostatic electropolymerization on Pt substrates at various current density from 0.6 to 1.6 mA cm^{-2} in 0.1 mol dm^{-3} $LiClO_4$/PC containing 0.05 mol dm^{-3} azulene monomer, while monitoring the electrode potential against time. The amount of deposited PAz was controlled by monitoring the charge passed during electropolymerization.

Cell assembly and electrochemical measurements.—A 0.283 cm^3 Pt plate and Pt wire were used as substrates for PAz deposition and counterelectrodes, respectively. All potentials were referred to a Li/Li$^+$ electrode in the same solution. Cyclic voltammetry was carried out in 1.0 mol dm^{-3} $LiClO_4$/PC solution deaerated with pure argon. A Li/$LiClO_4$/PAz battery was constructed with a PAz cathode and a Li anode pressed onto Ni-expanded mesh.

Charge-discharge tests were performed in 1.0 mol dm^{-3} $LiClO_4$/PC in argon gas atmosphere, when Li anode and solvent were used abundantly compared to the amount of cathode material, in order to evaluate the ability of polymer cathode. The cyclability of Li/$LiClO_4$/PAz (5C cm^{-2}) was checked by consecutive charge-discharge performances when charged to a 20% doping level at a current density of 0.5 mA cm^{-2}. The surface and cross-sectional conditions for free-standing PAz films peeled off from Pt substrate were inspected by scanning electron microscope (SEM).

Results and Discussion

Typical comparison of cyclic voltammogram of polyazulene with those of polypyrrole and polyaniline.—Figure 1 shows the comparison of typical cyclic voltammograms (5 mV s^{-1}) for anion doping-undoping processes at electrodeposited PAz, polypyrrole and polyaniline films. Although each film was prepared by passing the same amount of charge (1C cm^{-2}), the PAz film shows larger current values than the other two films. We estimated the amount of doping charge (Q_a) under anodic (and/or cathodic) current between 2.4 and 3.7V under low scan rates. The Q_a value corresponds to a redox capacity (reversibility exchangeable charge) of each film at the time scale of the scan rate. Table I lists the values of doping charge, Q_a, Q_{ag}, and Q_{av} where Q_a, Q_{ag}, and Q_{av} are the values per unit area (mC cm^{-2}), unit material weight (mC mg^{-2}) and unit material volume (C cm^{-3}). From this table, it is obvious that PAz films have the highest redox capacity among these 1C cm^{-2}-formed films at the time scale of this scan rate (5 mV s^{-1}).

* Electrochemical Society Active Member.
[1] Present address: Department of Chemical Engineering and Materials Science, University of Minnesota, Minneapolis, Minnesota 55455.

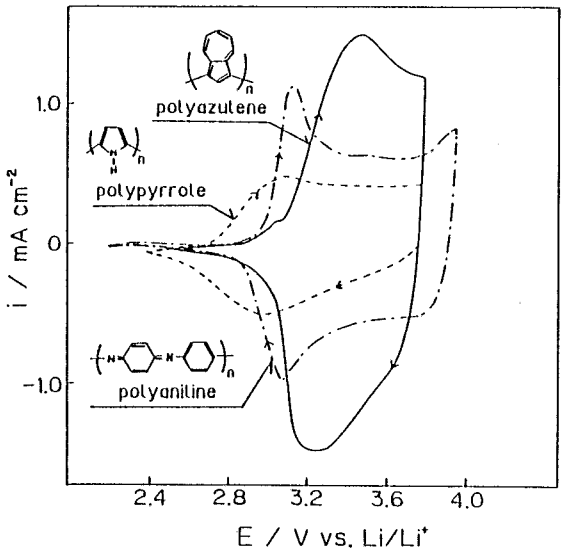

Fig. 1. Comparison of cyclic voltammograms (5 mV s^{-1}) for PAz, polypyrrole, and polyaniline film electrodes, all of which were prepared by passing 1C cm^{-2}. The polypyrrole film was formed at 4.2V vs. Li/Li^+ in (0.2 mol dm^{-3} pyrrole + 0.2 mol dm^{-3} $LiClO_4$)/PC. The polyaniline film was formed at 0.75V *vs.* Ag/AgCl in (0.1 mol dm^{-3} aniline + 0.1 mol dm^{-3} H_2SO_4) *aq*. The polyazulene film was formed as indicated in the Experimental section.

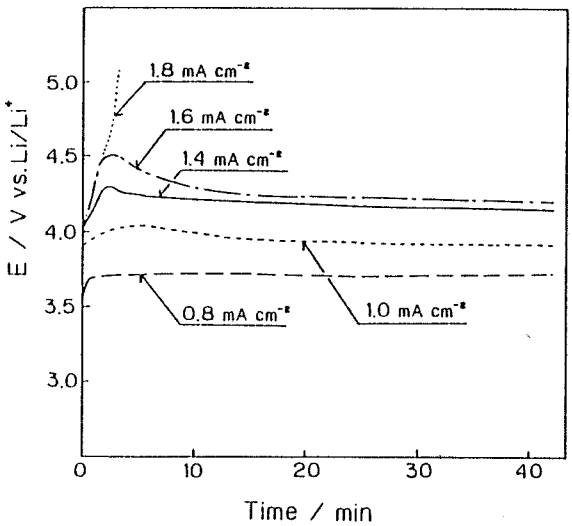

Fig. 2. Potential-time curves for galvanostatic polymerization of azulene in (0.05 mol dm^{-3} + 0.1 mol dm^{-3})/PC at various current densities.

The ratio of the weight of undoped films (w) divided by the molecular weight of each monomer (M), represents the number of monomer units in polymer films. These values are listed in Table I in comparison with Q_a values determined from the voltammograms in Fig. 1. Ratios of monomer-unit-number for polyazulene:polypyrrole: polyaniline films is approximately 10:7:2. The largest number of monomer units are involved in 1C cm^{-2} prepared PAz film among three films. That is, the polymerization efficiency is higher in the order: polyazulene > polypyrrole > polyaniline. On the other hand, Q_a values are larger in the order: polyazulene > polyaniline > polypyrrole. However, when we compare values of Q_{ag} (mC mg^{-1}), the order becomes polyaniline > polypyrrole > polyazulene because of the larger weight of the azulene monomer units. With respect to capacity (Ah kg^{-1}), the Li/PAz battery may be inferior to Li/polypyrrole and Li/polyaniline batteries. For values of Q_{av} (C cm^{-3}), polyazulene shows the maximum value as shown in Table I. Li/PAz battery appears to show the best capacity (Ah cm^{-3}). From the calculation of film density, which can be given from Q_{av}/Q_{ag}, the density of PAz, polypyrrole and polyaniline are 4.7, 2.65, and 4.2g cm^{-3}. Therefore, the best capacity of PAz may be given by the high density film. However even in high density film, the capacity would not become higher without the film structure of possessing smooth anion diffusion process which may depend on the film preparation conditions.

In terms of oxidation/reduction potentials (*vs.* Li/Li^+) of these voltammograms, the potential is observed to be more positive in the order: polyazulene > polyaniline > polypyrrole. Therefore, a Li/PAz battery will show higher discharge voltage than Li/polyaniline or Li/polypyrrole batteries. However, as already stated in the introduction, electrochemically formed PAz film may show considerable variation in Q_a values and the kinetic behavior depends greatly on formation conditions. Thus, we will describe results on optimization of polymerizing factors in order to obtain suitable PAz for plastic battery material.

Table I. Comparison of film weights and CV results. The numbers in brackets correspond to the relative ratios

	w/M (units/cm^2)	Q_a (mC cm^{-2})	Q_{ag} (mC mg^{-1})	Q_{av} (C cm^{-3})
Polyazulene	1.35×10^{19} [10]	170	60	283
Polypyrrole	7.87×10^{18} [7]	80	75.5	200
Polyaniline	2.81×10^{18} [2]	112	266	112

Potential (E)-time (t) curves at electropolymerization.— Polyazulene films can be formed either potentiostatically or galvanostatically. Since electrochemically deposited PAz film has rather low electrical conductivity (10^{-3}S cm^{-2}), a potential-control electropolymerization needs an extremely long time to produce even very thin films. PAz films formed by this procedure showed poor reproducibility in their electrochemical properties. We, therefore, used a current-controlled method for preparation of PAz films. First of all, we attempted to determine the current density range of which highly electroactive PAz film is electropolymerized. During electropolymeri-

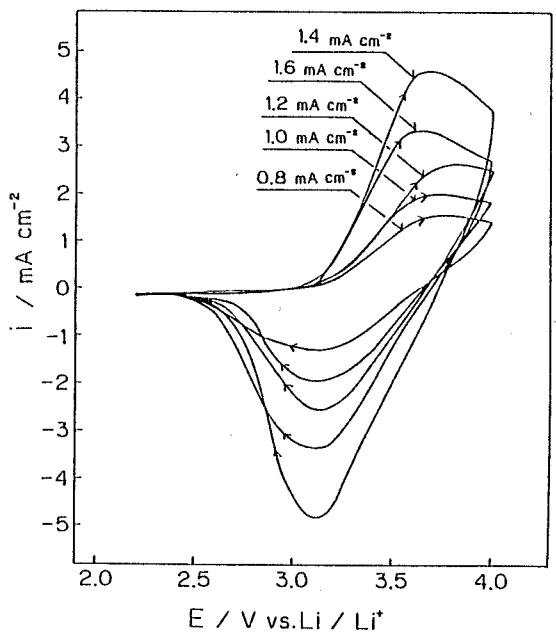

Fig. 3. Cyclic voltammograms for PAz electrode prepared at various current densities. Scan rate: 5 mV s^{-1}, film formation charge: 5C cm^{-2}.

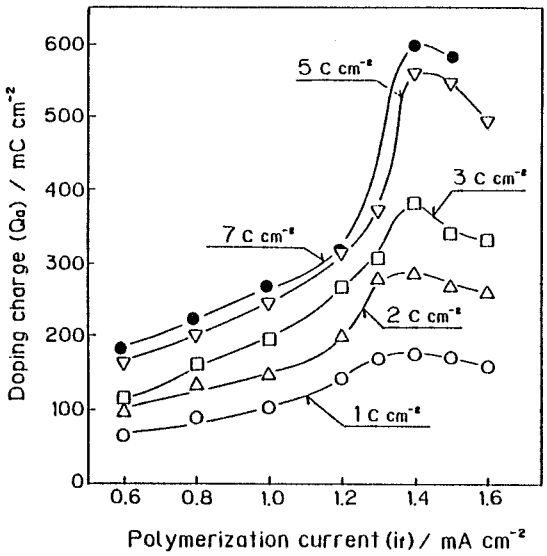

Fig. 4. Dependence of polymerization current density (i_f) on the doping charge (Q_a) of PAz electrodes at various formation charges.

zation at constant current, the potential of the PAz-coated Pt working electrode was monitored and plotted against time for various current density values (see Fig. 2). At high current density, the electrode potential shows an initial increase due to limitation by monomer diffusion toward electrode surface. After the first layer is deposited on Pt substrate, the potential remains constant, indicative of the steady-state polymerization of azulene on PAz-coated Pt electrodes. As the current density increases, the potential during electropolymerization increases. Nevertheless, over 1.6 mA cm^{-2}, the potential diverges because of limitations of the rate of monomer diffusion. Thus, polymerization cannot be performed at higher current density than this critical value. In PC solutions with monomer concentration of 0.05 mol dm^{-3}, PAz can be prepared only within the current density range from *ca.* 0.6 mA cm^{-2} (at which the electrode polarizes 3.6V: the onset potential for PAz polymerization) to 1.6 mA cm^{-2}.

Cyclic voltammetry and evaluation of charge-storing ability of PAz film.—Figure 3 shows typical cyclic voltammograms (CVs) for PAz film electrodes formed by passing 5C cm^{-2} at various current densities. Anodic and cathodic current peaks correspond to oxidation and reduction processes of doping and undoping of dopant anions into or out of the film, respectively. With an increase in polymerization current density, the CV response shows a steady increase and switching reversibility of the electrode process becomes more complete. However, at polymerization current higher than 1.4 mA cm^{-2}, *i.e.*, at 1.6 mA cm^{-2}, the current peak of the obtained cyclic voltammograms becomes smaller than that for the film formed at 1.4 mA cm^{-2}, indicating that the electrochemical activity of PAz formed at 1.6 mA cm^{-2} is degraded. As a reason for this behavior, the decomposition of PAz film and solvent is supposed to occur because an extraordinary high potential (*ca.* 4.5V *vs.* Li/Li$^+$) is observed at 1.6 mA cm^{-2}.

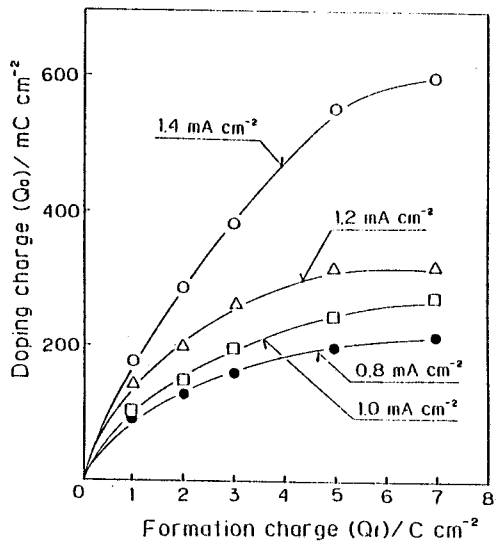

Fig. 5. Dependence of formation charge (Q_f) on the doping charge (Q_a) of PAz electrodes formed at various current densities.

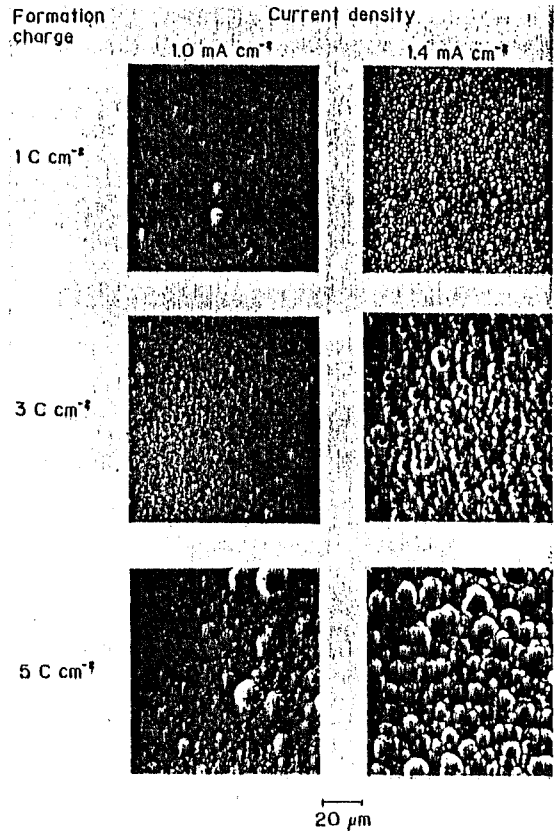

Fig. 6. SEM micrographs (top views) of PAz films polymerized under various conditions.

In order to clarify this effect, doping charge (Q_a) under anodic current curves in these cyclic voltammograms (at 5 mV s^{-1}) is plotted against polymerization current density (see Fig. 4). The data are shown for PAz films formed by passage of 1, 2, 3, 5, and 7C cm^{-2}. Independent of the deposition amount, all of the curves show maximum values at 1.4 mA cm^{-2}, which is well consistent with results obtained in Fig. 3. Up to current density of 1.4 mA cm^{-2}, the doping charge shows a gradual increase, indicating that the number of active sites increases. Over 1.4 mA cm^{-2}, PAz film may show oxidative decomposition, because of a very high potential, and therefore the degradation of the electroactivity is observed.

To optimize the electrochemical activity in regard to formation charge (Q_f), the data in Fig. 4 are plotted against Q_f (see Fig. 5). As Q_f increases, Q_a shows almost constant increase. However, over 5C cm^{-2}, Q_a values appear to level. There is an indication that charge-storing capability is not enhanced by forming PAz films by passing more than 5C cm^{-2}. The increasing rate (dQ_a/dQ_f) is largest at

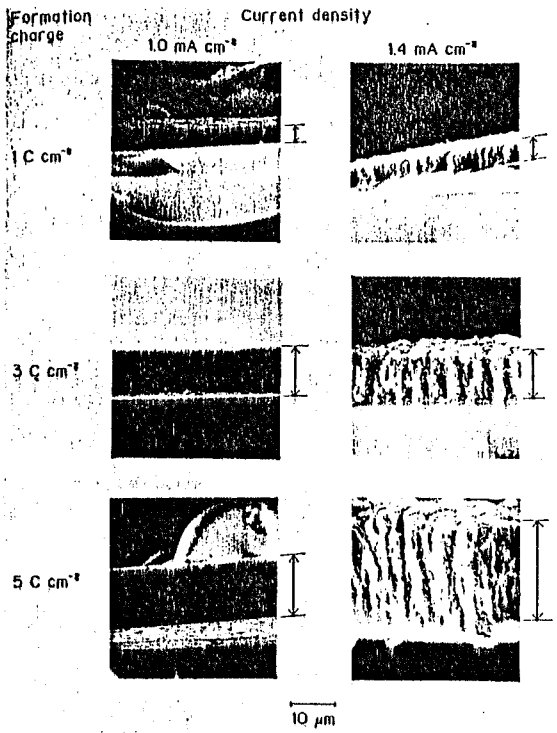

Fig. 7. SEM micrographs (cross-sectional views) of PAz films polymerized under various conditions.

1.4 mA cm $^{-2}$. Such dQ_s/dQ_f variation can be explained by considering differences in morphology. The most suitable PAz film for secondary battery material can be prepared at 1.4 mA cm $^{-2}$ by passage of 5C cm^{-2}.

Morphology of PAz films.—Variations of Q_s values of PAz films can be primarily determined by the morphology of resulting PAz films and the smoothness of dopant motion within PAz film within a certain time scale. Of particular interest here is how the surface and cross-sectional morphology related to the Q_s-Q_f dependence shown in Fig. 5. In Fig. 6, the top view of several PAz films formed at 1.0 and 1.4 mA cm^{-2} is shown as a function of Q_f (1, 3, 5C cm $^{-2}$). All of the films formed at 1.4 mA cm^{-2} appear to be rougher than those formed at 1.0 mA cm^{-2}. For the film prepared at 1.0 mA cm^{-2}, the surface morphology does not show noticeable change with an increase in the Q_f value. On the other hand, PAz films prepared at 1.4 mA cm^{-2} show remarkable change in their surface morphology, suggesting faster polymer growth than at 1.0 mA cm^{-2}.

The thickness of the same PAz films is roughly estimated from the cross-sectional view of SEM micrographs (see Fig. 7). As already expected from results in Fig. 4 and 5, these micrographs show that thicker or larger-volume PAz film has higher charge-storing capability. When polymerizing at 1.0 mA cm $^{-2}$, film thickness do not change very much for Q_f values above 3C cm^{-2}. On the other hand, cross sections of PAz films (1.4 mA cm^{-2}) show porous conditions and their thicknesses change almost proportionally with Q_f values up to 5C cm^{-2}. However, films polymerized beyond Q_f = 5C cm^{-2} show almost the same morphology and film thickness as those of 5C cm^{-2}. This fact indicates that a significant portion of the charge used to polymerize the material may be consumed in oxidative decomposition of films and/or solvent. From this, polymerization rates of 1.0 mA cm^{-2} and 1.4 mA cm^{-2} films are 0.28C cm^{-2}/μm (Q_f < 3C cm^{-2}) and 0.22C cm^{-2}/μm

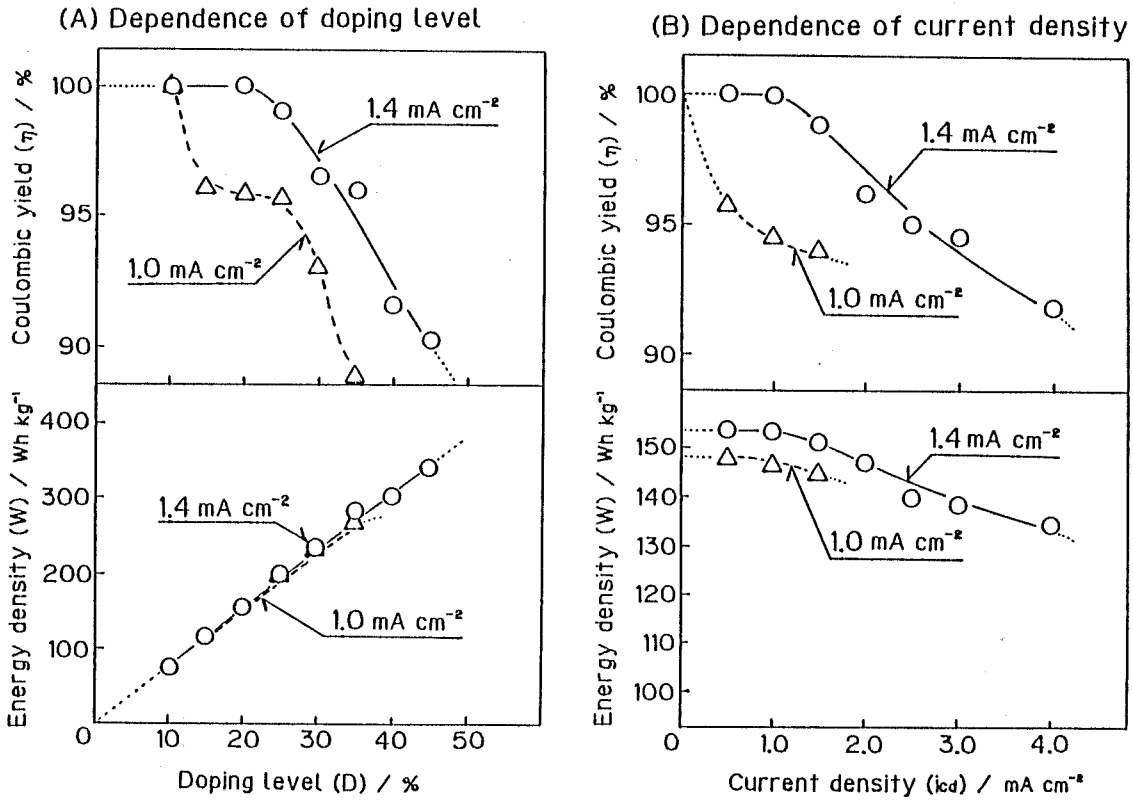

Fig. 8. Dependence of doping level (D) and current density (i_{cd}) on the charge-discharge characteristics of Li/LiClO$_4$/PAz (formed with 5C cm^{-2}) batteries as a function of the formation current density. The charge-discharge current was 0.5 mA cm^{-2} for (A). The cells were charged to a doping level of 20% for (B).

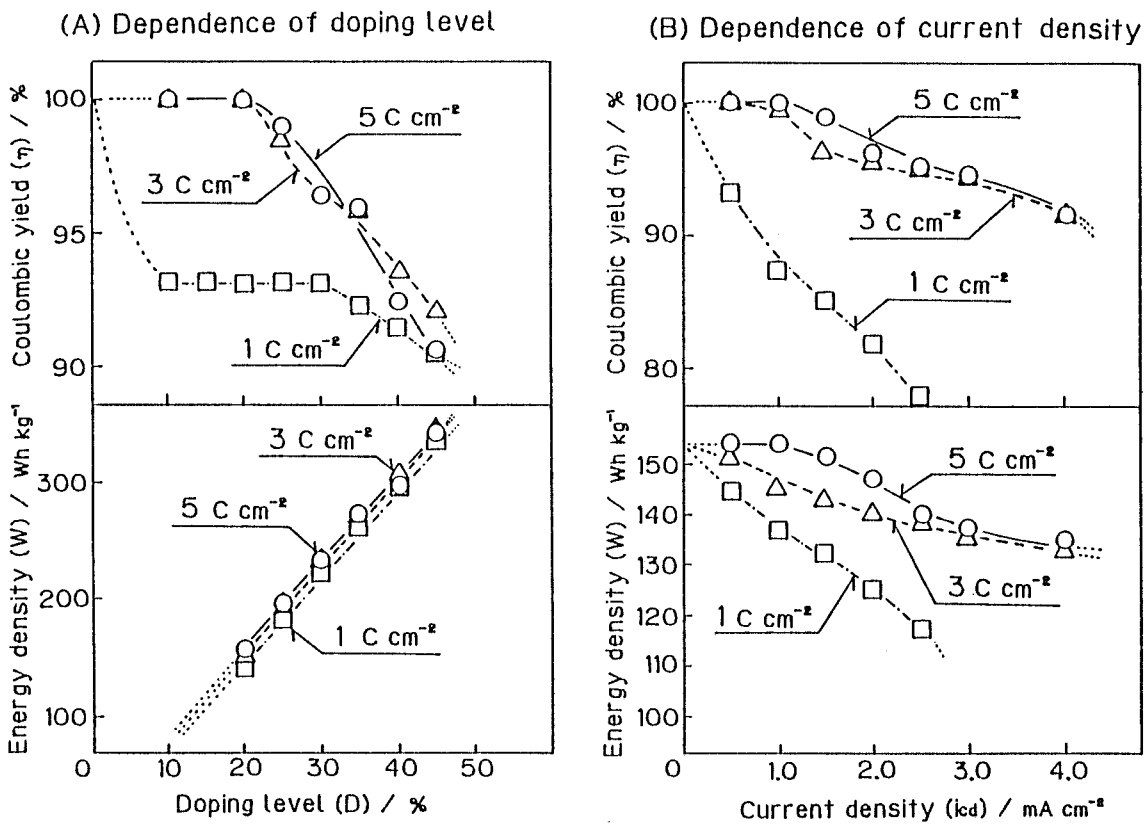

Fig. 9. Dependence of doping level (D) and current densities (i_{cd}) on the charge-discharge characteristics of Li/$LiClO_4$/PAz (formed at 1.4 mA cm^{-2}) batteries as a function of the formation charge of PAz films. The charge-discharge current was 0.5 mA cm^{-2} for (A). The cells were charged to a doping level of 20% for (B).

(Q_f < 5C cm^{-2}), respectively. The results are quite compatible with the behavior of the rise in doping charge with film thickness as shown in Fig. 5.

Charge-discharge performances of Li/$LiClO_4$/PAz battery.—The effect of electropolymerization current density on performance of a rechargeable Li/$LiClO_4$/PAz battery was investigated for the optimization of cathode material. PAz films formed at various current densities were assembled into cells with lithium anodes, and their charge-discharge performances were checked at various doping levels (D) and current densities (i_{cd}). Figure 8 shows results for 1.0 and 1.4 mA cm^{-2} formed PAz films. In Fig. 8(a), the dependence of the depth of charge (represented as doping level) on the coulombic yield (η) and energy density (W) are shown. The 20% doping level corresponds to charge of 440 mC cm^{-2} per unit weight of cathode material. As shown in Fig. 8, the battery using 1.4 mA cm^{-2} formed PAz cathode shows better performance than the battery using PAz film formed at 1.0 mA cm^{-2}. The battery (1.4 mA cm^{-2} PAz) keeps over 90% of the coulombic efficiency until D = 45%. In both cases, the energy densities show proportional rise against the doping level, indicating that PC solvents and PAz film itself do not decompose with deep charging. With respect to the dependence of i_{cd} on charge-discharge performance as indicated in Fig. 8(B), they are strongly dependent on the current dernsity at film preparation (i_f). Up to i_{cd} = 4 mA cm^{-2}, the Li/$LiClO_4$/PAz (1.4 mA cm^{-2}) keeps more than η = 90%. However, the battery using 1.0 mA cm^{-2}-formed PAz film cannot tolerate over i_{cd} = 1.5 mA cm^{-2}. It is commonly observed for those batteries that the energy density decreases with a rise in i_{cd} value. This fact means that some portion of the charging coulombs is consumed for the oxidative decomposition of PAz film and solvent because of an extraordinary high cell voltage owing to the anion diffusion's limitation within bulk polymer. Such drastic difference in charge-discharge performance is associated with the rougher morphology of PAz film formed at 1.4 mA cm^{-2}. Namely, the 1.4 mA cm^{-2}-formed PAz film has a large effective surface area and low packing density where dopant anions can move faster.

Performance of the Li/$LiClO_4$/PAz battery was then checked as a function of formation charge (Q_f) of PAz cathode as shown in Fig. 9. The properties were examined in the same way as in the previous figure. Although the battery using 1C cm^{-2} PAz performs very poorly, almost identical behavior is observed for batteries using PAz films formed by passage of 3 and 5C cm^{-2}. It appears that the Li/$LiClO_4$/PAz (5C cm^{-2}) battery shows the best performance. Therefore, PAz films formed at 1.4 mA cm^{-2} with 5C cm^{-2} can be the most effective material.

Charge-discharge curves for Li/$LiClO_4$/PAz (formed at 1.4 mA cm^{-2} with 5C cm^{-2}) are shown in Fig. 10. The discharge voltage is very high (*ca.* 3.2V) and flat. The highest voltage output is due to higher redox potential compared with polypyrrole and polyaniline. The flat output voltage can be explained as follows: since anion diffusion within bulk polymer is considered to be very fast as expected from rough morphology (see Fig. 7), the cell can maintain galvanostatic discharging without much polarization. At 45% doping level, the battery keeps over 90% of coulombic efficiency, and flat discharge curves. The current density dependence of battery performance also indicates that the battery can show high discharge voltage without losing the flatness in discharge curve. The cyclability of the same cell was checked at 0.5 mA cm^{-2} in Fig. 11. The battery keeps excellent charge-discharge characteristic up to 900 cycles. Energy density loss is negligible because coulombic yield is almost 100% until 900 cycles. PAz films are mechanically stable so that this material is tolerable for practical use.

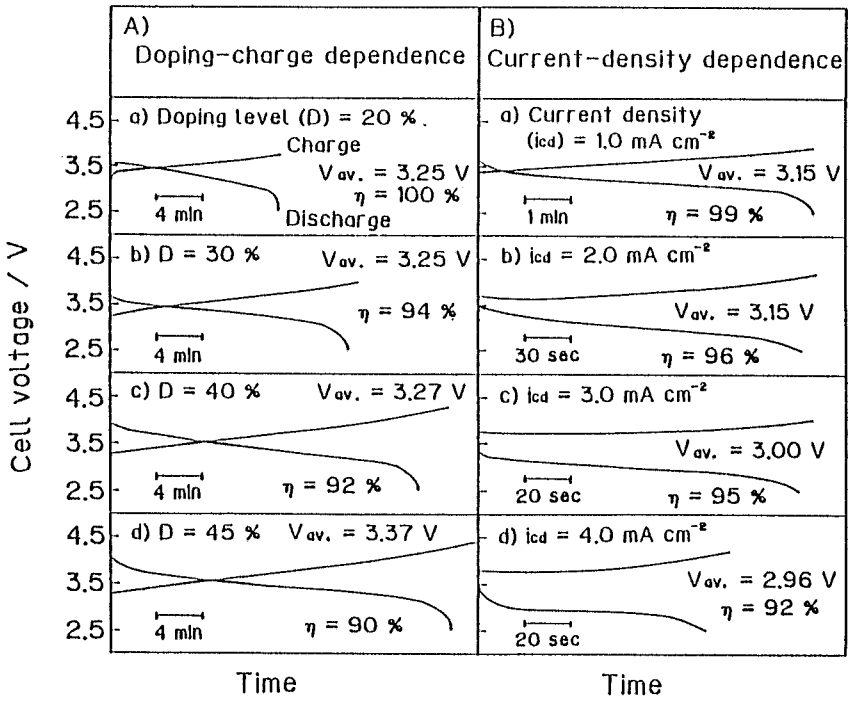

Fig. 10. Charge-discharge performances of Li/$LiClO_4$/PAz batteries. A) Doping-level (D) dependence at 0.5 mA cm^{-2}. B) Current-density (i_{cd}) dependence at the doping level of 20% (440 mC cm^{-2}). The PAz films were formed by passing 5C cm^{-2} at 1.4 mA cm^{-2}.

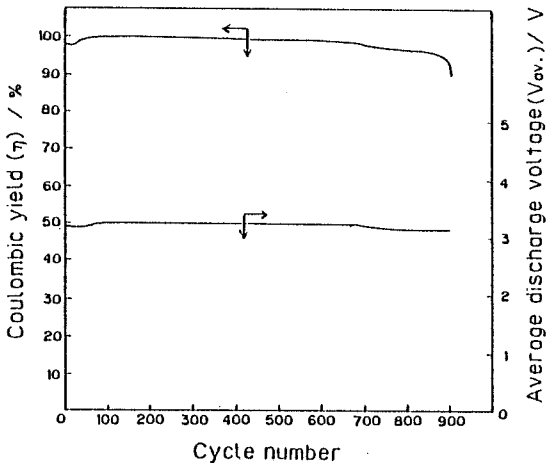

Fig. 11. Dependence of cycle number on coulombic yield (η) and average discharge voltage ($V_{av.}$) for Li/$LiClO_4$/PAz (formed at 1.4 mA cm^{-2} with 5C cm^{-2}) battery where the cell was charged up to 20% of doping level (440 mC cm^{-2}) at 0.5 mA cm^{-2}.

Conclusions

An electrochemically formed PAz film was found to be an excellent cathode material for plastic secondary batteries. The optimized polymer preparation conditions are 1.4 mA cm^{-2} (current density) and 5C cm^{-2} (formation charge) when films are prepared in (0.05 mol dm^{-3} azulene + 0.1 mol dm^{-3} $LiClO_4$)/PC solution. The charge-discharge performance is better than that for Li/polypyrrole batteries.

Acknowledgment

A part of this work was financially supported by a Grant for Scientific Research from the Ministry of Education of Japan.

Manuscript submitted March 28, 1988; revised manuscript received March 29, 1989.

Waseda University assisted in meeting the publication costs of this article.

REFERENCES

1. A. F. Diaz and J. A. Logan, *J. Electroanal. Chem.*, **111**, 111 (1980).
2. A. G. MacDiarmid, S-L. Mu, N. L. D. Somasiri, and W. Wu, *Mol. Cryst. Liq. Cryst.*, **121**, 187 (1985).
3. K. Abe, F. Goto, K. Okabayashi, T. Yoshida, and H. Morimoto, "The 27th Battery Symposium of Japan in Osaka," p. 201 (1986).
4. M. Ogawa, T. Fuse, T. Kita, T. Kawagoe, and T. Matsunaga, *ibid.*, p. 197 (1986).
5. A. Kitani, M. Kaya, and K. Sasaki, *This Journal*, **133**, 1069 (1986).
6. G. C. Farrington, B. Scrosati, D. Frydrych, and J. DeNuzzio, *ibid.*, **131**, 7 (1984).
7. E. M. Genies and C. Tsintavis, *J. Electroanal. Chem.*, **195**, 109 (1986).
8. S. H. Glarum and J. H. Marshall, *This Journal*, **134**, 142 (1987).
9. H. Sakai, K. Naoi, T. Hirabayashi, and T. Osaka, *Denki Kagaku*, **54**, 516 (1986).
10. A. F. Diaz, J. L. Castillo, J. A. Logan, and W. Y. Lee, *J. Electroanal. Chem.*, **129**, 115 (1981).
11. E. M. Genies and J. M. Pernaut, *J. Electroanal. Chem.*, **191**, 111 (1985).
12. A. Mohammadi, O. Inganaes, and I. Lundstroem, *This Journal*, **133**, 947 (1986).
13. H. Sakai, K. Naoi, T. Hirabayashi, and T. Osaka, *Denki Kagaku*, **54**, 75 (1986); T. Osaka, K. Naoi, and H. Sakai, and S. Ogano, *This Journal*, **134**, 285 (1987).
14. T. Osaka, K. Naoi, S. Ogano, and S. Nakamura, *Chem. Lett.*, 1986, 1687; T. Osaka, K. Naoi, S. Ogano, and S. Nakamura, *This Journal*, **134**, 2096 (1987).
15. J. Bargon, S. Mohmand, and R. J. Waltman, *Mol. Cryst. Liq. Cryst.*, **93**, 279 (1983).
16. R. J. Waltman, A. F. Diaz, and J. Bargon, *This Journal*, **131**, 1452 (1984).
17. G. Tourillon and F. Garnier, *J. Electroanal. Chem.*, **135**, 173 (1982).
18. T. Osaka, K. Naoi, and T. Hirabayashi, *This Journal*, **134**, 2645 (1987).
19. R. Burzynski, P. N. Presad, S. Bruckenstein, and J. W. Sharkey, *Synth. Met.*, **11**, 293 (1985).

Proc. of Sym. on Matl. and Processes for Lithium Batteries, Electrochem. Soc., 89-4, 269(1989)

LITHIUM SECONDARY BATTERIES: ROLE OF POLYMER CATHODE MORPHOLOGY

Katsuhiko Naoi and Boone B. Owens
Corrosion Research Center,
Department of Chemical Engineering and Materials Science, University of Minnesota,
221 Church St SE, Minneapolis, MN 55455, U.S.A.

Michiko Maeda and Tetsuya Osaka
Department of Applied Chemistry, School of Science and Engineering,
Waseda University, 3-4-1 Okubo, Shinjuku, Tokyo 160, JAPAN

ABSTRACT

Electrically conducting polymers have been utilized both as the cathode and as the electrolyte element of lithium secondary cells. Polymer cathodes were limited in their suitability for batteries because of the low energy content associated with low levels of doping and the inclusion of complex ionic species in the cathode. Recent studies have indicated that doping levels up to 100% can be achieved in polyaniline. High doping levels in combination with controlled morphologies have been found to improve the energy and rate capabilities of polymer cathodes. A morphology-modifying technique was utilized to enhance the charge/discharge characteristics of Li/liquid electrolyte/Polypyrrole cells. The polymer is electropolymerized in a preferred orientation morphology when the substrate is first precoated with an insulating film of nitrile butadiene rubber (NBR). Modification of the kinetic behavior of the electrode results from variations in the chemical composition of the NBR.

Heterocyclic conducting polymers such as polypyrrole[1-9] and polyaniline[10-12] are recognized as electroactive materials, which show redox process accompanied by concurrent doing-undoping ions in electrolyte solution. For this reason, these materials can potentially be utilized in rechargeable plastic batteries.[13-14]

Promising cathode materials for rechargeable lithium electrochemical cells include solid intercalation compounds such as metal oxides or sulfides and electroactive polymer cathode materials such as polyaniline or polypyrrole(PPy). The theoretical values for the specific energy of the electrode couples may be calculated for these two classes of cathodes; the solid oxide type cathodes exhibit theoretical specific energies in the range of 300-1000 Wh kg^{-1}, compared to values of about 200-400 Wh kg^{-1} for the polymeric cathode materials. Lithium/polymer cathode cells have intrinsically lower values for specific energy because of the low doping level of the polymer films and the requirement of ionic doping associated with the faradaic reaction. Further, slow ion diffusion within the bulk of the polymer films results in limitations on the rate behavior of such cell systems. Since the oxidation and reduction of a PPy film induces a concurrent doping-undoping of anions, the charge-discharge property of a Li/PPy battery is determined by

this process. In order to enhance the battery performance characteristics of a Li/PPy cell, the PPy cathode must have a high charge-storing ability(electroactivity) and rough morphology in which a large amount of anions can dope/undope smoothly to maintain the charge/discharge rate of the cells.

Recent studies on electropolymerized PPy films have revealed that the electropolymerization factors, *viz.*, electrolyte anion, potential, current and formation charge, play important roles in determining the electrochemical property and morphology of the resulting films.[12-14] In particular, the rate of anion diffusion across a PPy film was found to be strongly dependent on the morphology or packing density of the grown PPy films.[14,15] A remarkable enhancement of anion diffusivity has been observed at a controlled morphology PPy film formed with a guide of pre-coated insulating material, *e.g.*, NBR(nitrile butadiene rubber) film.[14] The preparation procedure for such a PPy film is illustrated in Fig.1.[11,14] First, the NBR film is coated on Pt substrate. Second, it is immersed in an acetonitrile solution containing pyrrole monomer and electrolyte and the PPy is grown by electropolymerization. Finally, after the PPy is electropolymerized along the etched tubular channels, the pre-coated NBR layer is totally rinsed away by an organic solvent(MEK). By virtue of the flexible and insulating nature of the NBR film, it can modify the morphology of the PPy film, especially in the perpendicular direction, where the pre-coated NBR film acts as a structure-modifying material, regulating the polymer growth in the direction normal to the Pt substrate.

It is noteworthy that the PPy film prepared by such a method satisfies the optimum conditions for an effective battery material. In fact, the lithium battery assembled with an NBR/PPy cathode tolerates a larger current density than the battery using a normal PPy cathode which is formed on a Pt substrate.[15] Therefore, it is interesting to further investigate the ionic transport at the NBR/PPy film as a basic approach of high energy plastic battery research. Of particular interest is to control the degree of morphology orientation and to accelerate the rate of anion doping-undoping process at polymer cathode. The authors attempted to control the orientation of PPy morphology by varying the chemical composition of NBR and its thickness. In this paper, it is described how the morphology of the PPy film is modified under various polymerization conditions, and how the anion diffusion behavior at the PPy film is related to the resultant morphology.

EXPERIMENTAL

Chemicals and Solutions

Reagent grade acetonitrile was used as obtained, without further purification. Acetonitrile solutions containing 0.2 mol dm^{-3} pyrrole monomer and 0.2 mol dm^{-3} electrolyte salts were used for the preparation of the polypyrrole(PPy) film. Electrochemical analysis was made in the acetonitrile solution containing 1.0 mol dm^{-3} of various electrolytes. Purified propylene carbonate(PC) containing 1.0 mol dm-3 LiClO4 was used as the electrolyte solution for the charge-discharge measurement. The morphology modified PPy films were grown utilizing various kinds of NBR films(Nippon Zeon Co., Ltd.).

Film Preparation

Conducting PPy films used in this work were prepared by the potentiostatic electro-oxidation method. The normal PPy films were grown directly on the Pt substrate at 0.8 V *vs.* Ag/Ag^+(0.01 mol dm^{-3} $AgNO_3$) by passing 1 C cm^{-2} of charge. For the preparation of NBR-modified morphology PPy film(NBR/PPy), the film was also grown at 0.8 V constant potential, following the procedures described previously.[14,15]

Cell Assembly and Measurements

The cell for the electrochemical measurements was assembled with a PPy-coated Pt working electrode, a stainless steel-plate(large surface area) counter electrode and an Ag/Ag^+ reference electrode. Cyclic voltammograms were obtained for a normal PPy and NBR/PPy electrodes formed with various types of NBR films. The separation potential of anodic and cathodic charges under the anodic curves was recorded at a quasi-stationary scan rate of 5 mv s^{-1}. The electrode impedance was measured at some doping potentials in the frequency ranges 10 mHz to 100 kHz by the FFT impedance method.[15] The surface and the cross-sectional morphologies of the NBR(5 μm in thickness)/PPy films formed by the passage of 10 C cm^{-2} were inspected with the scanning electron microscope (SEM).

RESULTS AND DISCUSSION

Model for PPy -Growth through NBR Film

To consider how an oriented morphology of PPy is constructed, a simple growth model for NBR/PPy film is illustrated in Fig. 2 in comparison with a cross-sectional SEM micrograph of a typical NBR/PPy film. These correspond to the initial stage of the PPy growth through the etched tubular channels formed in the vicinity of Pt/NBR interface. Two main factors affecting the construction of perpendicular PPy morphology are suggested here, *viz.*, (1) tubular channel formation by solvent etching, and (2) polymer growth by electropolymerization. Immediately after an NBR/Pt electrode is immersed in the acetonitrile solution of ($LiClO_4$ + pyrrole), the solution begins to etch fine tubular channels in the NBR film to establish the conduction paths from the solution to the substrate. As soon as the path reaches the surface of the substrate, PPy film begins to grow along these channels. The degree of morphology orientation and the diameters of fibrils can be determined by the relative balance of the rates of polymer growth and pore-etching(tubular channel formation). The rate of polymer growth is related to the potential, chemical stability and nucleophilicity of co-existing anions at electropolymerization. The potential for electropolymerization was fixed at 0.8 V in this work, and the polymerization anions used were ClO_4^-. Therefore, the growth rate of PPy was fixed in this study. On the other hand, the rate of pore etching and the dimension of the pores were related mainly to the solubility of NBR in the acetonitrile solvent and the thickness of the NBR film.

Effect of Acrylonitrile content in NBR on Electrochemical Behavior of NBR/PPy Film

In order to see how the solubility and/or flexibility of the NBR film affected the

morphology and electrochemistry of the resulting NBR/PPy films, electrochemical properties of these films were investigated. Figure 3 shows a typical effect of the acrylonitrile(AN) content in the NBR film on the cyclic voltammograms for the NBR/PPy(1 C cm^{-2}) films measured in 1.0 mol dm^{-3} $LiClO_4$. The values of m and n shown in the upper part of this figure correspond to the composition of butadiene and AN in NBR, respectively. As the AN content ($\frac{n}{m+n}$) of NBR decreases, the potential separation of anodic and cathodic current peaks becomes narrower. This indicates that the redox process in the NBR/PPy film becomes more reversible as the NBR film becomes more soluble and/or flexible. Therefore, the ion transport behavior NBR/PPy film was further investigated by varying the scan rate of the cyclic voltammetry.

Figure 4 shows the dependence of the AN content on the rate-determining stage of the electrode process at NBR/PPy films. From the cyclic voltammograms at different scan rates, anodic peak currents(i_{pa}) are proportional to x powers of scan rate(v), while x changes from 0.5 to 1.0 satisfying the following equation.

$$i_{pa} \propto v^x \quad (0.5 < x < 1.0) \qquad [1]$$

$x=0.5$; $i_{pa} \propto \sqrt{v}$ (diffusion controlled process)

$x=1.0$; $i_{pa} \propto v$ (reaction controlled process)

The x value for all curves increased up to NBR=5 μm, and saturated above this point. As the NBR becomes thicker, the over-all electrode process becomes much more limited by the charge-transfer process at electroactive sites in the NBR/PPy film. The behavior would be associated with an enhancement of anion diffusion within PPy layer. However, the acceleration of diffusion rate seems to reach a certain limiting value at 5 μm in thickness, and further thickening of NBR film does not cause any change.[14] Therefore, for the amount of PPy (1 C cm^{-2} formation charge), more than 5 μm-thick insulating layer makes the most optimum oriented structure PPy morphology. In order to further investigate how the doping-undoping kinetics change as a function of pre-coated NBR thickness, the NBR/PPy films were analyzed by FFT impedance spectroscopy.

Impedance results for NBR(AN=22%)/PPy(1 C cm^{-2})-ClO_4^- are indicated as Cole-Cole plots in Fig.5. In general, the absolute value of electrode impedance(|Z|) for NBR/PPy films decreases with increasing NBR thickness. This fact indicates that the redox reaction at NBR/PPy electrodes is enhanced by the acceleration of either charge injection or ion transport in and out of the active sites of PPy regime. Impedance behavior at low frequencies indicates that the rate-determining stage of the redox reaction changes from diffusion-controlled to charge-transfer-controlled by thickening the NBR film. This means the diffusion rate of ions within the PPy film is considerably accelerated with the modified morphology. The impedance spectra for NBR(5 μm)/PPy and NBR(8 μm)/PPy films appear essentially the same. This observation is consistent with the deductions from the scan rate dependence of cyclic voltammograms, suggesting that the electrode process does not change any more by further thickening.

The time scale relevant to the anion diffusion within NBR(5 μm)/PPy films is demonstrated as a function of AN content in NBR film. Figure 6 shows the Bode plots for various NBR/PPy films. The frequency range corresponding to the mass transfer

(indicated by the slope of 0.5) shows noticeable change upon varying the AN content. As the AN content increases, the corresponding frequency value at which the line of 0.5 gradient starts becomes lower. This fact again supports the evidence for the enhancement of the diffusivity of dopants within NBR/PPy film. The morphology guest polymer, *viz.*, PPy grows in the more perpendicular orientation to form a much more open structure, as the AN content becomes less.

Morphology of NBR/PPy Films

Surface and cross-sectional morphology of various kinds of NBR/PPy films was inspected by SEM (see Fig.7). When PPy is formed with a guide of NBR of higher AN content, the surface condition of remaining PPy film becomes grainy. On the other hand, for the film formed with NBR of lower AN content, the surface shows much rougher and more open structure. With respect to the side views of these micrographs, the manner of morphology orientation or the apparent thickness of these films are much clearly demonstrated. As the AN content becomes less, the polymer growth become faster, especially in the perpendicular orientation because the attraction force between the molecules of NBR is weak. This results in more bulky structure which tolerates high-rate charging and possibly leads to a high power density when such films are used as a cathode material for rechargeable cells.

Charge-Discharge Performance of Li/$LiClO_4$(PC)/(NBR/PPy)

NBR/PPy films were utilized as the cathode of a lithium cell with a liquid organic solvent, and the charge-discharge characteristics were observed. Figure 8 shows typical charge-discharge curves for Li/$LiClO_4$(PC)/[NBR(5 μm)/PPy(3 C cm^{-2})] cell. As was expected, the discharge recovery becomes better for NBR/PPy cathode formed with the lower AN-content NBR film.

Figure 9 shows the relationship between coulombic efficiency and the current density for these same cells. There is a clear indication that an NBR/PPy cathode formed with less AN-content NBR tolerates high current density. A Li/(NBR(AN=18%)/PPy) cell maintains as much as 80% coulombic efficiency when charging-discharging at 1.0 mA cm^{-2}.

Figure 10 shows the maximum power density for Pt/NBR films, estimated from the cyclic voltammograms in Fig.3. As the AN content in NBR decreases, the maximum power density increases. Especially, a big jump of maximum power density is observed at around AN=20%, and the value amounts to *ca.* 80 kW kg^{-1} at AN=18%. Therefore, an enhancement of ionic motion directly leads to make the power density bigger.

CONCLUSION

An enhancement of anion diffusivity was observed with modified-morphology polypyrrole films using a pre-coated insulating template(NBR). The electrochemical properties of such films could be interpreted on the basis of ion transport within the polymer layer with cyclic voltammetry, AC impedance, and SEM by varying the AN content in the NBR modified polymer. As the pre-coated NBR becomes thicker(up to 5

μm), the dopant movement within NBR/PPy film becomes faster. Also, as the AN content in the NBR decreases, the electrode process, especially the diffusion rate, becomes higher. This fact is supported by both the impedance measurements and the morphology observed with SEM. As the AN content of NBR becomes smaller, the NBR film becomes more soluble and flexible, so that the growth of polypyrrole is considered to be much perpendicularly-oriented to form much open and bulky structure. Such special morphology results in an acceleration of the diffusion rate of dopants within the grown NBR/PPy film and also increases the power density.

Further improvement in kinetic behavior of polymer cathodes should result from continuing investigations of these phenomena.

ACKNOWLEDGMENT

This work was financially supported in part by the Grant-in-Aid for Scientific Research from the Japanese Ministry of Education and also in part by the Defense Advanced Research Projects Agency and the Office of Naval Research.

References

1 A. F. Diaz and K. K. Kanazawa, *J.C.S. Chem. Commum.*, **1979**, 635 (1979).
2 A. F. Diaz and J. I. Castillo, *J.C.S. Chem. Commum.*, **1980**, 397 (1980).
3 A. F. Diaz and J. A. Logan, *J. Electroanal. Chem.*, **111**, 111(1980).
4 A. F. Diaz, J. M. V. Vallejo and A. M. Duran, *IBM J. Res. Dev.*, **25**, 42 (1981).
5 A. F. Diaz, J. I. Castillo, J. A. Logan and W. Y. Lee, *J.Electroanal. Chem.*, **129**, 115 (1981).
6 N. Mermilloid, J. Tanguy and F. Petiot, *J.Electrochem.Soc.*, **133**, 1073 (1986).
7 K. Abe, F. Goto, K. Okabayashi, T. Yoshida and M. Morimoto, Proceedings of 27th Battery Symposium in Japan, P. 201 (1986).
8 O. Niwa and T. Tamura, *J. C. S. Chem. Commum.*, **1984**, 817.
9 K. Naoi, H. Sakai, S. Ogano and T. Osaka, *J, Pow. Sourc.*, **20**, 237 (1987); T. Osaka, K. Naoi and S. Ogano, *J.Electrochem.Soc.*, in press.
10 A. Kitani, M. Kaya and K. Sasaki, *J. Electrochem. Soc.*, **133**, 1069 (1986).
11 H. Sakai, K. Naoi, T. Hirabayashi and T. Osaka, *Denki Kagaku*, **54**, 75 (1985); T. Osaka, S. Ogano and K. Naoi, *J.Electrochem.Soc.*,in press.
12 T. Osaka, K. Naoi, S. Ogano and S. Nakamura, *Chem. Lett.*, **1986**, 1687 (1986); T. Osaka, K. Naoi, S. Ogano and S. Nakamura, *J.Electrochem.Soc.*, **134**, 2096 (1987).
13 K. Naoi and T. Osaka, *Denki Kagaku*, **54**, 808 (1987); K. Naoi and T. Osaka, *J. Electrochem.Soc.*, **134**, 2479 (1987).
14 K. Naoi, A. Ishijima and T. Osaka, *J. Electroanal. Chem.*, **217**, 203 (1987); T. Osaka and K. Naoi, *Shokubai (Catalyst)* **29**, 130 (1987).
15 T. Osaka and K. Naoi, *Bull. Chem. Soc. Jpn.*, **55**, 36 (1982).

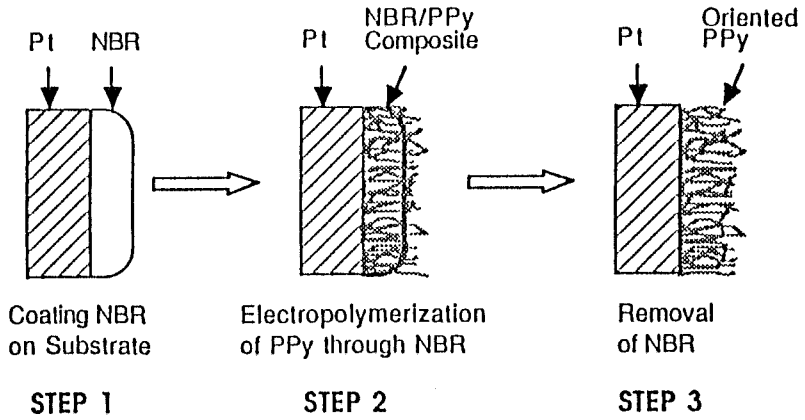

Fig.1 Preparation procedure of NBR/PPy(NBR-guided grown PPy) film.

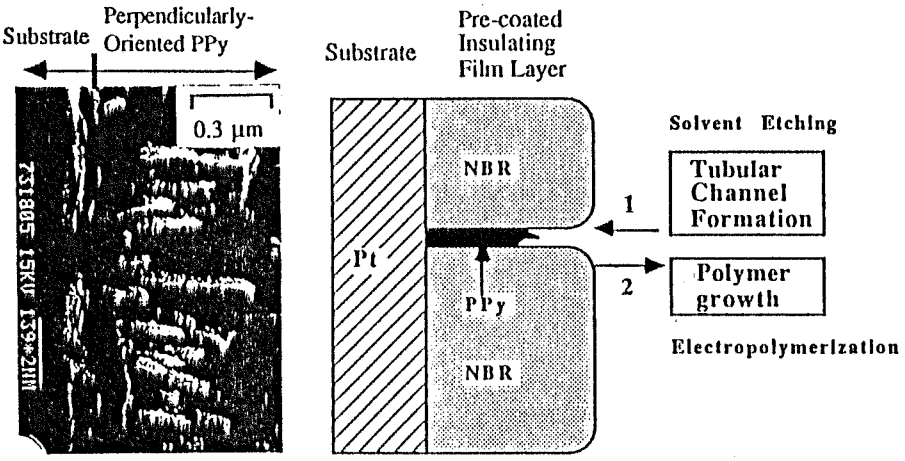

Fig.2 Cross-sectional SEM micrographs of typical NBR/PPy-BF_4^- film and schematic model of the tubular channel formation and PPy growth through them.

NBR

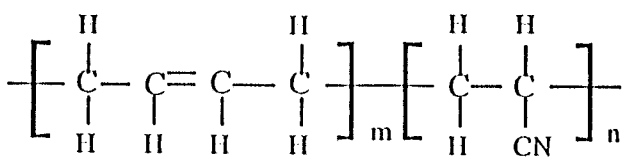

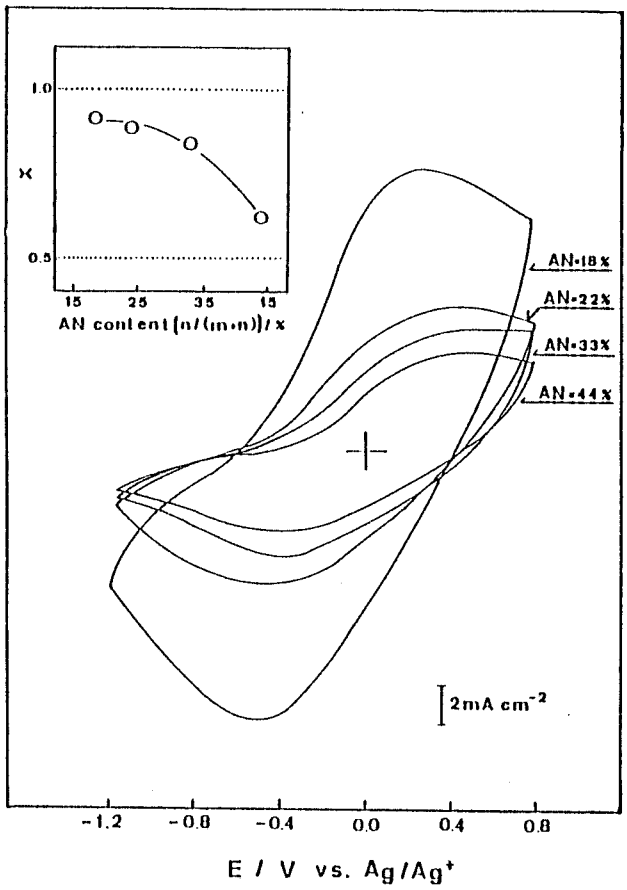

Fig. 3 Typical cyclic voltammograms for NBR/PPy(1 C cm^{-2}) film electrodes in 1.0 mol dm^{-3} $LiClO_4$ at 50 mv s^{-1}, where the thickness of pre-coated NBR film is varied in the range 0.0 to 11.3 μm.

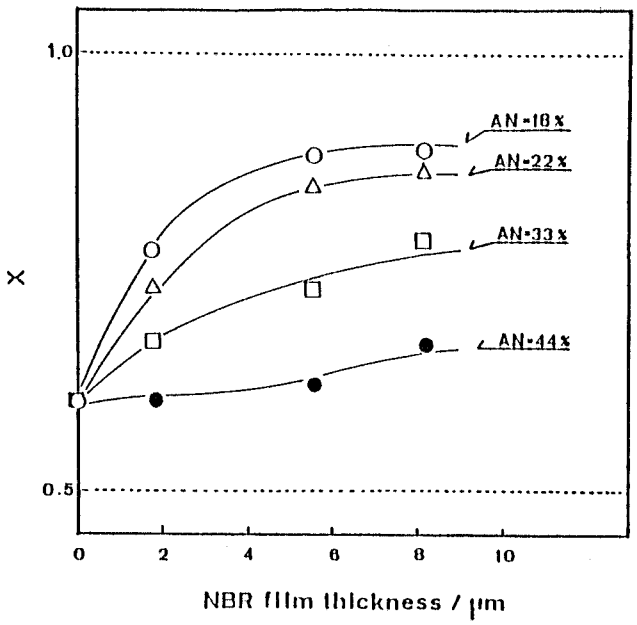

Fig.4 Variation of rate-determining stage for NBR(AN=18-44%)/PPy(1 C cm^{-2}) film electrodes upon changing the thickness and acrylonitrile content in NBR.

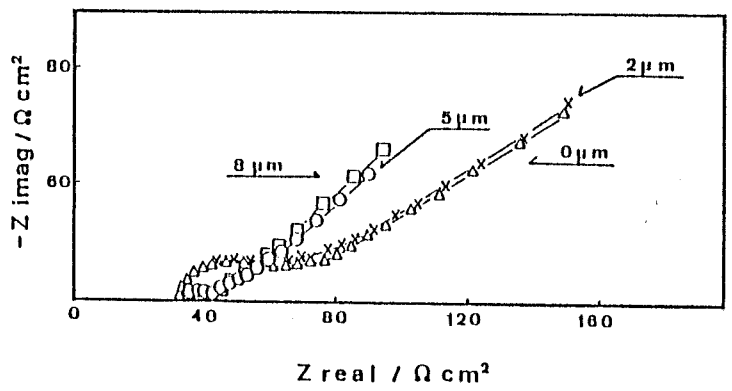

Fig.5 Cole-Cole plots for NBR(0-8 μm)/PPy(1 C cm^{-2}) films.

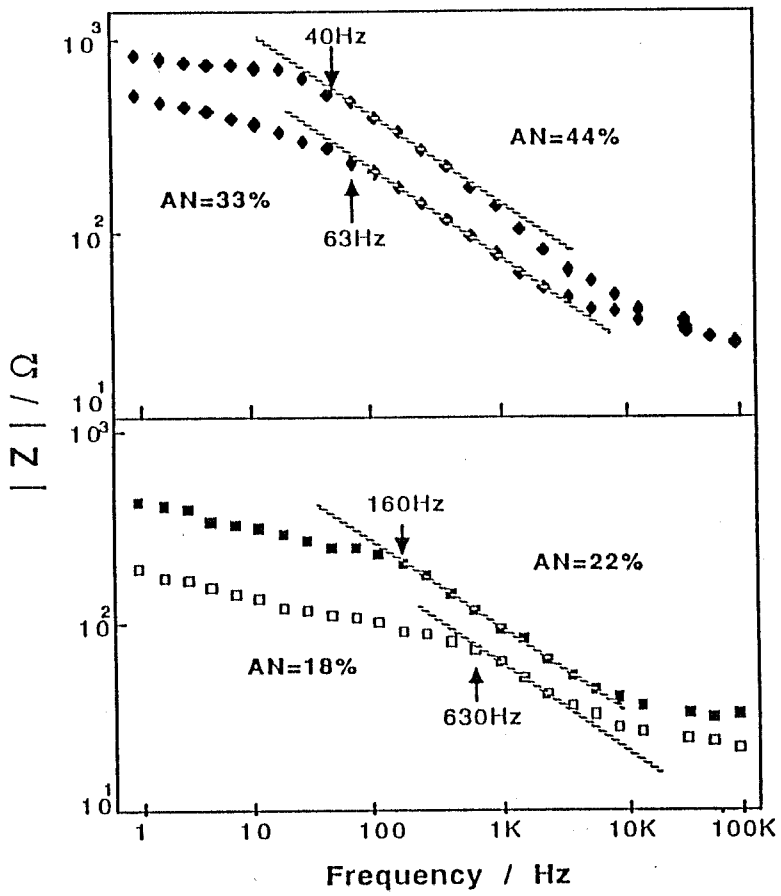

Fig.6 Effects of acrylonitrile content in NBR on the Warburg frequency region in Bode plots for NBR(5 μm)/PPy(1 C cm^{-2}) film.

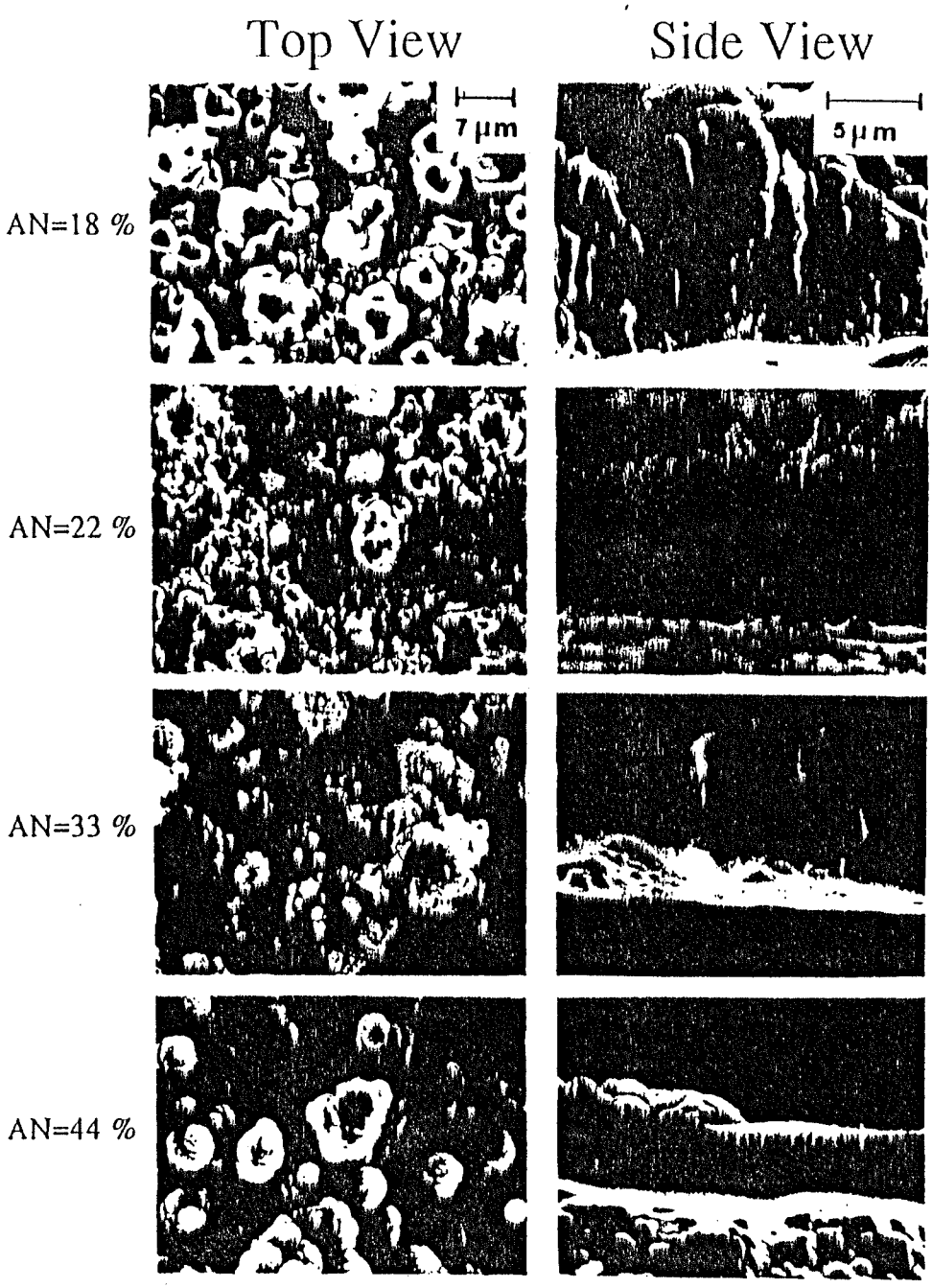

Fig.7 SEM micrographs of NBR(5 μm)/PPy (10 C cm^{-2}) films formed with various kind of NBR films.

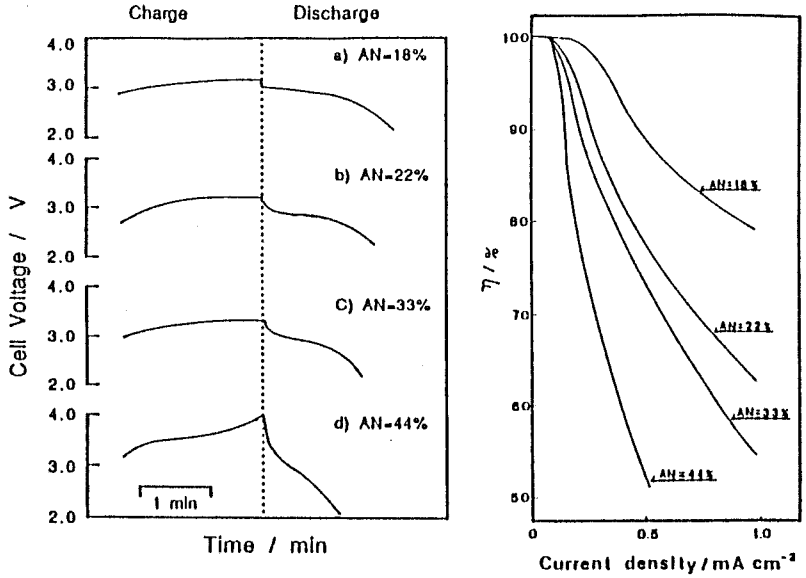

Fig.8 (Left) Charge-discharge curves for Li/$LiClO_4$/(NBR(5 μm)/PPy(5 C cm^{-2}) cells. The cells were charged to 60 mC cm^{-2} at 0.5 mA cm^{-2}.
Fig.9 (Right) Current-density dependence of coulombic efficiency for the above.

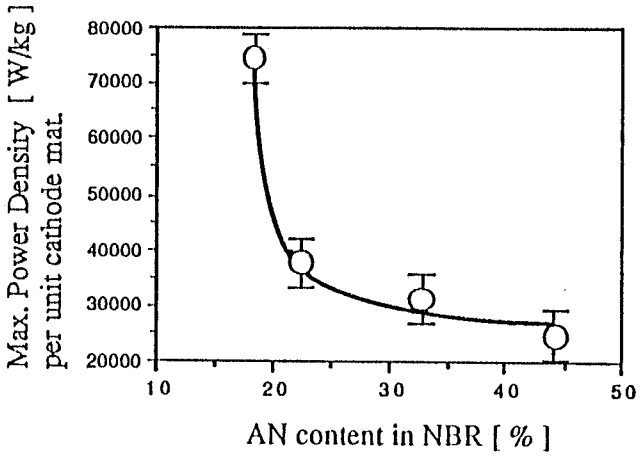

Fig.10 Maximum power density per unit cathode material for Li/$LiClO_4$(PC)/PPy cell.

Subject index

Reprinted from JOURNAL OF THE ELECTROCHEMICAL SOCIETY
Vol. 137, No. 2, February 1990
Printed in U.S.A.

Impedance Analysis of Ionic Transport in Polypyrrole-Polyazulene Copolymer and Its Charge-Discharge Characteristics

Katsuhiko Naoi,*,[1] Ken-ichi Ueyama, and Tetsuya Osaka*

Department of Applied Chemistry, School of Science and Engineering, Waseda University, 3-4-1 Okubo, Shinjuku, Tokyo 160, Japan

William H. Smyrl*

Department of Chemical Engineering and Materials Science, University of Minnesota, Minneapolis, Minnesota 55455

ABSTRACT

Ionic transport behavior across an electropolymerized polypyrrole/polyazulene composite film was investigated by using ac impedance analysis, and its charge-discharge characteristics were also studied. Co-electropolymerization of pyrrole and azulene was well defined and fairly stoichiometric in propylene carbonate solution. The charge capacity for the composite films showed a remarkable increase for films with about 50 to 75% of azulene monomer content, and the behavior was correlated with morphological and diffusivity changes. The charge-discharge characteristics were examined for cells with a lithium anode and various polypyrrole/polyazulene composite cathodes. Pure polypyrrole cathodes behaved exactly like a capacitor at low frequency, while pure polyazulene cathodes showed excellent rechargeable behavior with very flat discharge curves. Composite cathodes showed intermediate behavior.

Electropolymerization has been gathering growing interest recently, as an elegant new way of preparing conducting polymer films, *e.g.*, polyaniline (1-7) and polypyrrole (PPy) (8-14). The process is fairly stoichiometric and simple without using the strong oxidizing agents like halogens or AsF_5 that are used in conventional chemical processes. With the electrochemical technique, various qualities of polymeric films can be prepared by simple electro-oxidation of monomers with varied polymerization factors. The factors include, for example, kind of monomer, electrolysis mode [controlled potential (11) and controlled current (3, 11)], electrolyte anion (11, 12), and passed charge (thickness) (12). By choosing appropriate conditions for these factors, we can deliberately design the structure/morphology and electrochemical redox properties of resulting films so as to tailor them to specific applications, such as energy storage or microelectronics.

The electropolymerization method is also a powerful means to prepare random copolymerized or composite polymers by mixing different kinds of monomers in the starting polymerization solution. In general, co-electropolymerization of different monomers gives amorphous films with little interaction among monomers (16). The resulting film is then a polymer composite in the sense of its elemental composition. However, in some cases, it shows noticeable changes in morphology compared to the individual pure polymers. The morphological changes result in changes (acceleration/retardation) in ionic transport behavior across the film. The ionic transport behavior is especially important for controlling the rate capability of energy storage devices (12).

Among conducting polymers, polypyrrole-based composite films are the most extensively studied. Co-polymerization of pyrrole has been reported with other kinds of monomers such as thiophene (15), azulene (16), and N-substituted pyrrole with methyl (17-19) or phenyl groups (19, 20). One of the best examples is the co-polymerization of pyrrole and azulene, which shows fairly stoichiometric and reproducible polymerization behavior. Since pyrrole and azulene show similar electro-reactivity (oxidation potentials) and polymerization scheme (α-α' linkage at 5-membered rings, (21-24), they mix with each other fairly well during electro-polymerization to form a uniform composite film. Electropolymerized polyazulene (PAz) shows moderately high conductivities (10^{-2}-10^{0} Ω^{-1} cm^{-1}) (21) in the dry state, and a bulky morphology that depends greatly on the kind of coexisting anion (23). Also, PAz film is an effective cathode material in lithium cells because it has a high redox potential and high switching reversibility (22, 24).

The combination of PPy and PAz is a kind of composite of bulky (azulene) and less bulky (pyrrole) monomers. The insertion of the bulky azulene group into a PPy matrix causes the PPy/PAz composite film to look much rougher than PPy itself, and to show various packing structures that depend on the pyrrole/azulene monomer ratio in the film. This kind of rough film is specifically suitable for application as an energy-storage material like a redox capacitor (28), or rechargeable battery, which can tolerate high-rate charging/discharging.

So far, PPy/PAz film has received only limited attention except for structural analysis by IR spectroscopy (16). The authors have investigated the ionic transport phenomena across the PPy/PAz composite film using the same techniques that have been used earlier for polyvinylferrocene (PVF) (27), i.e., by cyclic voltammetry and ac impedance spectroscopy (25-27). The emphasis of the present paper is to report the variations in redox capacity and diffusivity of anions for different PPy/PAz composite films, and how these properties are related to the morphology observed by scanning electron microscopy (SEM).

Experimental

Chemicals and solutions.—Reagent grade $LiClO_4$ and propylene carbonate (PC) were used as the electrolyte salt

* Electrochemical Society Active Member.
[1] Present address: Corrosion Research Center, Department of Chemical Engineering and Materials Science, University of Minnesota, Minneapolis, MN 55455.

and solvent, respectively. PC was used after purification by percolating through activated alumina. Water in the PC was removed by adding molecular sieves to it and letting it stand for a few days until use (11, 12, 18, 24). Highest grades of azulene (Az) and pyrrole (Py) monomers were used as obtained without further purification.

PC solutions (degassed with Ar gas) containing 0.1 mol dm^{-3} $LiClO_4$ plus Py and/or Az monomers were used for the preparation of polymer films. The total concentrations of Py and Az monomers were kept contant (0.05 mol dm^{-3}). Monomer ratios for the five different solutions are shown in Table I. In this table, the solutions of Az% = 0 and 100 correspond to 100% Py and 100% Az solutions, respectively. Cyclic voltammetry, impedance spectroscopy, and charge/discharge performance tests were carried out in 1.0 mol dm^{-3} $LiClO_4$/PC solution.

Film preparation.—Polypyrrole/polyazulene composite films were prepared on a Pt plate (0.283 cm^{-2}) in the PC solutions mentioned above using a cell assembly described elsewhere (11, 12, 18, 24). Electropolymerization was performed at a constant potential of 4.2 V (*vs.* Li/Li^+ in the same solution, at which the oxidation of both Py and Az occurs at almost equal electroreactivity under diffusion control (16). Total deposition amounts of the polymers were determined by monitoring the charge consumed during electropolymerization. Free-standing films, prepared by the passage of the same amount of charge (2 C cm^{-2}), were inspected by SEM.

Electrochemical measurements.—Cyclic voltammetry was employed for surveying both electropolymerization behavior at a scanned potential (10 mV s^{-1}) and redox (doping/undoping) processes at grown polymer films. As for impedance measurements, an ac voltage signal (maximum amplitude = 5 mV peak to peak) superimposed on dc bias was applied to the cell as a perturbation, and the response current signal was analyzed using FFT techniques. The range of frequencies was 5 mHz to 100 kHz. Li/1.0 mol dm^{-3} $LiClO_4$-PC/(PPy/PAz) cells were assembled with a (PPy/PAz)/Pt cathode and Li/Ni-mesh anode in a small container purged with dry and pure Ar gas. Charge-discharge tests were conducted at constant current densities (0.1-1.4 mA cm^{-2}). Discharge of the cells was terminated when the cell voltage reached 2.5V. All the results of cyclic voltammograms and charge-discharge curves in this work were obtained after stabilization for several cycles in ambient temperature (25°C).

Results and Discussion

Polymerization curves.—Figure 1 shows consecutive cyclic voltammograms for the polymerization of PPy, PAz, and their composite films at a Pt electrode in $LiClO_4$ solutions containing: a) 100% Py monomer (Az% = 0); b) Py and Az monomer (Az% = 50); and c) 100% Az monomer (Az% = 100), respectively. In terms of the polymerization behavior at the first scan, each voltammogram has almost the same onset oxidation potential (*ca.* 3.6V) and shows a limiting current beyond *ca.* 4.1V for 100% pyrrole, and *ca.* 4.2V for 100% azulene solutions. Azulene monomer shows a wider limiting current region than pyrrole, which is consistent with the results obtained by Burzynski *et al.* (16). However, the rate of monomer feed would be more or less the same in this diffusion-controlled region of over *ca.* 4.2V. Therefore, the polymerization potential for the following results was set at 4.2V. In the solution of Py/Az = 50/50, intermediate behavior of these two monomers was observed. No cathodic currents were observed

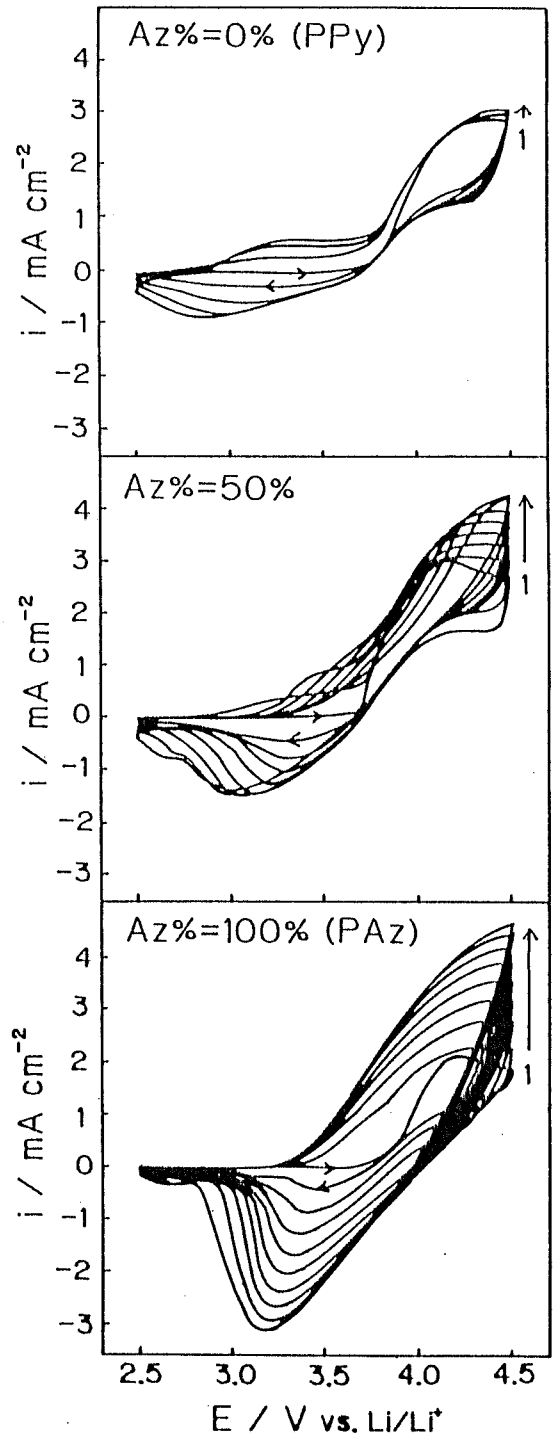

Fig. 1. Cyclic voltammograms for the co-polymerization of Py/Az monomers in various Py/Az solutions at a scan rate of 10 mV s^{-1}.

Table I. Composition of solutions at electropolymerization

	Solutions	Azulene content [mol dm^{-3}]	Pyrrole content [mol dm^{-3}]
A	Az% = 0	0.0000	0.0500
B	Az% = 25	0.0125	0.0375
C	Az% = 50	0.0250	0.0250
D	Az% = 75	0.0375	0.0125
E	Az% = 100	0.0500	0.0000

for the first scan except for that due to undoping anions. This indicates that both Py and Az monomers were oxidized to form radical cations to yield polymeric films, and the films do not decompose cathodically in this range.

From the second scan, anodic and/or cathodic currents in the voltammograms grow in each succeeding cycle (indicated by arrows). The current involves oxidation of

monomers (radical cation formation) at over 3.6V, as well as the oxidation of polymer films themselves on the substrate. The oxidation/reduction process of polymer films has concurrent anion doping/undoping at their active sites. The interesting observation is that continuous current growth occurs for azulene and pyrrole/azulene solutions, but the 100% pyrrole solution shows saturation in the oxidation region (over *ca.* 4.0V). The former two cases suggest that electroactive conducting polymers are continuously deposited layer after layer from the solutions. It is likely that the diffusivity of dopants limits the current for polymer growth when the polymerization speed is very high and the concentration gradient becomes very steep across the interface between polymer film and electrolyte. Because PPy films are more compact than PAz films (24), the film deposition for PPy shows saturation, but PAz deposit is in the conditions investigated here.

Elemental analysis of composite films.—Table II shows the results for the elemental analysis of PPy, PAz, and PPy/PAz composite films prepared from PC solutions of various Az content at 4.2V *vs.* Li/Li$^+$. The numbers X and Y correspond to the monomer ratios of Py and Az, respectively, found in composite polymer films $[-(Py)_x-(Az)_y]_n$. From this table, it can be seen that the films contain exactly the same ratios of Py and Az monomers as in the starting solutions. Hence the polymerization occurred at almost the same efficiencies for the two monomers at the potential of 4.2V.

Cyclic voltammograms for PPy/PAz composite films.—Figure 2a shows typical cyclic voltammograms at 5 mV s^{-1} for PPy, PPy/PAz, and PAz films deposited from various PC solutions of Az% = 0, 25, 50, 75, and 100%. In these voltammograms, the anodic and cathodic currents correspond to anion doping and undoping processes accompanied by the oxidation and reduction of the film itself. The voltammograms were repeatedly cycled without any decay of current, meaning that all the films were chemically stable and reproducible in the potential range between 2.5 and 3.8V.

The voltammogram of each PPy/PAz film has well-defined single redox peaks, and the redox potential ($\approx E_{pac} = E_{pa} + E_{pc}/2$) increases linearly in proportion to Az% in the film as seen in Fig. 2b, where E_{pa} and E_{ac} are the potentials of the anodic and the cathodic peaks, respectively. The relationship between E_{pac} and Az% suggests that the PPy/PAz films prepared are not simple mixtures of PPy and PAz but completely random copolymers whose electrochemical properties are intermediate between the pure polymers (17, 18).

Since all the voltammograms were obtained at a scan rate of 5 mV s^{-1}, the overall electrode process was quasi-stationary, controlled mainly by the electron exchange reaction, but still partly controlled by ionic transport within the bulk of the films. The detected anodization or cathodization charge reflected the effective number of active sites associated with the faradaic reaction at the time scale of the measurement. As the Az% was increased, the oxidation charge (Q_a) of the films became larger, *i.e.*, the total number of active sites participating in redox reaction became larger with an increase in Az% in the composite film. However, the value of Q_a did not vary linearly as a function of Az%; instead, the value showed an increase from 50 to 75%, as seen in Fig. 2b. This implies that around this value of Az%, there was some drastic structural or morphological change of the composite film.

Table II. Elemental analysis of PPy-PAz composite films

	Solution	Composition of CHN	Monomer ratio in composite film Pyrrole : Azulene	
A	Az% = 0	$C_{0.49}H_{0.39}N_{0.12}$	0	100
B	Az% = 25	$C_{0.54}H_{0.39}N_{0.07}$	25	75
C	Az% = 50	$C_{0.57}H_{0.39}N_{0.04}$	50	50
D	Az% = 75	$C_{0.60}H_{0.38}N_{0.02}$	75	25
E	Az% = 100	$C_{0.61}H_{0.39}$	100	0

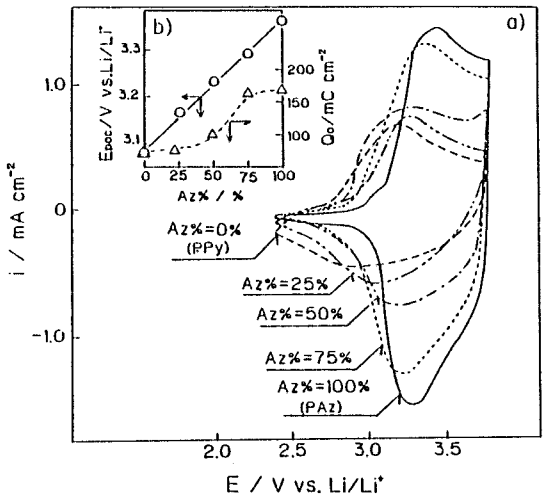

Fig. 2. a) cyclic voltammograms for PPy/PAz composite polymers (prepared by passing charge of 1 C cm^{-2}) at a scan rate of 5 mV s^{-1}. b) Dependence of Az% on redox potential (E_{pac}) and oxidation charge (Q_a) estimated from the voltammograms in 2a.

The scan rate dependence of the cyclic voltammograms can be summarized as in the manner described previously (11, 12). The anodic current peaks (i_{pa}) for PPy, PAz, and PPy/PAz films were plotted against the scan rate (v) on a logarithmic scale; the plot was linear, with a slope, x, in the scan rate range 5 to 50 mV s^{-1}. Therefore, the simple relationship between i_{pa} and scan rate can be written as follows

$$i_{pa} \propto v^x \quad [1]$$

The value of x ($0.5 < x < 1.0$) gives information about the rate-determining process of the overall redox reaction at the polymer film electrode. So, the x value found for each film was plotted against Az% for various PPy/PAz composite films, and is shown in Fig. 3. The dashed lines at $x = 0.5$ and 1.0 correspond to diffusion-controlled and reaction-controlled processes, respectively. The x value shows a gradual increase from Az% = 0 to 50 and attains saturation above Az% = 50. This means that the electrode process be-

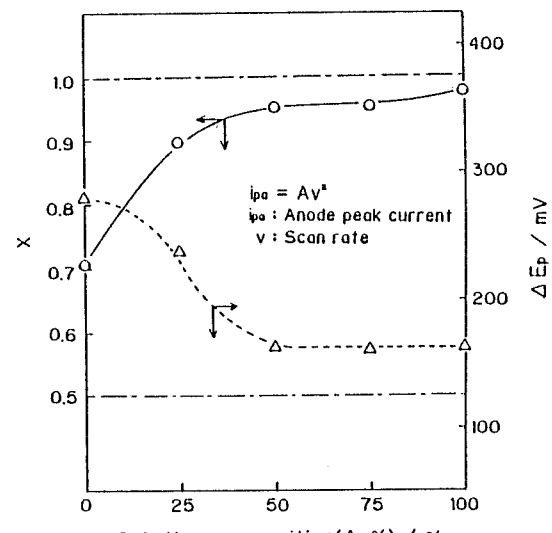

Fig. 3. Correlation of x and ΔE_p for PPy/PAz composite films (1 C cm^{-2}) against Az%.

comes limited by charge injection with an increase in Az%, and ionic transport in the film is fast enough to maintain electroneutrality above Az% = 50.

The value of ΔE_p (peak separation potential) shows exactly the mirror image of the curve of x value, indicating that PPy/PAz films lose the ability to switch reversibility below 50% in correspondence with the change in limiting process. These two observations indicate that switching reversibility is controlled by the ionic transport of dopants. The most appreciable change in the diffusion coefficient, D, is observed at Az% = 25-50, which is evidently consistent with the relationship x *vs.* Az%. Thus, the enhancement of the diffusivity of anions is considered to be closely related to the rate-determining step of the electrode reaction. However, the capacity value, C_L, variation against Az% seems somewhat different from that of the diffusion coefficient. Namely, the most noticeable change occurs at Az% = 30-45. The C_L variation is more likely to depend on the morphological change observed in Fig. 7, which is described later. This is reasonable because the deferential capacity is very sensitive to the active surface area, and change in this number is most likely when the morphological change at the polymer surface is observed. The behavior of D and C_L values against Az% correlates to that in Fig. 9.

Impedance analysis and estimation of diffusion coefficient and capacity value.—In order to analyze the details of kinetic and diffusion processes across the PPy/PAz films as a function of Az%, impedance spectroscopy was used. The potential dependence of the D and C_L values shows a peak at around $E_{p/2}$ in the cyclic voltammogram for each film (25). So, the impedance spectra at around the anodic peak potential are compared. Figure 4b shows typical Cole-Cole plots for PPy/PAz films (prepared with the same charge of 1 C cm^{-2}) at the potential of each anodic peak potential of the cyclic voltammogram. These impedance spectra show the behavior typical of thin redox and electronically conductive polymer films (like PVF) as shown in Fig. 4a (26, 27). Namely, at high frequencies (region A), charge transfer domination is observed with a semi-circle and, at lower frequencies (region B), diffusion of the anion in the polymer film dominates the impedance results. Finally, at the lowest frequency (region C), the finite film thickness limits the extent of diffusion behavior, and the locus rises vertically, owing to the saturation of resistance and capacitance (C_L) components.

In the diffusion-controlled region, where the impedance phase angle is $\pi/4$, the magnitude of the impedance is given by Eq. [2]

$$Z = \frac{C_L * L}{\sqrt{D^* \omega}} \qquad [2]$$

where C_L, D, and L are the low-frequency redox capacitance, diffusion coefficient, and the polymer film thickness, respectively. Values of C_L were estimated from the low-frequency impedance data (charge saturation region: $\omega \ll L^2/D$). In this range, the phase angle approached $\pi/2$ and C_L was calculated using Eq. [3]

$$\frac{1}{C_L} = \frac{d(-Z_i)}{d(\omega^{-1})} \qquad [3]$$

At very low frequencies (≤ *ca.* 30 mHz) in Fig. 4b, the locus for each film becomes vertical, and plots of $-Z_i$ *vs.* $1/\omega$ become linear, as shown in Fig. 5. From the slope of the curves in Fig. 5, the redox capacitance of each film was calculated by using Eq. [3].

At intermediate frequencies (*ca.* 40 mHz < f < 210 mHz), each locus was linear with unit slope. In this region, a plot of Z *vs.* $1/\sqrt{\omega}$ showed a straight line as indicated with Eq. [2]. By adopting the results of Fig. 5 to Eq. [2], values of the diffusion coefficient were obtained. In Fig. 6, the values of D and C_L are plotted against Az% for each PPy/PAz film. The obtained D values (1.0 – 7.5 × 10^{-8} cm^2 s^{-1}) are in reasonable agreement with those estimated from pulse measurements (12). The D value depended on Az% non-linearly, but jumped in the region between Az% = 25 and 50 by approximately a factor of 5. This change is unexpected in view of the uniform increase in Az% in the PPy/PAz composite film which was found by elemental analysis. Above Az% = 50, the D values approach saturation, indicating that the diffusion attains a limiting stage (*ca.* 7.0 × 10^{-8} cm^2 s^{-1}) and that the structure becomes open enough to allow dopants to move smoothly in and out of the films.

The redox capacity becomes larger as Az% increases above 50. Compared to the change in D, the extent of the change in C_L (0.5 – 1.2 × 10^{-4} F) is smaller and occurs at higher Az% values. The increase of C_L could be associated with the volumetric change of films caused by the incorporation of bulky azulene into the PPy matrix. This is very similar to the behavior of Q_a estimated from the cyclic voltammograms at slow scan rates. Previous reports have discussed purely capacitive behavior of polymer films at low frequenices (27, 28). Considering the above, surface roughness did not appear to change appreciably against Az%, since the ratio (Q_a/C_L) was constant against Az% in the whole range.

Morphology of composite films.—The lower diffusion rate at low Az% may be related to the change of film morphol-

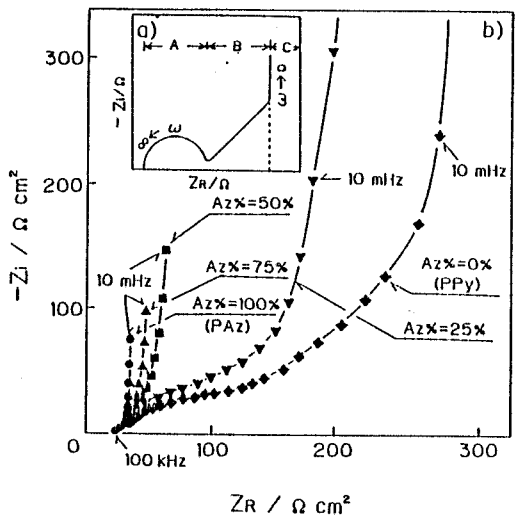

Fig. 4. a) Ideal impedance behavior for redox polymer film. b) Cole-Cole plots for various PPy/PAz composite films (1C cm^{-2}) at each anodic peak potential.

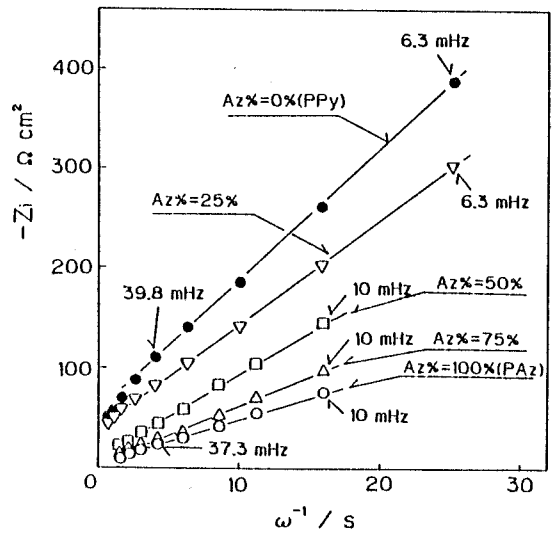

Fig. 5. $-Z_i$ vs. $1/\omega$ plots for various PPy/PAz composite films (1 C cm^{-2})

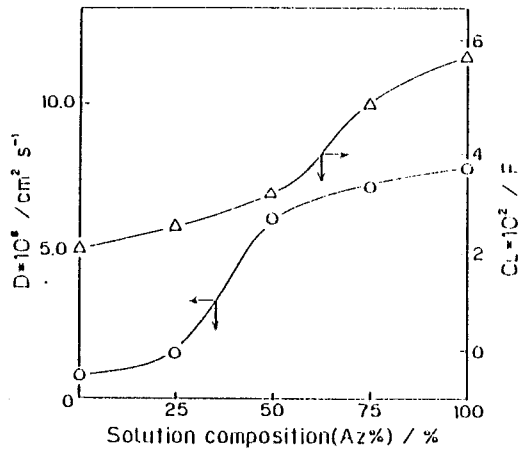

Fig. 6. Correlation of diffusion coefficient (D) and redox capacitance (C_L) for various PPy/PAz composite films (1 C cm $^{-2}$) against Az%.

ogy. In order to test this possibility, the film structures of PPy, PAz, and PPy/PAz films were observed with SEM. The SEM micrographs (side views) of PPy, PAz, and two PPy/PAz films (Az% = 25, 50) are shown in Fig. 7. Pure PPy and even PPy/PAz (Az% = 25) films show a very smooth and compact structure, suggesting that polymer grows equally in every direction. On the other hand, pure PAz and PPy/PAz (Az% = 50) films show rough and perpendicularly oriented structure. This means that the incorporation of PPy into bulky PAz matrix of more than 50% makes the morphology somehow oriented to be like columns. The orientation of the polymer film makes more space for the flux of anion doping/undoping into/out of polymer films, and leads to an enhancement of anion diffusivity (D value). The behavior (acceleration of diffusivity of anions and structure orientation) is very similar to the observation for the NBR-modified PPy films (12). The orientation of polymer films also results in the noticeable variation of film thickness. The thickness of these four films was estimated to be *ca.* 10 μm for both PAz and PPy/PAz (Az% = 50) films, and *ca.* 6 μm for both PPy and PPy/PAz (Az% = 25) films. A remarkable change in the thickness values occurred between the films of Az% = 25 and 50, i.e., the thicknesses of PAz and PPy/PAz (Az% = 50) are almost twice those of PPy and PPy/PAz (Az% = 25).

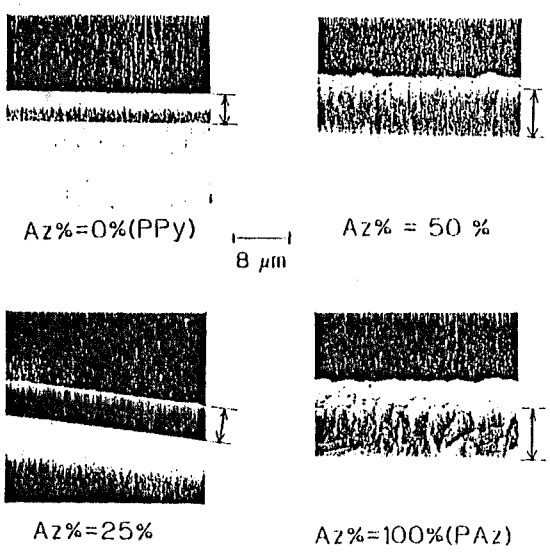

Fig. 7. SEM micrographs of the cross-sections of various PPy/PAz (2 C cm $^{-2}$) composite films.

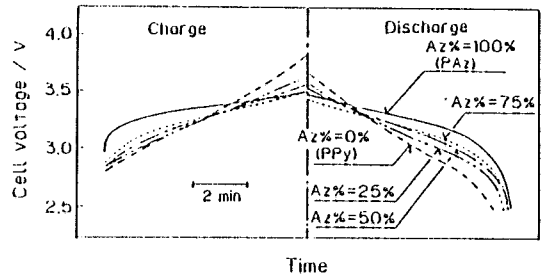

Fig. 8. Charge-discharge curves for Li/1.0 mol dm $^{-3}$ $LiClO_4$(PC)/(PPy/PAz(1 C cm $^{-2}$)) cells. Charge depth = 90 mC cm $^{-2}$; current density = 0.2 mA cm $^{-2}$.

Charge-discharge characteristics of Li/$LiClO_4$(PC)/(PPy/PAz) cells.— Figure 8 shows a typical comparison of the charge-discharge curves for the two electrode cells with lithium and various PPy/PAz films, all of which were formed by the passage of 1 C cm $^{-2}$. Each cell was charged to 90 mC cm $^{-2}$ at 0.2 mA cm $^{-2}$. The coulombic efficiencies and the average discharge voltages were calculated as follows: 94%, 3.06V (PPy); 98%, 3.09V (Az% = 25); 100%, 3.15V (Az% = 50); 100%, 3.19V (Az% = 75); 100%, 3.24V (PAz). A striking difference was observed in the shape of discharge curves, i.e., the discharge voltage became flatter and higher with an increase in Az%. In other words, 100% PPy behaved more like a pure capacitor with the linear increase/decrease in the charge/discharge curves, while 100% PAz had a flat discharge. The latter behavior is due to the higher diffusivity and higher redox potential of pure PAz (D = 7.5 × 10 $^{-8}$ cm^2 s $^{-1}$; E_{pac} = *ca.* 3.05V) compared to that of pure PPy (D = 1.0 × 10 $^{-8}$ cm^2 s $^{-1}$; E_{pac} = *ca.* 3.35V). The pure PAz cathode shows high capacity (low angle for V *vs.* t curve), but PPy shows a completely linear behavior

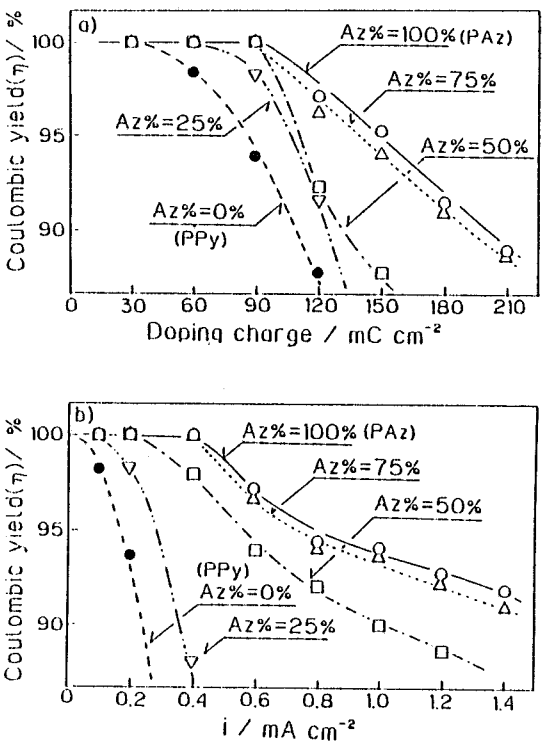

Fig. 9. Coulombic efficiency for charge-discharge curves in Fig. 8. a) Dependence of charge depth in terms of doping charge; current density = 0.2 mA cm $^{-2}$. b) Dependence of charge/discharge current density; charge depth = 90 mC cm $^{-2}$.

in Fig. 8. A higher capacity value for the pure PAz film is attributed to higher electroactivity of PAz relative to PPy, because the capacity value is closely associated with the faradaic reaction itself (28). The linear charge-discharge behavior observed for pure PPy can be explained by an ideal polarization at the PPy cathode at this rate of charging and/or discharging. In other words, rate of measurement is too fast for dopants to penetrate deeply into the PPy regime; charges accumulate at the polymer/electrolyte interface just like an ideally polarizable electrode. This explanation is likely because PPy cathodes show much flatter charge/discharge characteristics at slower rates than 0.2 mA cm^{-2} (12). However, for such kinds of films, the charging is limited up to a certain voltage because of an excessive polarization of the cell over 4.5V, at which solvents start to decompose.

The charge-discharge characteristics were further checked as a function of: a) depth of charge, and b) charge-discharge rate as shown in Fig. 9. Figure 9a shows the doping charge dependence on coulombic efficiency (η) at 0.2 mA cm^{-2}. The cell with a higher Az% composite film could be charged up to 210 mC cm^{-2}; keeping more than 90% of charge retention. The charge capacity was appreciably smaller below Az% = 50. At smaller Az%, the loss of charge is more likely to be used for the polarization and/or accumulation of charges at the cathode surfaces because of the compact film morphology and therefore the slow diffusion of ions within the bulk of film. This is why the pure PPy cathode behaves more like a pure capacitor.

The rate capability of these cells was examined by varying the current density during the charge/discharge cycles. For example, the PPy/PAz cathodes containing more than Az% = 50 keep more than 90% of coulombic efficiency up to 1.0 mA cm^{-2}. On the other hand, the cathode films containing below Az% = 25 show the same coulombic efficiency only at slow rates of less than 0.4 mA cm^{-2}. This means that the difference in the value of the diffusion coefficient directly reflects the rate capability of these cells. For example, the ratio of the rate tolerance (PAz/PPy = 1.4/0.2 = 7) at η = ca. 92% would correspond to the ratio of diffusion coefficients (PAz/PPy) = $7.5 \times 10^{-6}/1.0 \times 10^{-6} = 7.5$).

Conclusions

The impedance analysis used for PVF in our previous work (27) has been adopted to co-electropolymerized PPy/PAz films. From cyclic voltammograms, the redox potential for composite films shifted linearly to more positive values with an increase in azulene content (Az%) in the films. The oxidation charge, Q_a, of active sites showed a remarkable increase for films with more than 50 to 75% of azulene monomers. From the ac impedance analysis, the diffusion coefficient of dopant (ClO_4^-) and redox capacity were estimated. Low values of D caused the electrode process to change from charge-transfer-limiting to diffusion-limiting at Az% = 25 to 50% and lower. A noticeable change in C_L was observed around Az% = 50 to 75%, in the same range where the morphology changed from compact to a rougher condition.

The charge-discharge characteristics were examined for two electrode systems with a lithium anode and PPy, PAz, and various PPy/PAz composite cathodes. 100% PPy cathodes showed pure capacity-like charge and discharge. On the other hand, the 100% PAz cathode showed a very flat discharge behavior. Composite films are intermediate in behavior. A bulky PPy/PAz composite film at high Az% tolerated high current-density charging/discharging. Figure 9a suggests that an appreciable increase in C_L value (at Az% = 50-75) corresponds to higher doping level or higher energy density of the composite films. The enhancement of diffusivity (at Az% = 25-50) leads to a higher rate capability or higher power density, as shown in Fig. 9b.

Acknowledgments

The authors would like to acknowledge financial support from the Darpa/ONR and the General Sekiyu Research and Development Encouragement & Assistance Foundation.

Manuscript submitted March 23, 1989.

The University of Minnesota assisted in meeting the publication costs of this article.

REFERENCES

1. A. F. Diaz and J. A. Logan, *J. Electroanal. Chem.*, 111, 111 (1980).
2. A. G. MacDiarmid, S-L Mu, N. L. D. Somasiri, and W. Wu, *Mol. Cryst. Liq. Cryst.*, 121, 187 (1985).
3. K. Abe, F. Goto, K. Okabayashi, T. Yoshida, and H. Morimoto, The 27th Battery Symposium of Japan in Osaka, p. 201 (1986); M. Ogawa, T. Fuse, T. Kita, T. Kawagoe, and T. Matsumaga, *ibid.*, p. 197 (1986).
4. A. Kitani, M. Kaya, and K. Sasaki, *This Journal*, 133, 1069 (1986).
5. G. C. Farrington, B. Scrosati, D. Frydrych, and J. DeNuzzio, *ibid.*, 131, 7 (1984).
6. E. M. Genies and C. Tsintavis, *J. Electroanal. Chem.*, 195, 109 (1986).
7. H. Sakai, K. Naoi, T. Hirabayashi, and T. Osaka, *Denki Kagaku*, 54, 516 (1986).
8. A. F. Diaz, J. L. Castillo, J. A. Logan, and W. Y. Lee, *J. Electroanal. Chem.*, 129, 115 (1981).
9. E. M. Genies and J. M. Pernaut, *ibid.*, 191, 111 (1985).
10. A. Mohammadi, O. Inganaes, and I. Lundstroem, *This Journal*, 133, 947 (1986).
11. H. Sakai, K. Naoi, T. Hirabayashi, and T. Osaka, *Denki Kagaku*, 54, 75 (1986); T. Osaka, K. Naoi, H. Sakai, and S. Ogano, *This Journal*, 134, 285 (1987).
12. T. Osaka, K. Naoi, S. Ogano, and S. Nakamura, *Chem. Lett.*, 1986, 1687; K. Naoi and T. Osaka, *This Journal*, 134, 2479 (1987); T. Osaka, K. Naoi, S. Ogano, and S. Nakamura, *ibid.*, 134, 2096 (1987).
13. J. Bargon, S. Mohmand, and R. J. Waltman, *Mol. Cryst. Liq. Cryst.*, 93, 279 (1983).
14. R. J. Waltman, A. F. Diaz, and J. Bargon, *This Journal*, 131, 1452 (1984).
15. O. Inganaes, B. Liedberg, and W. Chang-ru, *Synth. Met.*, 11, 239 (1985).
16. R. Burzynski, P. N. Prasad, S. Bruckenstein, and J. W. Sharkey, *ibid.*, 11, 293 (1985).
17. K. K. Kanazawa, A. F. Diaz, M. T. Krounbi, and G. B. Street, *ibid.*, 4, 119 (1981).
18. K. Naoi, T. Hirabayshi, I. Tsubota, and T. Osaka, *Bull. Chem. Soc. Jpn.*, 60, 1213 (1987).
19. J. R. Reynolds, P. A. Poropatic, and R. L. Toyooka, *Synth. Met.*, 18, 95 (1987).
20. M. V. Rosenthal, T. A. Skotheim, A. Melo, M. I. Florit, and M. Salmon, *J. Electroanal. Chem.*, 185, 297 (1985).
21. J. Bargon, S. Mohmand, and R. J. Waltman, *Mol. Cryst. Liq. Cryst.*, 93, 279 (1983).
22. R. J. Waltman, A. F. Diaz, and J. Bargon, *This Journal*, 131, 1452 (1984).
23. G. Tourillon and F. Garnier, *J. Electroanal. Chem.*, 135, 173 (1982).
24. T. Hirabayashi, K. Naoi, and T. Osaka, *This Journal*, 134, 750 (1987).
25. T. Osaka and K. Naoi, Unpublished data.
26. C. Ho, I. D. Raistrick, and R. A. Huggins, *This Journal*, 127, 343 (1980).
27. T. B. Hundter, P. S. Tyler, W. H. Smyrl, and H. S. White, *ibid.*, 134, 2198 (1987).
28. J. Tanguy, N. Mermilloid, and M. Hoclet, *ibid.*, 134, 795 (1987).

—受賞講演—

機能材料としての導電性高分子薄膜の合成と評価

逢坂哲彌

1 はじめに

電解酸化重合により得られる導電性高分子は，化学重合によるポリアセチレンなどとともに合成金属材料として興味がもたれているが，新しい機能をもった薄膜に対する基礎的な興味ばかりでなく応用をふまえた見地からも注目され，活発に研究されるようになってきた[1]．

導電性高分子の機能性薄膜としての可能性をTable 1に示す．この中で特に二次電池カソード材料としての可能性が最も実用に近いターゲットであり[2]，すでに電解重合ポリアニリンがコイン形リチウム二次電池のカソード材料として実用化されている[3]．また，高容量コンデンサー，エレクトロクロミック表示素子，センサー，スイッチング素子等の可能性について研究が行われ，有機膜による半導体素子の可能性も検討が加えられている．このような現状において，我々が研究を行っている電池材料への応用を中心に電気化学的に活性な高分子薄膜の合成と評価について紹介する．

Table 1 Application of conductive polymers to electronic devices.

Electrochemical doping behavior	・Electrode material of rechargeable battery ・Electrochromic device ・ISFET (sensor), Microsensor ・Capacitor
Undoped state or slightly doped state	・Switching device (MIM) ・Schottky junction with metal (diode, transistor)

早稲田大学理工学部応用化学科（〒169 東京都新宿区大久保3-4-1）

2 導電性高分子の分類と電気化学的特性評価

研究初期には，最も軽量で，電気化学的活性の高いポリアセチレン（白川法により合成）が研究対象であったが，ポリアセチレンは空気中の水分および酸素により劣化し，自己放電性が高い．従って，ポリピロール，ポリアニリン等，安定でかつ電気化学的に合成可能な導電性高分子材料が注目されるようになった．Fig. 1に代表的な導電性ポリマーを構造的に分類した．電解重合により合成可能な導電性高分子の中で，ポリピロールが材料の安定性及び作製の容易さから多く研究されている．リチウムと組み合わせた時の二次電池としては，もっとも可能性のある材料としてポリアニリンが注目されているがポリピロールによる積層型電池も試作されている[4]．

導電性高分子膜では膜中へのイオンドーピングが，膜中電荷の保持および導電性に大きい影響を及ぼす．ポリ

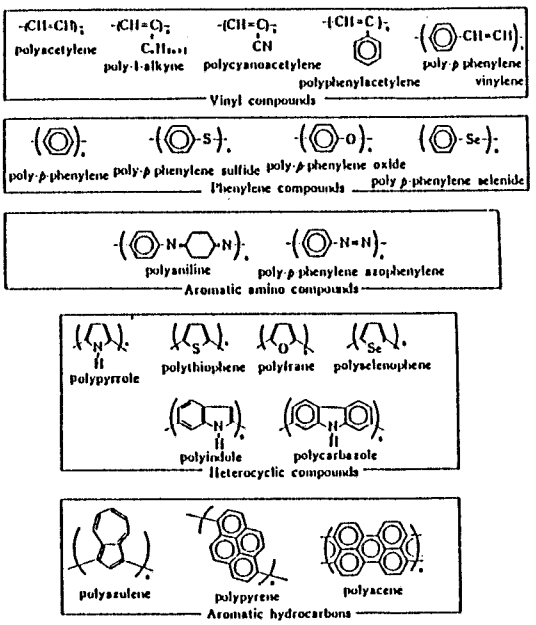

Fig. 1 Lists for typical conducting polymers.

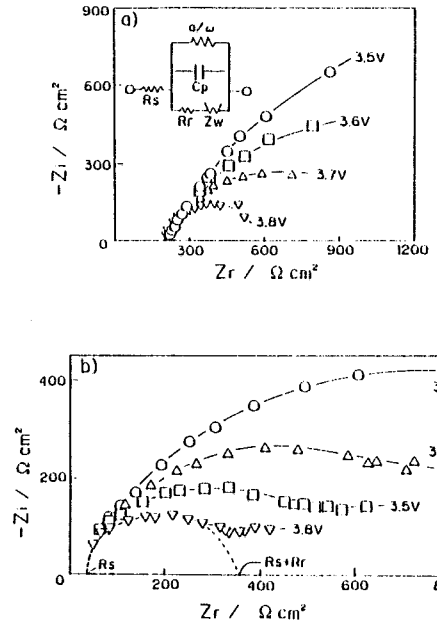

Fig. 2　Impedance representations of polyacetylene and polypyrrole electrodes at anion doping process. a) doping process of polyacetylene in 1 mol dm^{-3} $LiBF_4$／PC, b) doping process of polypyrrole in 1 mol dm^{-3} $LiClO_4$／PC at various potentials (V vs. Li/Li^+).

アセチレンがイオンドーピングにより高導電性を示すことが1977年MacDiarmidらのグループによりまず見出され，さらに1979年電解液中でポリアセチレンが電気化学的に可逆なイオンドーピング・脱ドーピングを行う過程により二次電池活物質としての可能性をもつことが示唆された[2]．これが，ポリマー電池開発研究の端緒となった．このような高分子中へのイオンドーピング・脱ドーピング過程を評価することが，最も重要である．迅速な測定法であるFFTインピーダンス法[5]は，このような過程を評価するのに適した方法である．Fig. 2にポリアセチレンおよびポリピロール膜のアニオンドーピング過程にFFTインピーダンス法を適用した例を示す[6]．この結果は代表的なRandles型等価回路を適用して結果を扱うことができる．膜の導電性に関与している抵抗成分 R_r を半円の直径から求めると，Fig. 3にみられるようにポリアニンが最もドーピング・脱ドーピング過程の可逆性が高いことが容易に評価できる．導電性高分子のインピーダンス法による解析例は，Hunterらにより示されている[7]．すなわち，Hoらが WO_3 膜に適用したインピーダンス解析法[8]を高分子薄膜に適用し，Fig. 4aに示すようなA（反応律速），B（拡散律速），C（電荷飽和）の三領域に分類することにより各

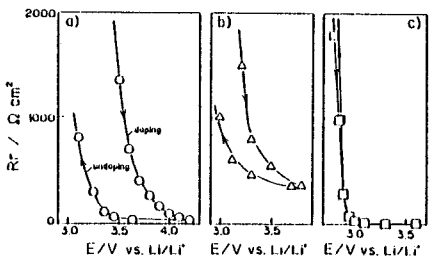

Fig. 3　Potential dependence of resistive component, R_r, for ClO_4^- doping-undoping process in 1 mol dm^{-3} $LiClO_4$／PC. a) polyacetylene ; b) polypyrrole ; c) polyaniline.

因子を算出している．領域Cの低周波数域から高分子薄膜のレドックス容量 C_L，領域Bの中間周波数域から膜内ドーパントイオンの拡散係数Dを算出することができる．

低周波数領域では，

$$C_L^{-1}=d(-Zi)/d(\omega^{-1}) \qquad (2-1)$$

中間周波数領域では，

$$|Z|=(C_L^{-1}L)/\sqrt{D\omega} \qquad (2-2)$$

ここでZ，L，ωは電極インピーダンス，高分子膜厚，角周波数である．

ここで，電解重合により2種類の特徴ある膜を共重合膜として得る場合にこのインピーダンス解析法を適用した例を示す[9]．Fig. 4bはピロールとアズレンモノマーを含む重合液から共重合（または複合）膜を得るよう電解重合を行い，得られたPPy（ポリピロール）－PAz（ポリアズレン）高分子膜のインピーダンス挙動である．得られた膜は元素分析によると重合液中のモノマー混合比と同じ比の組成であった．PPy-PAzを複合的に電解重合した膜のインピーダンス挙動（Fig. 4b）は，明らかにFig. 4aのモデルに対応している．この膜はアズレン含有量（Az%）50%のところで急激に膜厚が倍以上のバルキーな膜になりポリアズレンの特徴が顕著になる（SEM観察による）．この膜のインピーダンス法によるアニオン膜内拡散係数Dとレドックス膜容量 C_L の計算結果がFig. 4cである．明らかに膜容量 C_L は膜のかさ密度に対応してAz%が50～75%の領域で大きくなる．また，拡散係数DはAz%が25%～50%の領域で増加しており，これはサイクリックボルタモグラムから予想されるイオンドーピング反応速度が速くなる領域に一致している．この膜によるLi／PPy-PAz電池特性はFig. 4bの電気化学的基礎特性とよく対応し，電池容量はAz%が50%～75%で，また出力電流はAz%が25～50%の領域で特性が著しく向上している．このように共重合により特徴ある膜を作製することが可能で，その膜の電気化学的基礎特性をインピーダンス法で的確に評価

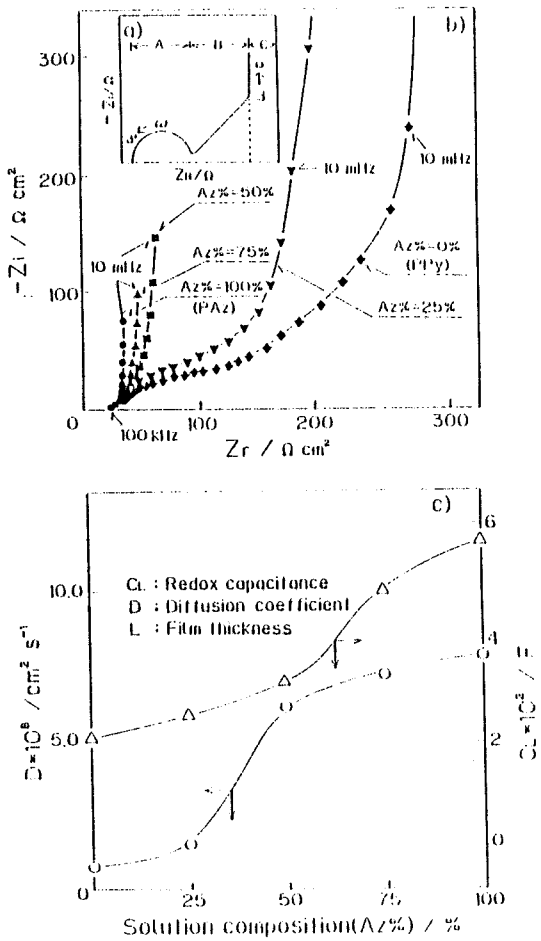

Fig. 4 a) Schematic representation of Cole Cole plot. b) Cole-Cole plots for various PPy(polypyrrole)-PAz (polyazulene) composite films (1 C cm^{-2}) at each anodic peak potential in 1 mol dm^{-3} $LiClO_4$/PC. c) Correlation of diffusion coefficient (D) and redox capacitance (C_L) for various PPy PAz composite films (1 C cm^{-2}) against Az composition.

することができ，その評価結果は電池カソードとしての特性とよい相関性をもつ．

次に，膜中イオンの出入りを重さによって評価できるin-situ 水晶振動子マイクロバランス（QCM：Quartz Crystal Microbalance）法の例を示す[10]．本法は石英結晶上に金を析出させた電極を試料極として利用する．この石英結晶にたとえば6 MHzの周波数を印加しておくと，その電極上に析出させた膜重量の変化を周波数変化として検出することができる．導電性高分子膜をこの試料極上に析出させた場合には膜中へのイオンドーピング・脱ドーピングによる重量変化が周波数変化として測定可能である．重量変化はng変化程度まで検出可能で，重量変化Δmと周波数変化Δfの関係は，次式に従う．

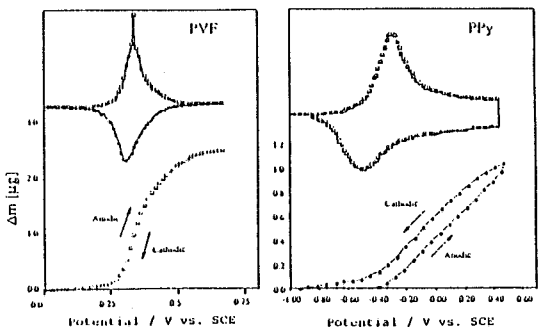

Fig. 5 Typical mass changes at PVF (polyvinylferrocene) and PPy (polypyrrole) electrodes during cyclic voltammetry at 1 mV s^{-1} in 0.1 mol dm^{-3} $LiClO_4$/AN. The top curves are the respective cyclic voltammograms.

$$\Delta f = -\frac{2f_0^2}{\sqrt{\rho_Q \mu_Q}} \cdot \frac{\Delta m}{A} \qquad (2\text{-}3)$$

ここでf_0は共鳴周波数，ρ_Q，μ_Qおよび A は石英密度，剛性率（shear modulus）および表面積である．共鳴周波数6 MHzの石英を用いた場合は次式のような関係になる．

$$\Delta f = -0.25\ A^{-1}\Delta m \qquad (2\text{-}4)$$

Fig. 5にPVF（ポリビニルフェロセン）とPPy（ポリピロール）膜のドーピング・脱ドーピングをQCM法で測定した代表例を示す[11]．PVFは分子量80,000のものをメチレンクロライドにとかし，スピンコートしてかわかした膜厚1000 Åの膜であり，PPyは0.8 V vs. Ag/Ag$^+$で膜厚1000 Åに重合した膜である．Fig. 5の上部には1 mV/sのサイクリックボルタモグラム（CV）を示すが，この条件で同時にQCMデータをサンプリングしている．ここで特徴的なことは，アニオンドーピング・脱ドーピング過程に伴うイオン重量変化はPVFでは可逆性が高くアノード，カソード方向がよく一致しているが，PPyではアノード，カソード方向は一致せず可逆性が低い結果となっている．この挙動はCV挙動から予想される結果ではあるが，QCM法による膜内へのアニオンドーピング過程の重量変化からも確認できたことになる．

さらにこれら2つの膜の容量値をCV法およびインピーダンス法から求めて比較すると Fig. 6 のような興味深い結果となる*．すなわちPVF膜では，CV法からとインピーダンス法からの容量値はよく一致するが，

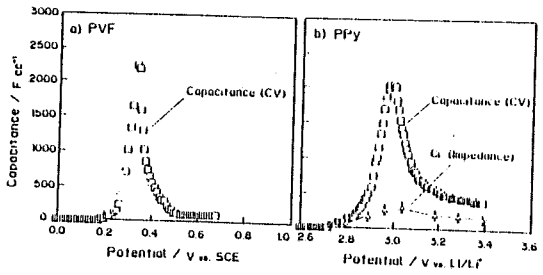

Fig. 6 Potential variation of capacitive values derived from CV and impedance methods for PVF(a) and PPy(b) electrodes.

PPy 膜では両者は一致せずインピーダンスから得た C_L 値の方が全体的に低い値となる．この結果はインピーダンス法からの C_L 値は単にファラデー過程に関与する項に相当するため，非ファラデー成分（おそらく容量成分）を含まない PVF ではよく一致するが，非ファラデー成分を含む PPy 膜は，その部分がうまくつかまらないため一致しないと考えられる．いずれにしてもまだ議論の残る部分である．

このような結果は，PDIM (Phase Detection Interferometric Microscope) の表面プロファイルを比較することによりほぼ議論できるであろう．PDIM 法とは，レーザー光により表面モルフォロジーおよびラフネスを正確に測定する方法で，特に垂直方向に 0.6 nm の高解像度をもつ[12]．Fig. 7 に PVF と PPy の PDIM プロファイルとそれぞれに相当するドーピング過程のモデル図をあげた．PVF 膜では表面がフラットでレドックスの可逆性が高い膜のため，ドーピング過程によりかなり深くまで入ったイオンのファラデー過程が主体で，表面電荷は無視できるが，PPy 膜では表面のラフネスが高く，表面に弱くトラップされたイオンによる電荷量が多く無視できない．そのため，表面部分のトラップイオンは非ファラデー成分としてインピーダンスからの C_L 値に反映せず，かつ QCM 法による重量変化でもアノード，カソード方向の不一致として現れると考えられる．

このように，いくつかの in situ 法の組み合わせにより，広い角度からの考察と結論とが可能となるであろう．

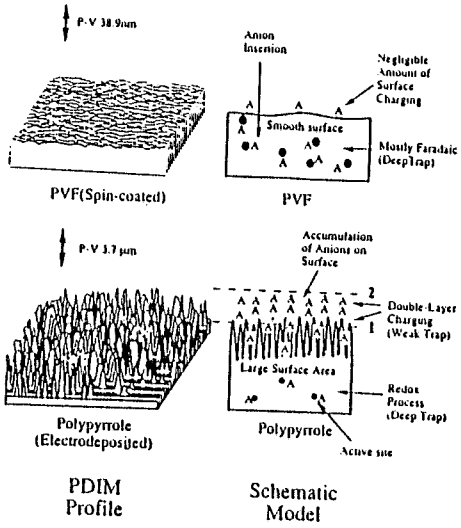

Fig. 7 Phase detection interferometric microscopic profiles and schematic model of ion-doping conditions for PVF and PPy electrodes in 0.1 mol dm^{-3} $LiClO_4$／AN.

3 ポリマー電池への応用

3.1 ポリマー電池の分類と動作原理

導電性高分子を導体化するには，酸化還元処理によりキャリアを注入する必要がある．酸化処理により正のキャリアを注入することを p 型ドーピング，還元処理により負のキャリアを注入することを n 型ドーピングという．このドーピングは化学的方法だけでなく，電気化学的に外部電力により電解液中のカチオン，アニオンを膜中あるいは膜外へドーピング・脱ドーピングすることができ，この反応を利用してポリマー電池を構成することができる．ポリマー電池はリチウムとの組み合わせで，Li／p 型ポリマー（カソード），Li／n 型ポリマー（カソード），n 型ポリマー（アノード）／p 型ポリマー（カソード）の 3 種類に分類することができる．これらの反応例を示すと，

p 型ポリマー（カソード）の場合

$$(P)_x + (xy)A^- + (xy)Li^+ \underset{\text{放}}{\overset{\text{充}}{\rightleftarrows}} \{(P^{y+}(A^-)_y\}_x + (xy)Li \qquad (3\text{-}1)$$

n 型ポリマー（カソード）の場合

$$\{P^{y-}(Li^+)_y\}_x \underset{\text{放}}{\overset{\text{充}}{\rightleftarrows}} (P)_x + (xy)Li \qquad (3\text{-}2)$$

ここで，導電性高分子を $(P)_x$（x は分子鎖長），アニオンを A^-，ドーピング量を y として示している．これらの電池の特徴を Table 2 に示す．ここで特徴的なこ

---

*CV からの容量 C 値は，電流値 i を時間で積分して電荷 Q 値を求め，さらに Q 値を電位 E で微分して求める．

$$C = dQ/dE = \frac{dQ}{dt} \cdot \frac{dt}{dE} = i \cdot v^{-1}$$

ただし，v は走査速度である．

インピーダンスからの C_L 値は前述のように式 (2-1) から求まる．

Table 2 Various types of lithium/polymer batteries.

	Plastic battery	Lithium battery		
Battery type	p/n	p	n	n
Construction (+/−)	polymer/polymer	polymer/Li	polymer/Li	inorganic/Li
Electrolyte	non aq./salt	non-aq./Li salt	non-aq./Li salt	non-aq./Li salt
Dopant	anion, cation	anion	Li^+ ion	Li^+ ion
Charging	doping	doping	undoping	deintercalation
Cell volt.	fair	high	fair	fair
Electrolyte conc. during charging	decrease	decrease	constant	constant

とはLi/p型ポリマー電池は電圧は高くとれるが充放電で電解液濃度が変わるため，比較的多くの電解液量を必要とするのに対し，Li/n型ポリマーは電圧は低いが電解液濃度一定で電解液量を多くは必要としない．従って，n型ポリマーは，無機系インターカレーション化合物同様，電解液が少ない利点を持つが，現状ではn型ドーピング反応は可逆性および安定性も悪い．また，n型ポリマーは，ポリアセチレン，ポリアセン，ポリパラフェニレンなどごく少数である．これらの問題点を解決する一つの方法として，ポリマーアニオンを導入した導電性高分子膜を正極に用いるリチウム電池の研究が行われ始めた[13]．このタイプの電池では，充電時にポリマーから電子が引き抜かれた時，導電性高分子膜中のポリマードーパントのアニオンサイトが電荷の中性化に寄与する(3-3)式参照)．一方，放電時には，高分子膜が中性化するにつれてフリーになったアニオンサイトがリチウムイオンを捕捉する．

$$P/PA^- \ Li^+ \underset{\text{放}}{\overset{\text{充}}{\rightleftarrows}} P^+/PA^- + Li \qquad (3\text{-}3)$$

従って，原理的にはp型ポリマーを用いた場合と全く同じであるが，見かけ上はリチウムイオンのみが反応に関与し，充放電時の電解液の濃度はn型ポリマーを用いた場合と同様に変化しないので，電解液は少量ですみ，また，固体電解質などの利用も可能となるので，今後このような利用を考えた材料開発も可能性があるであろう．このタイプの導電性ポリマーをカソードとしてリチウムと組み合わせた場合の理論計算が最近示され，かなりの高エネルギー密度で高出力な電池が可能であることが示されている[14]．

3.2 ポリマー電池の特徴

ここでリチウム/ポリマー二次電池の特徴をあげると，(1)形状加工が自由で，フィルム状薄型バッテリーが可能，(2)単位重量当たり比較的大きいエネルギー密度を持つが(カソード当たり200～400 Wh kg^{-1})，現状では無機インターカレーション材料よりはやや劣っているか同等と考えられている．また，(3)ポリマー電極ではポーラスな高分子マトリックス全体で反応がおこるため有効電極面積が大きく，かつ，ドーピングレベルが大きいため，瞬間的に放電可能な出力密度が大きい．以上の点を考慮すると将来的には形状フレキシブルでエネルギー密度が高くかつ出力密度が大きい二次電池が期待できる．反面，単位容積当たりのエネルギー密度が小さく自己放電が大きい．無機インターカレーション化合物と比べて多量の有機電解液を必要とし，過充電に弱いといった実用化の上でのいくつかの問題点も指摘されている．

3.3 ポリピロール膜を利用したリチウム二次電池用カソード特性

ポリピロールは空気中で非常に安定であり，機械的な膜強度も良好なため，多くの研究がなされている．通常の電解重合ポリピロール膜はち密な膜のためイオンの出入りが容易でなく，ドーピングレベルが小さい．しかしポリピロールは重合時のアニオン種により膜のモルフォロジーを制御することができ，膜特性が大きく変化する[15]．Fig. 8は重合時のアニオンを変えた場合のポリピロール膜の充電量（ドーピング量）の変化を重合電位に対して調べたもので，$CF_3SO_3^-$ と PF_6^- アニオン重合膜では0.3 V付近で最大値を示している[15]．従ってこの重合電位において最大のドーピング量を得ることができる．Fig. 9はこれらの膜を正極に用いた時のリチウム二次電池の定電流充放電特性の結果である（図中に示されたアニオンは重合時に用いたものである）．Fig. 9はFig. 8の結果によく対応し，重合時のアニオンを BF_4^-，ClO_4^- から PF_6^-，$CF_3SO_3^-$ に変えると充放電容量が大幅に向上している．この変化はポリピロール膜のモルフォロジーに対応していることがSEM観察により確認されている．また，Fig. 10に示すような絶縁性NBR（ニトリルブタジエンラバー）を介して

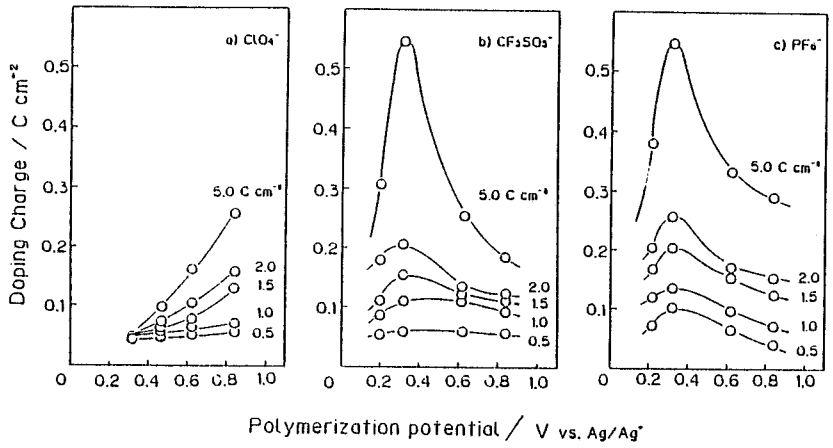

Fig. 8 Dependence of polymerization potential on the doping charge of polypyrrole films as a function of formation charge (C cm^{-2}) in 1 mol dm^{-3} $LiClO_4$/PC.

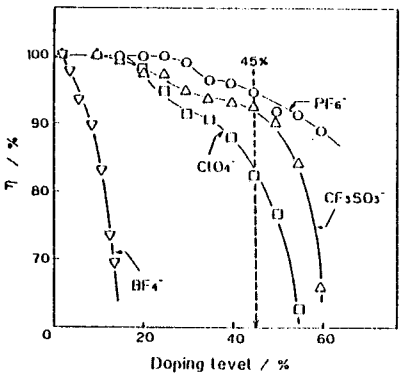

Fig. 9 Properties of Li/PC, 1 mol dm^{-3} $LiClO_4$/PPy batteries, where polypyrrole films were formed with various anions.

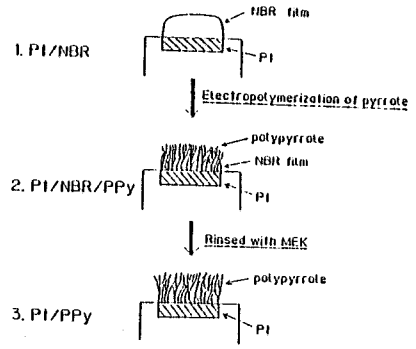

Fig. 10 Schematic model of the preparation procedure of NBR-aided grown PPy electrode (Pt/NBR/PPy).

ポリピロールを重合し，膜を垂直配向させたのち，NBRを溶しだすことにより得られたポリピロール膜では，膜中アニオン拡散速度が大幅に向上することが報告されている[16]．Fig. 11 に示すインピーダンス法によってその特性向上がよく確認でき，ドーピング開始電位付近（−0.25 V vs. Ag/Ag^+）で，NBR/PPy 膜は抵抗値に比例する半円がすでに小さくなり，膜中イオンドーピングが良好に起こることによるレドックス特性向上が示されている．この膜をカソードとして利用したリチウム二次電池特性は Fig. 12 に示すように充放電速度（出力）の点で大幅な向上が見られる[16]．このように，高分子膜では活性点の数とイオンドーピング過程速度を十分に高めることが，膜モルフォロジー制御により行なえることが明らかである．

4　高容量コンデンサーへの応用

導電性高分子は，二次電池カソード材料として非常に高い出力と比較的高いエネルギー密度を持つという特徴がある．これは，導電性高分子材料が高い電気化学活性と速い電荷のやりとり（スイッチング特性）を示すことに起因する．また，導電性高分子は異常に高い誘電特性を示すこともあって，小型大容量コンデンサーへの応用が考えられ，今後大きな期待ができる．特に，電解重合法等により作製したポリピロール，ポリチオフェン，ポリアニリンは，電解質溶液と接触すると，その界面および膜内に電気二重層ができ，レドックス反応とは別に容量性の大電流が流れることが知られている[17~20]．

例えば，アセトニトリル中（0.1 M $LiClO_4$/AN）における電解重合法により作製したポリピロール(PPy)

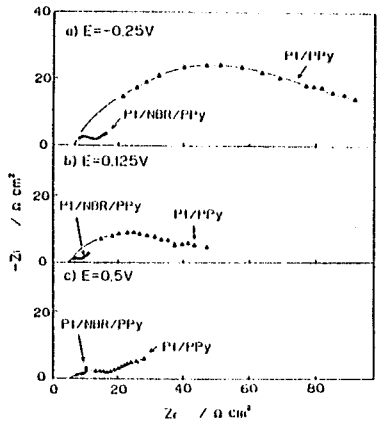

Fig. 11 Typical Cole Cole plots for Pt／PPy and Pt／NBR／PPy electrodes in 0.1 mol dm^{-3} T*n*BAClO$_4$／AN at doping potentials (V vs. Ag／Ag^+).

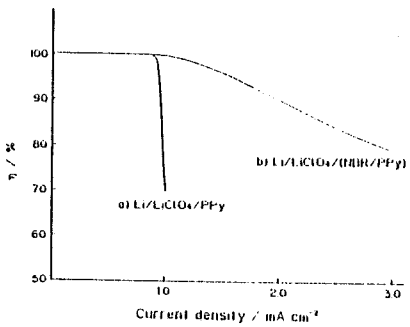

Fig. 12 Current density dependence of coulombic yield (η) for charge-discharge tests with charge depth 60 mC cm^{-2} (doping level 15%) ; a) Li／PC, 1 mol dm^{-3} $LiClO_4$／PPy ; b) Li／PC, 1 mol dm^{-3} $LiClO_4$／(NBR (2 μm)／PPy). Each polymer was prepared by passing charge of 1 C cm^{-2}.

膜のサイクリックボルタモグラムを Fig. 13 の上部に示した．レドックスピークのあとに平坦な領域（容量電流）が観測できる．この大きな容量電流の要因に関しては，未だに明らかにされておらず，二重層充電だけでは説明することはむずかしいため[18]，非ネルンスト系のレドックス過程であるとも考えられている[17~19]．PPy の微分容量値（ポリマー容量 1 cc 当たり）を電位に対してプロットし同じく Fig. 13 に示した．

PPy 電極上ではピーク電位付近で速い充電が起こり，ピーク電位以上では容量電流に対する遅い充電が起こっていることがわかる．充放電曲線もコンデンサー特有の三角形に近く，膜の合成条件（特にモルフォロジー）を

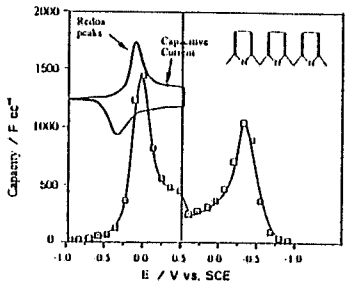

Fig. 13 Cyclic voltammogram for polypyrrole film (1 μm thick) and capacitance per unit volume (1 cc) of polypyrrole in 0.1 mol dm^{-3} $LiClO_4$／AN. Scan rate = 1 mV s^{-1} : The polypyrrole film was prepared at 0.7 V vs. SCE.

制御することにより，完全な三角波にすることも可能である．また，非常に可逆性の高いレドックスポリマーであるポリビニルフェロセン（PVF）等と比べると，動作電位範囲も広く，コンデンサーへの応用に適している[20]．微分容量はピーク値で約 2000 F cc^{-1}（充電時），約 1500 F cc^{-1}（放電時），平均値では，400－500 F cc^{-1}（充放電時）と非常に高い値を示す．

PPy の微分容量値を異なった種類のカーボン材料と比較したものが，Fig. 14 である[21]．カーボンの二重層容量値は，有効面積，電解質の種類によって種々の値を持つ．ここでは有効表面積（BET 値）の異なる三種類のカーボン材料，すなわち，グラファイト，カーボンブラック，活性炭の二重層容量値を示している．最近，二次電池材料にも用いられ始めた最も高い BET 値を示す活性炭（BET＝450－1000 m^2 g^{-1}）に比べても，同等かそれ以上の容量を PPy は示している．また，Li／2M $LiClO_4$－PC／PPy のセル当たりの容量値を電位に対してプロットすると Fig. 15 のようになる．カソードあたりの容量値と比べるとセルあたりでは 1／4.85 とかなり小さくなる．動作電圧 2.0 V～3.25 V の範囲の平均値で 120 F cc^{-1}，充電時，放電時の最大値はそれぞれ 340 F cc^{-1}，240 F cc^{-1} となる[10]．このように，導電性高分子材料を用いたコンデンサーの容量値は一般に充電時の方が放電時に比べて瞬間的に高い値を持つという特徴がある．

Li／PPy の平均容量値を従来のコンデンサー（Al，Ta，セラミックス）および二重層コンデンサー（Ag／$RbAg_4I_5$／カーボン）と比較すると Fig. 16 のようになる．理論値で比較すると大容量の Ag／カーボンキャパシターに比べても更に 1 桁高い値を示す．またエネルギー密度的に考えても，セル当たり（ハードウェアを含む）理論値で 100 Wh kg^{-1} というコンデンサーとしては比較的高い値を持っている．

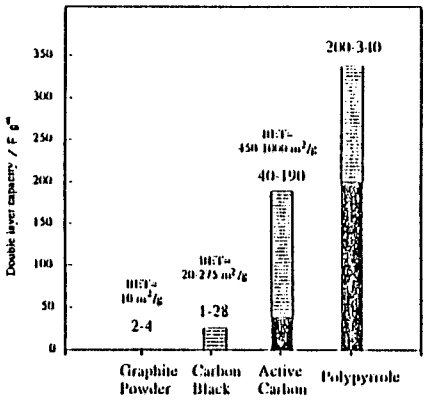

Fig. 14　Comparison of double layer capacity values.

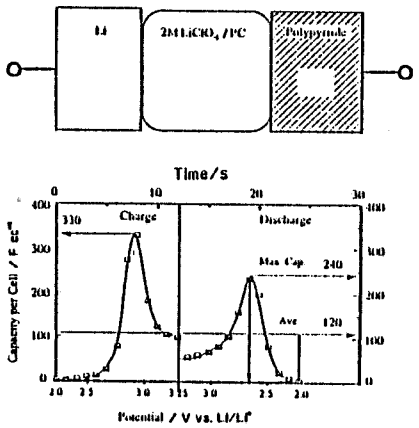

Fig. 15　Capacitance values per cell : Li／2 mol dm^{-3} $LiClO_4$, PC／PPy as a function of voltage during charge／discharge process. The polypyrrole film was prepared in the same manner as in Fig. 13.

このように，ポリピロール等に代表される導電性高分子材料は，小型大容量コンデンサーとして大きな可能性を秘めている．問題点としては，動作電圧の範囲が狭い事，充放電時の電流のリーク等があげられる．国内ではすでにマルコン電子(株)がポリピロールを負極にしたチップ型アルミ固体電解コンデンサーを開発し，電解液型の従来品よりも優れた周波数特性を持つことが報告されている[22]．今後この分野での導電性高分子の利用が拡がるものと考えられる．

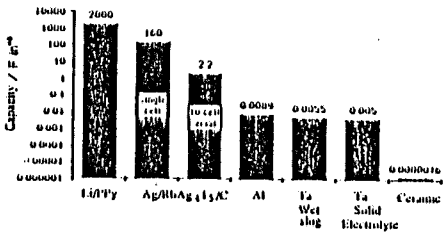

Fig. 16　Comparison of capacity value of Li／2 mol dm^{-3} $LiClO_4$, PC／PPy cell with conventional capacitor devices.

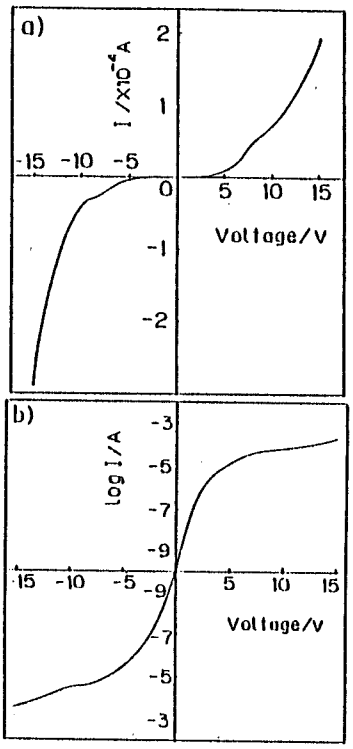

Fig. 17　The I-V(a) and log I-V(b) characteristic of ITO／PMPy (undoped)／ITO cell ; where the thickness and diameter of PMPy (polymethylpyrrole) were 1 μm and 300 μm.

5　MIM 非線形素子への応用

スイッチング素子としてMIM (Metal Insulator Metal) 素子を用いて液晶カラー画像ディスプレーが商品化されているが，この方式は従来のTFT（薄膜トランジスタ）をスイッチとして利用するパネルよりも工程が少なく，高い生産性が得られる．実際に用いられている組み合わせはガラス基板上に300 nm Taをスパッタし，エッチング後Ta表面を陽極酸化により約60 nm

程度酸化，Ta_2O_5絶縁膜を形成する．その上にCrをスパッタし，最後にITOパターンを行い液晶駆動電極を作る．素子は$5\times5\mu m^2$サイズである．Ta／Ta_2O_5／Cr構造をもつMIMにかわって，絶縁膜部分に電解重合高分子膜を利用すると，多くの素子部分の絶縁膜を一度に容易に作製でき，また液晶駆動用のITO電極をそのままMIM素子のMetal部とすることができるため，パネルの大面積化が容易に行える可能性がある．Fig. 17に，我々が試みたITO／ポリマー／ITOのスイッチング特性を示す[23]．ポリマーとしてはポリNメチルピロールを用い，脱ドープを行いITOでサンドイッチ化している．ポリマー膜厚1.0μm以上，素子面積の直径300μm以下でこのように5桁変化するスイッチング応答が可能であった．従って，今後このような分野でも導電性ポリマーが利用できる可能性が考えられる．

6 おわりに

本解説では，主として，導電性高分子を評価するいくつかの例およびその膜を応用するいくつかの例について概説し，その際の基礎的な考察と研究例を中心に紹介した．応用例としてリチウム／ポリマー電池，高容量コンデンサーおよびMIM素子を紹介したが，この分野はまだまだ若い分野であり，それだけに多くの実りある成果に発展する可能性を秘めているので，多くの研究者・開発者の参加を期待したい．

謝 辞

本稿内容は，平成元年度電気化学協会学術賞「電気化学的手法を利用した機能性薄膜の合成とエレクトロニクス材料への応用」の対象内容のうち，無電解めっきによる機能性薄膜作成の部分は割愛し，電気化学的手法による導電性高分子作成の部分を中心にまとめたものである．著者は1989年夏期期間中にミネソタ大学に客員教授として滞在し，SmyrlおよびOwens両教授との共同研究を行ったが，その成果の一部を本稿の内容の一部に加えた．その成果に対し，SmyrlおよびOwens両教授に深謝する．また，本研究室で博士論文をまとめ現在ミネソタ大学博士研究員である直井勝彦君には，本稿をまとめるに当り多くの協力をいただいたので，ここに深謝する．

文 献

1) たとえば，清水剛夫，蒲田智一，膜，11，71 (1986)；千田貢，相沢益男，小山昇，高分子機能電極，学会出版センター，1983；雀部博之，導電性高分子材料，シーエムシー出版，1983.
2) P.J. Nigrey, A.G. MacDiarmid, A.J. Heeger, JCS Chem., Commun., 1979, 594 (1979).
3) 小川雅男，第27回電池討論会要旨，p. 197 (1986)；大福英治，川越隆博，松永孜，電気化学，57，557 (1989).
4) H. Munsted, G. Kohler, H. Mohwald, D. Naegele, R. Bitthin, E. Meissner, *Synthetic Metals*, 18, 259 (1987).
5) T. Osaka, K. Naoi, *Bull. Chem. Soc. Jpn.*, 55, 36 (1982).
6) T. Osaka, K. Kitai, *Bull. Chem. Soc. Jpn.*, 57, 759 (1984)；57, 3386 (1984).
7) T.B. Hunter, P.S. Tyler, W.H. Smyrl, H.S. White, *J. Electrochem. Soc.*, 134, 2198 (1987).
8) C. Ho, I.D. Rainstrick, R.A. Huggins, *J. Electrochem. Soc.*, 127, 343 (1980).
9) 逢坂哲彌，上山健一，日本化学会第57秋季年会講演・予稿集I，p. 250 (1988)；K. Naoi, K. Ueyama, T. Osaka, W.H. Smyrl, *J. Electrochem. Soc.*, 137(2), 494(1990).
10) G. Sauerbrey, *Z. Phys.*, 155, 206 (1959).
11) K. Naoi, M.M. Lien, W.H. Smyrl, B.B. Owens, *Appl. Phys. Commn*, 9, 147(1989).
12) W.H. Smyrl, R.T. Atanasoski, L. Atanasoska, L. Hartshorn, M. Lien, K. Nygren, E.A. Fletcher, *J. Electroanal. Chem.*, 264, 301 (1989)；W.H. Smyrl, R.T. Atanasoski, L. Atanasoska, L. Hartshorn, K. Nygren, E.A. Fletcher, *J. Electroanal. Chem.*, 267, 67 (1989).
13) 清水敦，山高一則，河野正志，1988電気化学秋季大会予稿集，p.53 (1988)；大谷彰，樋口浩之，阿部正男，清水剛夫，1988電気化学秋季大会予稿集，p.53 (1988).
14) K. Naoi, W.H. Smyrl, B.B. Owens, Ext. Abst. The 176th Electrochem. Soc. Meeting (Hollywood, Florida), Vol. 89 2, p. 92 (1989)；Proc. Symp. of Rechargeable Lithium Batteries of ECS, Vol. 89 2, 1990 印刷中.
15) T. Osaka, K. Naoi, S. Ogano, *J. Electrochem, Soc.*, 135, 1071 (1988).
16) K. Naoi, T. Osaka, *J. Electrochem. Soc.*, 134, 2479 (1987)；K. Naoi, A. Ishijima, T. Osaka, *J. Electroanal. Chem.*, 217, 203 (1987).
17) S.W. Feldberg, *J. Am. Chem. Soc.*, 106, 4671 (1984).
18) B.J. Feldman, P. Burgmayer, R.W. Murray, *J. Am. Chem. Soc.*, 107, 872 (1985).
19) J. Tanguy, N, Mermilliod and M. Hoclet *J. Electrochem Soc.*, 134, 795 (1987).
20) K. Naoi, W.H. Smyrl, B.B. Owens, M.M. Lien, The 175th Electrochem. Soc. Meeting (Los Angels, CA), Extd. Abst. #576 (1989).
21) K. Kinoshita ed., "Carbon" p.293, John Wiley & Sons, Inc., (1988).
22) 伊佐功，日経ニューマテリアル1989，1，30号，p.48.
23) T. Osaka, K. Ueyama, K. Ouchi, *Chem. Lett.*, 1989, 1543.

Reprinted from JOURNAL OF THE ELECTROCHEMICAL SOCIETY
Vol. 137, No. 7, July 1990
Printed in U.S.A.

Electroactive Polyaniline Film Deposited from Nonaqueous Organic Media

II. Effect of Acid Concentration in Solution

Tetsuya Osaka* and Toshiki Nakajima

Department of Applied Chemistry, School of Science and Engineering, Waseda University, 3-4-1 Okubo, Shinjuku-ku, Tokyo 169, Japan

Katsuhiko Naoi* and Boone B. Owens*

Corrosion Research Center, Department of Chemical Engineering and Materials Science, University of Minnesota, Minneapolis, Minnesota 55455

ABSTRACT

Polyaniline films electrodeposited from acidified nonaqueous organic media were investigated for their electropolymerization behavior and charge-discharge characteristics. The solution system used for the electropolymerization of polyaniline film was CF_3COOH acidified propylene carbonate, which was previously found to be the best system for the preparation of a highly electroactive conducting polymer film. Electroactive polyaniline films only form in solutions where the mole ratio of acid (CF_3COOH) to aniline monomer is greater than one. As the acidity is increased, the resultant polyaniline film exhibits greater electroactivity and better charge-discharge performance of Li/polyaniline cathode cell. This effect may be ascribed to the high current efficiency in electro-oxidative polymerization and high redox reversibility of PAn films prepared in the high acid content solutions.

Electrodes modified by electrodeposited polyaniline (PAn) films have been investigated extensively in recent years (1-11). Such polymer-coated electrodes may be applicable to a wide range of practical devices such as capacitors, polymer batteries, ion switching devices, and electrochromic devices. Polyaniline is one of the most promising materials because of its high doping level (>50-80%) and fast switching rate. Many investigations of the electropolymerization of aniline in aqueous solutions using several different strong acids, including H_2SO_4, HNO_3, HCl, HBF_4, $HClO_4$, and CF_3COOH, have been attempted (6-9). Genies *et al.* tried to analyze the intermediate at the polymerization of polyaniline in nonaqueous fluoride salt media (12). However, the electrodeposition of polyaniline out of nonaqueous organic media (i.e., propylene carbonate (PC)) has only been reported by the present authors (1, 2).

In previous investigations, the polyaniline films deposited from nonaqueous solutions with an organic acid (CF_3COOH) of appropriate electrolyte content were highly electroactive and porous, with large charge capacity and high rate capability as well as those deposited from acidic aqueous solutions (2a). It is widely believed that the polymerization of polyaniline occurs in acidic media involving the coupling of aniline radical cations (13). The other intermediate dependent on the pH of acidified media is also discussed (14). In nonaqueous PC solutions, it may be possible to form aniline radical cations to produce active polymer films efficiently with acid addition. Thus, to acidify a PC solution without decomposing it at the same time, we tried the following five acids whose *p*Ka values varied stepwise (2b): three inorganic acids, perchloric acid ($HClO_4$), sulfuric acid (H_2SO_4), hydrochloric acid (HCl), and two organic acid, trifluoroacetic acid (CF_3COOH) and acetic acid (CH_3COOH). In the presence of HCl or $HClO_4$, PC solution was unstable due to hydrolysis in the presence of the 30-40% of water which inevitably existed in these acids. In the case of the H_2SO_4/PC solution, anilinium salts ($(Ph\text{-}NH_3)_2SO_4$) were readily precipitated. By using acetic acid or trifluoroacetic acid, the PC solvent could be acidified without any hydrolysis and only in the stronger acid medium, CF_3COOH, an electroactive PAn was successfully deposited.

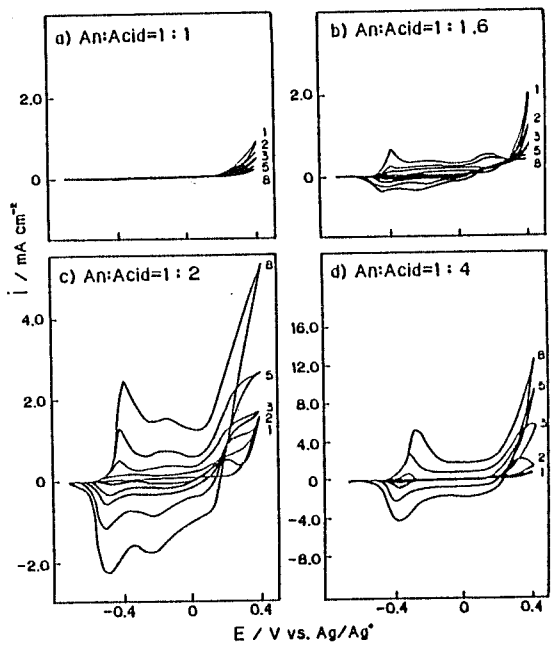

Fig. 1. Cyclic voltammograms for electropolymerization of aniline in PC solutions containing 0.5 mol dm^{-3} aniline monomer, 0.5 mol dm^{-3} $LiClO_4$ and various molarity (0.5-2.0 mol dm^{-3}) of CF_3COOH. Molar ratio of aniline monomer to acid are a) 1:1, b) 1:1.6, c) 1:2, and d) 1:4, respectively. Cycle numbers are given in figures.

* Electrochemical Society Active Member.

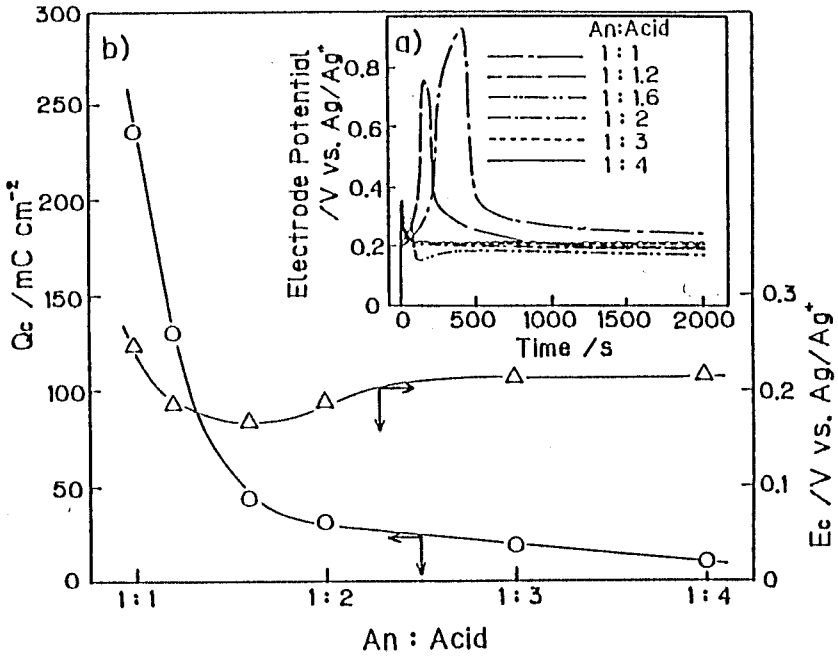

Fig. 2. (a) Potential vs. time curves during electropolymerization of polyaniline in (0.5 mol dm^{-3} aniline monomer + 0.5 mol dm^{-3} $LiClO_4$ + (0.5-2.0 mol dm^{-3}) CF_3COOH/PC solutions under galvanostatic conditions of 0.5 mA cm^{-2}. (b) Q_c and E_c values estimated from (a).

The present paper reports the effect of the relative concentrations of acid and aniline monomer in the polymerization solutions on the basically electrochemical behavior and further on the charge-discharge characteristics of polyaniline cathode in a lithium cell system.

Experimental

Solutions and film preparation.—Polymerization solutions contained 0.5 mol dm^{-3} aniline monomer, 0.5 mol dm^{-3} $LiClO_4$, and various amounts of acid (CF_3COOH). The PC (Merck) solvent was purified by percolating through activated alumina. Reagent grade products of CF_3COOH (Kanto Chemical) and $LiClO_4$ (Mitsuwa Chemical) were used without further purification. Water in the polymerization solutions was removed by adding molecular sieves.

Polyaniline films were deposited on Pt substrates (0.283 cm^2) in a three-electrode cell under argon gas atmosphere. Pt wire or plate was used as a counterelectrode and the potentials were referred to a Ag/Ag^+ (0.01 mol dm^{-3} $AgNO_3$/PC) reference electrode. Electro-oxidative polymerization method of PAn films was either a controlled-current of 0.5 mA cm^{-2} or a scanned potential between −0.7 and 0.4V at 10 mV s^{-1}.

Electrochemical measurements.—Cyclic voltammograms of the PAn films were performed in 1.0 mol dm^{-3} $LiClO_4$/PC at the same three-electrode cell. The PAn film was prepared by galvanostatic electropolymerization with a loading of up to 1 C cm^{-2}. The voltammetric apparatus included a FUSO Model 949 potentiostat modulated by function generator coupled to HOKUTO HF-201 digital coulombic-meter.

Charge-discharge tests were carried out on a Li/1.0 mol dm^{-3} $LiClO_4$, PC/PAn cell where the polyaniline was prepared with a loading of up to 20 C cm^{-2}. Li was mounted on Ni mesh electrode. Discharge of the cell was terminated when the cell voltage reached 2.0V.

SEM observations.—The morphology of the polyaniline films formed with 5 C cm^{-2} was inspected by scanning electron microscopy.

Results and Discussion

Electrochemical polymerization behavior.—Figure 1 shows the consecutive voltammograms in PC solutions containing aniline monomer. By using trifluoroacetic acid, the acid content was varied while maintaining the aniline monomer concentration at 0.5 mol dm^{-3}, and the subsequent polymerization was observed over the voltage range from 0.2 to 0.4V. As shown in Fig. 1a, when the acid content was also 0.5 mol dm^{-3}, i.e., the monomer/acid ratio = 1, electroactive film was not formed. As long as the ratio of aniline monomer to acid was greater than 1:2 (see Fig. 1a and b), currents due to the oxidative-polymerization of aniline became lower with increasing cycle number. This suggests that the film is not very conductive.

However, when the ratio was less than or equal to 1:2 (see Fig. 1c and d), an electrically conducting and electrochemically active polyaniline film was continuously formed. Furthermore, when the ratio was 1:4, the resulting film exhibited a very high electroactivity. The peak currents in the 1:4 ratio solution were twice those in the 1:2

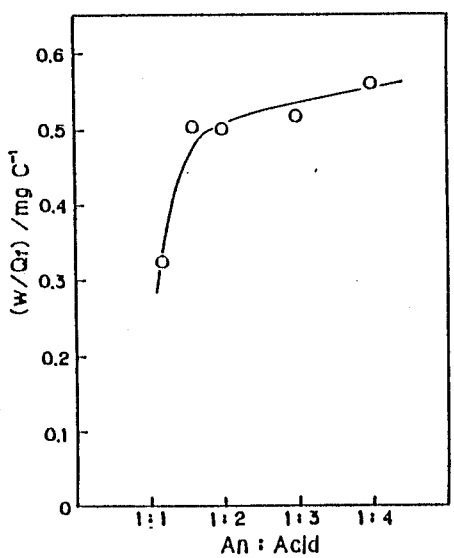

Fig. 3. Correlation of w/Q_r (weight of as deposited 1C passed polyaniline film) against the ratio of aniline to acid in polymerization solutions.

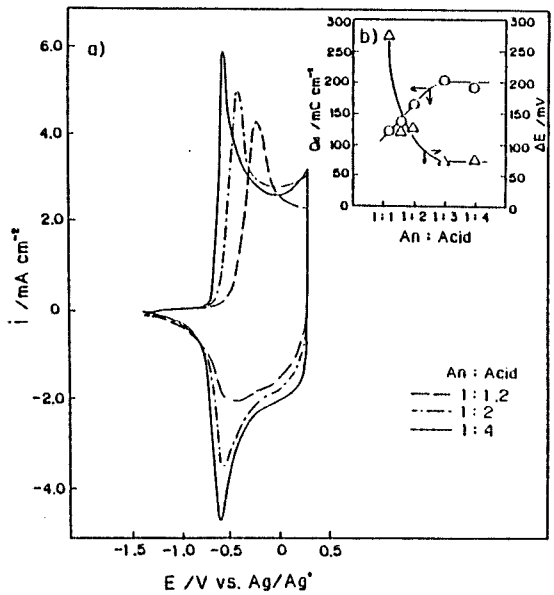

Fig. 4. (a) Cyclic voltammograms for polyaniline films (1 C cm $^{-2}$) in a 1.0 mol dm $^{-3}$ $LiClO_4$/PC solution at a scan rate of 5 mV s $^{-1}$. (b) Doping charge (Q_d) and peak separation (ΔE) values estimated from (a).

ratio solution and more than five times greater than those in the less acidic 1:1.6 ratio solution.

In the same solutions, we performed constant-current electropolymerization of 0.5 mA cm $^{-2}$ and the electrode potential was observed against the lapsed time as shown in Fig. 2a. When the ratio was 1:1, the electrode polarized to a very high potential at the initial region, and there was no electroactive polyaniline deposit on the substrate but just polyaniline oligomers dissolved into the solution, which could be confirmed by the dark green color in the solution. When the ratio was changed to 1:1.2, there was still a large amount of oligomer flow, but some polyaniline deposit was also observed on the substrate. In contrast, in the solution whose ratio is less than 1:1.6, the polymerization potential peak which appears in the initial region in potential-time curve becomes smaller, and the polymerization potential keeps constant, *ca.* 0.2V. Since the initial potential peak is assumed to be due to the initial layer formation on a bare Pt electrode, this result means that the initial layer formation on bare Pt becomes easier with a decrease in monomer/acid ratio. Figure 2b shows the effect of aniline monomer/acid ratio on the charge until constant potential (Q_c) and the constant potential (E_c), where the Q_c value is assumed to be the initial film formation charge on bare Pt. The Q_c value was measured by the coulomb meter as the charge value until the time at which electrode potential reached the potential plateau. The E_c potential decreases with monomer/acid ratio decreasing from 1:1 to 1:1.2 but after the region it increases (as shown in Fig. 2b). The reason why the E_c value exhibits high potential at the initial region of monomer/acid ratio more than 1:1.2 can be due to less film conductivity or no electroactive polyaniline deposit on bare Pt. At the region below monomer/acid ratio 1:1.6, the E_c potential increases with a decrease in monomer/acid ratio because of increasing anilinium ion.

On the other hand, the Q_c values clearly decrease with a decrease in monomer/acid ratio. It shows that an electroactive polyaniline easily deposits on bare Pt with increasing acid content in the solution. Genies *et al.* reported on PAn polymerization that an electrochemically produced cation radical reacts and makes PAn chains (12). We expect by the above results that PAn chain growth effectively occurs without side reaction when the acid content increases, though the anilinium ion monomer produced by acid addition is oxidized at higher potential (13-14).

Since the polymerization efficiency (w/Q_t) is estimated by dividing the weight (w) of deposited polymer by the charge (Q_t) passed during an electropolymerization, the relation between w/Q_t and acid/monomer ratio is shown in Fig. 3. With an increase in the acid content, the efficiency becomes higher and close to saturation in a solution containing more acid than 1:1.6. The lower value in a solution whose monomer/acid ratio is greater than 1:1.6, means that no polyaniline deposited remains on the substrate. Also the saturation in the region of solution containing more acid than 1:1.6 indicates that the polymerization efficiency becomes more than 90%.

Electrochemical doping-undoping processes.—Figure 4a shows a comparison of cyclic voltammograms (CV) for various PAn films of 1C cm $^{-2}$ equiv. amount formed in various acidified PC solutions. The scan rate for these CVs was 5 mV s $^{-1}$. There is an enhancement of the reversibility of the electrode process since the ΔE of the potential difference of anodic and cathodic peaks becomes small as shown in Fig. 4b, which may be due to a higher reversibility of the PAn film with increasing acid content. The doping charge Q_d, which is also enhanced, as shown in Fig. 4b, saturates at the monomer/acid = 1:3.

SEM observations.—Figure 5 shows SEM photographs for polyaniline films prepared from nonaqueous solutions with varying the monomer/acid ratio. As already reported

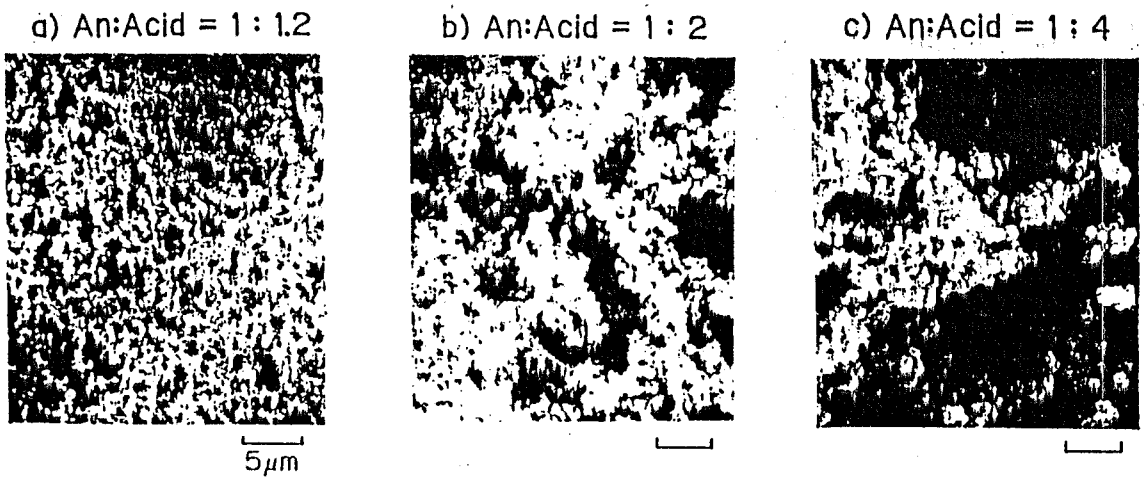

Fig. 5. SEM micrographs (top view) of polyaniline films (5 C cm^{-2})

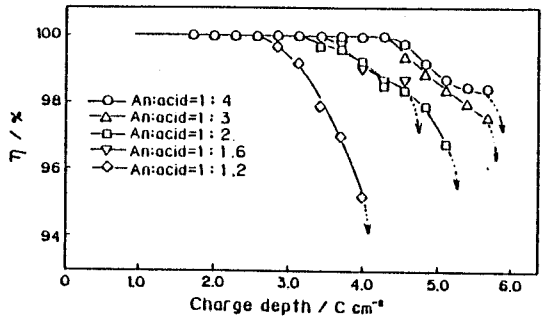

Fig. 6. Effect of charge depth on the coulombic efficiency of charge-discharge curves for $Li/LiClO_4$, PC/PAn (20 C cm^{-2}) cells. The current density at charge-discharge test was 8 mA cm^{-2}.

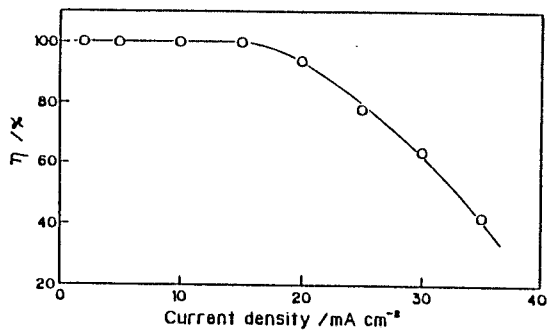

Fig. 7. Effect of charge-discharge current density on the coulombic efficiency of $Li/LiClO_4$, PC/PAn (20 C cm^{-2}) cells. The charge depth at charge-discharge test was 3.4 C cm^{-2}.

(1) the PAn film prepared in the aqueous $HClO_4$ solution has a fibrous structure. On the other hand, the film prepared in the acidified PC solution has a grainy structure. Such a grainy structure of PAn is clearly changed with a decrease in monomer/acid ratio, i.e., the grain size and the surface morphology become larger and rougher. Since PAn chain grows favorably without oligomer flow, then the polymerization results in such large size grains from higher acid content solution.

Charge-discharge performance of Li/PAn batteries.—We assembled cells with various types of PAn films and lithium electrodes, and charge-discharge tests were performed in 1.0 mol dm^{-3} $LiClO_4$/PC solutions. As is shown in Fig. 6, a remarkable enhancement of the charge capacity of the battery is observed for PAn cathode prepared in a more acidic solution. The behavior corresponds very well to the basically electrochemical properties in the cyclic voltammetric results.

In contrast the current density did not display as large a difference in the region. The dependence of preparation of PAn films from various acid contents did not display as large a difference in the region less than monomer: acid = 1:2. Figure 7 shows the most effective results on the coulombic efficiency for various current densities at a charge depth of 3.4C cm^{-2}. The Li/PAn battery maintains a 90% coulombic yield up to the current density of 20 mA cm^{-2}.

Conclusions

Two main factors are considered to be necessary for obtaining electroactive PAn from PC or other nonaqueous solutions. One is the existence of protons from an organic acid whose acidity is as high as that of CF_3COOH; the other factor is the existence of sufficient concentration of electrolyte to enhance the ionic conductivity of the nonaqueous solution. With an increase in acid content of the solution, the polymerization efficiency as well as the electroactivity of PAn films show striking enhancement. Enhancement of charge-discharge performance of Li/PAn batteries correlates well with the properties of electrochemical fundamentals of PAn films deposited from nonaqueous solutions.

Acknowledgment

This work was financially supported in part by the Grant in Aid for Scientific Research, the Ministry of Education, Science and Culture, the General Sekiyu Research and Development Foundation and also in part by the Office of Naval Research and the Defense Advanced Research Projects Agency.

Manuscript submitted July 31, 1989; revised manuscript received Dec. 5, 1989.

Waseda University assisted in meeting the publication costs of this article.

REFERENCES

1. T. Osaka, S. Ogano, and K. Naoi, *This Journal*, 135, 539 (1988).
2. (a) K. Naoi, S. Ogano, and T. Osaka, Abs. 6, p. 9, The Electrochemical Society Extended Abstracts, Vol. 88-1, Atlanta, GA, May 15-20, 1988; (b) T. Osaka, S. Ogano, K. Naoi, and N. Oyama, *This Journal*, 136, 306 (1989).
3. T. Osaka, Y. Ohnuki, N. Oyama, G. Katagiri, and K. Kanisako, *J. Electroanal. Chem.*, 161, 399 (1984).
4. T. Kobayashi, H. Yoneyama, and H. Tamura, *ibid.*, 177, 281 (1984).
5. S. W. Feldweig, *J. Am. Chem. Soc.*, 106, 4671 (1984).
6. A. Kitani, J. Izumi, J. Yano, Y. Hiromoto, and K. Sakaki, *Bull. Chem. Soc. Jpn.*, 57, 2254 (1984).
7. J. C. Chiang and A. G. MacDiarmid, *Synth. Met.*, 13, 193 (1986).
8. A. G. MacDiarmid, J. C. Ching, M. Halpern, W. H. Huang, S. L. Mu, N. L. D. Somasiri, W. Wu, and S. I. Yaniger, *Mol. Cryst. Liq. Cryst.*, 121, 173 (1986).
9. A. Kitani, M. Kaya, and K. Sasaki, *This Journal*, 133, 1069 (1986).
10. G. Zotti, S. Cattarin, and N. Comisso, *J. Electroanal. Chem.*, 239, 387 (1988).
11. K. Takei and K. Ishihara, "Research and Development of Lithium/Polyaniline Battery," Komae Research Laboratory Report, CRIEPE, Japan (1988).
12. E. M. Genies and M. Lapkpwski, *J. Electroanal. Chem.*, 220, 67 (1987); *ibid.*, 236, 189 (1987); *ibid.*, 236, 199 (1987).
13. R. N. Adams, *Acc. Chem. Res.*, 2, 175 (1969).
14. J. Bacon and R. N. Adams, *J. Am. Chem. Soc.*, 20, 6596 (1968).

PROCEEDINGS OF THE SYMPOSIUM ON

RECHARGEABLE LITHIUM BATTERIES

Edited by

S. Subbarao
Jet Propulsion Laboratory
California Institute of Technology
Pasadena, California

V. R. Koch
Covalent Associates Inc.
Woburn, Massachusetts

B. B. Owens and W. H. Smyrl
University of Minnesota
Minneapolis, Minnesota

BATTERY DIVISION

Proceedings Volume 90-5

THE ELECTROCHEMICAL SOCIETY, INC., 10 South Main St., Pennington, NJ 08534-2896

RECHARGEABLE LITHIUM/POLYMER CATHODE BATTERIES

Tetsuya OSAKA, Toshiki NAKAJIMA, Koh SHIOTA
and Boone B. OWENS*

Department of Applied Chemistry,
Waseda University
Okubo, Shinjuku-ku, Tokyo, Japan 169

*Corrosion Research Center,
University of Minnesota
221 Church St. SE, Minneapolis, MN 55455

Abstract

Lithium/polymer cathode batteries have high energy density and cell design flexibility. Ability of the electropolymerized polymers are controllable by some methods (e.g. polymerized with various anions, electrolytic conditions, NBR guided grown method). Among these polymers, an electrochemically-formed PAn appears to be most promising candidate. On the viewpoint of the application in Li batteries, the polymerization of PAn in non-aqueous solutions is advantageous because of no contamination by water. Usually, electroactive PAn is electropolymerized in acidic aqueous solutions. However, we have successfully prepared electroactive PAn in non-aqueous solutions.

Recently lithium/polymer cathode batteries as shown in Fig.1 have been developed. The Bridgestone Corp. & SEIKO Instruments Inc. group utilize an electropolymerized polyaniline(PAn) as the cathode material in a Li-Al/PC-DME, $LiBF_4$/PAn battery(1). In a prototype Li/PC,$LiClO_4$ /polypyrrole(PPy) battery by the BASF/VARTA group(2), the cathode is an electropolymerized PPy multilayer.

Extensive investigations of electropolymerized conductive polymer films have created such cathode material in recent years. Figure 2 demonstrates the practical potential region of Li/polymer cathode batteries, where the capacity(Ah kg^{-1}) is given per cathode material weight(3). In Fig. 2, the data for inorganic intercalation compounds as cathode are adopted under the stable charging-discharging conditions given by Yamaki(4). The capacity of Li/polymer batteries is clearly equal or inferior to that of Li/inorganic intercalation materials or Ni-Cd batteries. However, the energy density is superior because of its high cell voltage such as 3.0-3.2 V. Since the

feature of a polymer is that it is flexible and form free, it corresponds basically to any cell design. Among electropolymerized polymers, polypyrrole(PPy), polyaniline(PAn) and polyazulene(PAz) have the highest possibility for use as cathode materials of rechargeable Li batteries. Examples of the Li/polymer cathodes under laboratory level are listed in the Table(5,6,7). The value of MnO_2 is tabulated for reference(8). The energy densities in the table are the values per weight and volume of cathode materials under the conditions of stable rechargeable region.

In our research group, we have first investigated PPy with varying preparation methods, namely, polymerization with various anions(7) and with NBR(nitrile butadiene rubber)-guided-grown method(9,10). Since an electrochemically-formed PAn appears to be one of the most promising candidates for the cathode material because of its high electroactivity and relatively high doping level as is seen in the table, we have recently continued to investigate the new preparation method of PAn as well as that of PPy. Usually, electroactive PAn is prepared by electropolymerization in acidic aqueous solutions. However, we have successfully prepared electroactive PAn in non-aqueous solutions(5). In light of the application in Li batteries, the polymerization of PAn in non-aqueous solutions is advantageous because of no contamination by water.

In this paper, we report the electroactive PAn prepared from a non-aqueous solution and compare it with PPy prepared from some methods.

Properties of PPy films can be controlled by varying the anions at the polymerization. When polymerized with PF_6^- or $CF_3SO_3^-$ anion, the PPy films become to give higher doping capacity of ClO_4^- anion at the condition of $LiClO_4$-PC solution, and the Li/PC,$LiClO_4$/PPy battery assembled with the PPy cathode formed with PF_6^- keeps 100% coulombic yield up to the current density of 2.5 mA cm^{-2} (7). Moreover, PPy preparation through the host polymer of NBR insulating film can make the structure for accelerating anion diffusion in the film(9). The NBR-guided-grown PPy (PPy/NBR), where NBR is removed after PPy polymerization, especially improves the anion doping-undoping process. The battery assembled with PPy/NBR cathode can output more than 3 times larger current density especially at low doping level(10).

Figure 3 shows the schematic diagram of polymerization conditions of PAn films. An electroactive PAn film was successfully obtained by electropolymerization from non-aqueous propylene carbonate(PC) solution containing CF_3COOH and $LiClO_4$. The most important factor to form electroactive PAn is protons from an organic acid. Its

acidity strongly affects the activity and reversibility of anion doping-undoping.

The comparison of the cell properties and film morphology of PAn prepared in aqueous and non-aqueous solutions are given in Fig.4. Though the morphology between them is quite different, the cell properties and performances are almost equal to each other.

In order to confirm the effect of acid content, one of the most important factors to affect the electrochemical activity of the films, the basic properties of PAn films were investigated as is seen in Fig.5.

Figure 5 shows the effect of acid content at the polymerization and the highest ratio of acid : aniline in the polymerization solution gives beautiful reversibility of anion doping-undoping. The PAn film formed with the condition of ratio 4:1 finally gives the excellent battery performance as is seen in Figure 7.

In conclusion, the lithium/polymer cathode batteries have high energy density and are corresponding to any shape of cell design. Ability of electropolymerized films can be controlled by some methods. Especially, the electropolymerized PAn, which has high electrochemical activity, can be prepared in non-aqueous solution as well as in aqueous solution.

References

1. M. Ogawa, T. Fuse, T. Kita, T. Kawagoe, and T. Matsunaga, *Proc. Battery Meeting of Jpn.*, p197(1986).
2. H. Munsted, G. Kohler, H. Mohwald, D. Naegele, R. Bitthin, and E. Meissner, *Sythetic Metals*, 18, 259(1987).
3. T. Osaka, and K. Ueyama, *Kagaku Kogyo (Chemical Industry)*, 40, 231(1989).
4. J. Yamaki, *Denki Kagaku*, 56, 5(1988).
5. T. Osaka, S. Ogano, K. Naoi, and N. Oyama, *J. Electrochem. Soc.*, 136, 306(1989).
6. T. Osaka, K. Naoi, and T. Hirabayashi, *J. Electrochem. Soc.*, 134, 2645(1987).
7. T. Osaka, K. Naoi, and S. Ogano, *J. Electrochem. Soc.*, 135, 1071(1988).
8. N. Furukawa, T. Saito, K. Teraji, and I. Nakano, *Proc. Symp. on Primary and Secondary Ambient Temperature Lithium Batteries*, Electrochemical Soc. Inc., p557(1988).
9. K. Naoi, and T. Osaka, *J. Electrochem. Soc.*, 134, 2479(1987).
10. K. Naoi, A. Ishijima, and T. Osaka, *J. Electroanal. Chem.*, 217, 203(1987); T. Osaka, and K. Naoi, *Shokubai (Catalyst)*, 29, 130(1987).

Table Performance of Li/polymer secondary batteries (experimental data).

Cathode materials	Doping level [%]	Output voltage [V]	Charge capacity [Ah kg^{-1}]	Energy density [Wh kg^{-1}]	[Wh l^{-1}]
Polyaniline(5)	60	3.0	127	382	180
Polyazulene(6)	30(45)	3.3	70(102)	226(338)	187(279)
Polypyrrole(7)	25(45)	3.0	81(130)	243(390)	223(361)
MnO_2 (8)	0.14(e/Mn)	2.7	40	108	473

( ): Values at maximum doping level.

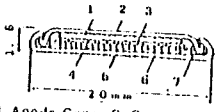

1. Anode Case 2. Current collector
3. Anode 4.Separator
5. Cathode 6. Cathode Case
7. Gasket

a) Coin type LI/PAn battery
(Bridgestone Corp., Seiko I)

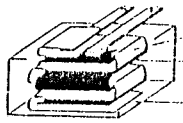

b) LI/PPy multilayer
type battery (BASF/BARTA)

Fig.1 Examples of lithium /polymer cathode batteries.

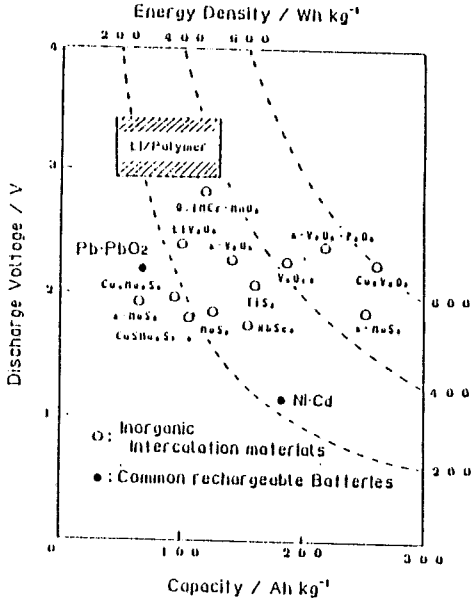

Fig.2 Characteristics of cathode materials in lithium/inorganic intercalation compound batteries and lithium/polymer batteries.

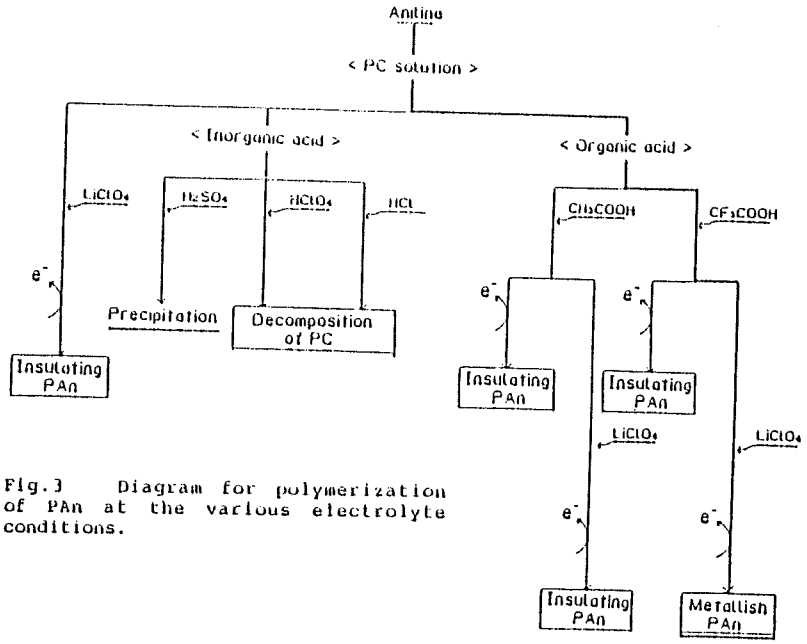

Fig.3 Diagram for polymerization of PAn at the various electrolyte conditions.

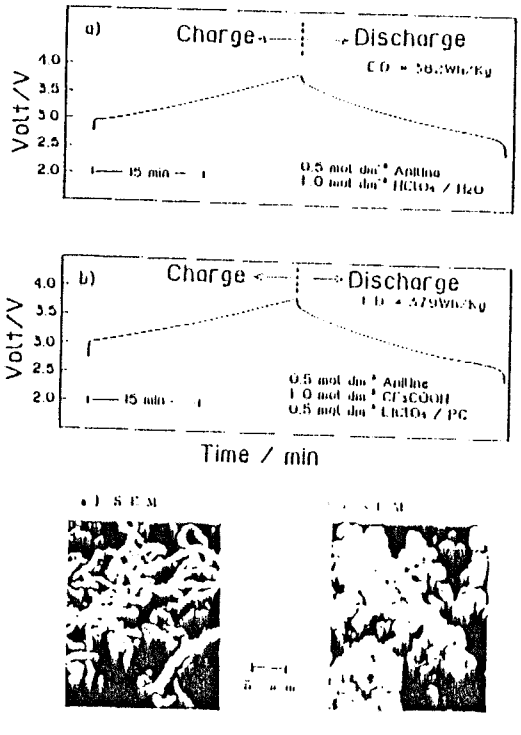

Fig.4 Charge-discharge performances of Li/PC,$LiClO_4$ /PAn batteries and SEM photographs. Polyaniline films were deposited from a) H_2O and b) PC solutions.

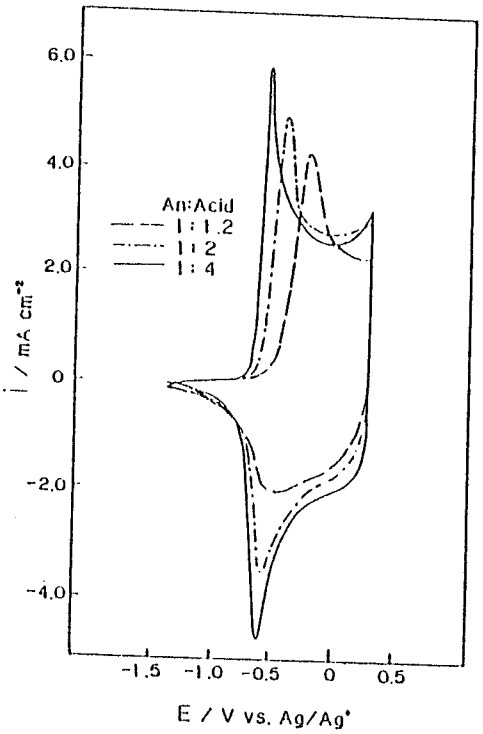

Fig.5 Cyclic voltammograms for PAn films (1 C cm^{-2}) in 1.0 mol dm^{-3} $LiClO_4$/PC solutions. The scan rate is 5 mV s^{-1}. PAn films are prepared in (0.5 mol dm^{-3} aniline + some concentration of CF_3COOH + 0.5 mol dm^{-3} $LiClO_4$)/PC solutions.

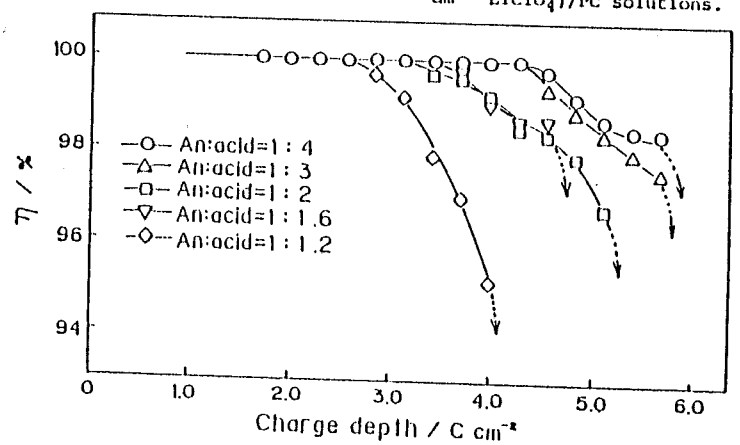

Fig.6 Dependence of charge depth on the coulombic yield for Li/PC,$LiClO_4$/PAn(20 C cm^{-2}) batteries. The charge- discharge current density was 8 mA cm^{-2}.

CHEMISTRY LETTERS, pp. 1535 1538, 1990.

An Application of Polypyrrole Films Electropolymerized in NaOH Aqueous Solution to Non-linear MIM Devices

Tetsuya OSAKA,* Kiyoshi OUCHI, and Toshihiro FUKUDA
Department of Applied Chemistry, School of Science and Engineering,
Waseda University, 3-4-1 Okubo, Shinjyuku-ku, Tokyo 169

Thin films of electroinactive polypyrrole(PPy) were electropolymerized in NaOH aqueous solutions on ITO(indium tin oxide) electrode. The PPy films were used at as-prepared condition without undoping process. The metal-insulator-metal(MIM) structure was fabricated by sputtering ITO on the PPy films to give ITO/PPy/ITO devices. The devices showed non-linear and symmetric I-V characteristics, where the currents sharply increased at ca. ±5 V.

An MIM(Metal-Insulator-Metal) device is practically used as a switching device for driving liquid crystal(LC) and expected to realize a larger area LC display because of its simple manufacturing process.[1] Many studies of organic insulating layers for MIM devices have been reported, for example, LB(Langmuir Blodgett) films,[2] evaporated polymer films such as polyethylene,[3] and so on. With regard to an electropolymerized film as an insulator, we first reported the I-V characteristics of the MIM device using the undoped poly-N-methylpyrrole(PMPy) film.[4] Since the as-prepared PMPy film containing ClO_4^- anion is conducting, it has to be undoped to obtain an insulating state for non-linear characteristics. If an electroinactive film can be obtained directly at as-prepared condition, it is more useful for its application. Electroinactive films such as polyphenol[5] and polyaniline prepared in non-acidified conditions[6] have already been reported, however, we failed to get a suitable film from these polymers concerning the adherence to ITO electrode. Then we found that an inactive PPy film electropolymerized in a NaOH aqueous solution is suitable for the insulator owing to its adherence and low conductivity. The preparation of the nonconducting PPy in the NaOH solution has only been stated briefly by Murthy et al. without detailed conditions.[7] In this letter, we will report the proper conditions of preparing the PPy film in the basic solution for the application to the insulator of MIM device and refer to its I-V char-

acteristics.

The electrolytes were 0.1 mol dm^{-3}(M) and 0.01 M NaOH aqueous solutions containing 0.25 M pyrrole. The PPy films were formed on ITO electrode (ca. 400 nm) by constant potential electrolysis at 1.5 V vs. Ag/AgCl. ITO/PPy/ITO devices were fabricated by sputtering ITO(ca. 60 nm) on the PPy films which were washed in water and dried with the stream of argon gas after electropolymerization. The pattern profile of the MIM devices used here was the same as in the previous experiments,[4] where the hole sizes for polymer layer were 100, 300, 500, 700, 1000 μm in diameter. In the experiments, the device of each hole size gave the same results of I-V characteristics, and thus all the results were represented with the devices of 300 μm diameter. I-V characteristics were measured between $\pm$10 V by 0.5 V step.

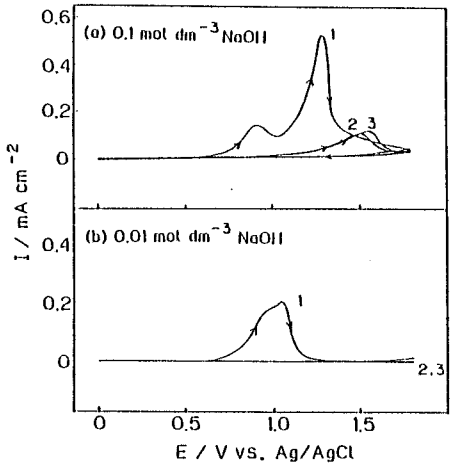

Fig. 1. Cyclic voltammograms at 10 mV s^{-1} in NaOH aqueous solutions containing 0.25 M pyrrole: (a) 0.1 M NaOH, (b) 0.01 M NaOH. Figures indicate the cycle numbers.

Electroactivity of the PPy was investigated by cyclic voltammetry in the two aqueous electrolytes. Figures 1(a) and 1(b) show the cyclic voltammograms in the electrolyte of 0.1 M and 0.01 M NaOH, respectively, scanned at 10 mV s^{-1} over the range between 0.0 V and 1.8 V vs. Ag/AgCl. At the first cycle, irreversible anodic currents are observed in both (a) and (b), and simultaneously PPy thin films are deposited on the ITO electrode. On the other hand, the polymerization current decreases sharply(a) or scarcely flows(b) after the first cycle. This means that the PPy films deposited from the NaOH basic solutions are electroinactive and nonconducting. It was reported by Li et al.[8] that OH^--doping and undoping of an electroactive PPy are observed by cyclic voltammetry in a NaOH solution with a decrease in the conductivity of the PPy, but that OH^- ion reacts irreversibly upon the PPy chain at the high potential electrolysis. Judging from the inactivity of the PPy films in our experiment, it was supposed that the irreversible reaction occurs between the PPy or pyrrole monomer and OH^-. The reaction might take place between α or β-carbons and OH^- and form C=O groups in the polymer chain leading to the shortening of the π-conjugation length, which is similar to the overoxidation suggested by F. Beck et al.[9]. The shape of the voltammogram (a) in the 0.1 M solution has another large peak at the first cycle, in contrast to (b) in the 0.01 M solution. The anodic peak at more positive potential in the voltammogram (a) is related to an oxygen evolution current judging from the results of

blank solution. In the blank solution without pyrrole monomer, the current for the oxygen evolution was distinctly detected at more than 0.90 V in the similar voltammogram of both NaOH concentrations. Therefore, the PPy film from the 0.01 M NaOH solution is suggested to be more tight, and the morphology of the PPy is probably influenced by the OH^- concentration. From scanning electron microscopy(SEM) observations, the PPy film from the 0.1 M solution became rougher and thicker film compared with that from the 0.01 M solution. Accordingly, we selected the 0.01 M NaOH solution for preparing the insulation layer of the MIM device.

The electropolymerization of the PPy for the MIM device was operated by potentiostatic electrolysis, which prepared the same inactive PPy film at 1.5 V vs. Ag/AgCl. The PPy film in the 0.01 M NaOH solution was ascertained by the SEM graphs to be thin and smooth, and the MIM device using the PPy film gave reproducible I-V characteristics. Figure 2 shows the relation between current and voltage for the MIM device using the PPy film electropolymerized for 50 min. The positive and negative directions in Fig. 2(a) and 2(b) correspond to positive and negative bias to the ITO electrode, respectively. It can be seen in Fig. 2(a) that the current behavior is symmetrical for positive and negative voltage, and the increase of non-linear current becomes nearly 5 orders between 0.5 V and 10 V. The device shows the possibility of practical use for switching by the threshold sharpness at $\pm$5 V in Fig. 2(b).

Since the initially deposited PPy film was insulated state, the current flow for electrolysis and the growth of film ceased immediately after the start of potentiostatic control. No appreciable change of the film thickness(ca. 0.2 μm) was actually observed between the films electrolyzed for 15 min and 60 min by SEM or a talysurf measurement. However, the

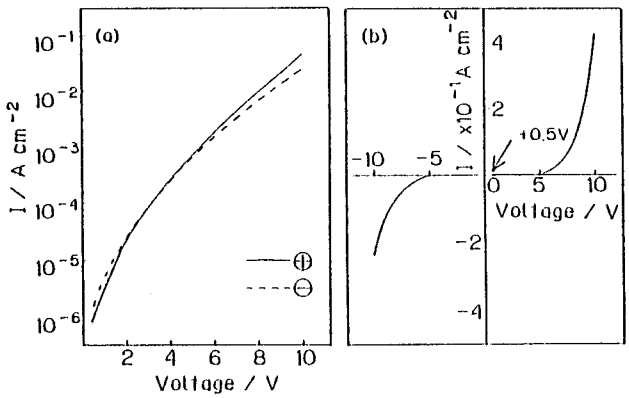

Fig. 2. I-V characteristics of an ITO/PPy/ITO device. PPy was electropolymerized for 50 min: (a) logI-V, (b) I-V.

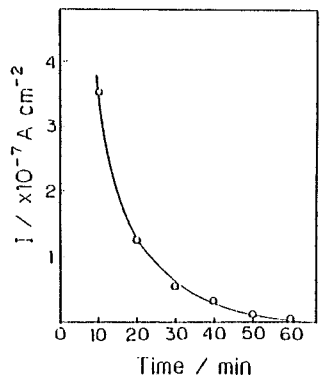

Fig. 3. Currents through the devices at the voltage of +0.5 V as a function of electrolyzed time.

currents at the bias voltage of 0.5 V in the I-V curves clearly change as a function of the electrolyzed time, i. e., the insulation resistance of the PPy increases with electrolyzed time. The currents at 0.5 V(see an arrow position in Fig. 2 (b)) are shown in Fig. 3. The increase in the insulation resistance may imply the decrease in pin-hole condition of the film, which is supported by the results that the MIM devices using the PPy films polymerized less than 20 min easily become breakdown at the high electric field of 10 V. Thus, the satisfactorily tight and pinhole-free PPy film is considered to be formed with sufficient electrolysis time irrespective of no growth of film thickness.

In conclusion, the electroinactive and nonconducting PPy film electropolymerized in the NaOH solution was proved to be an excellent insulator for the MIM device. It can be used as-prepared condition, which is more desirable for the application to the MIM device than the previously reported one.[4] Moreover, the MIM device using the PPy deposited from the NaOH solution is also superior to the previous one with respect to the stability of I-V characteristics.

A part of this work was financially supported by Grants of Scientific Research from the Japanese Ministry of Education, Science and Culture, and of General Sekiyu Research & Development Encouragement & Assistance Foundation.

References

1) D. R. Baraff, J. R. Long, B. K. MacLaurin, C. J. Miner, and R. W. Streater, Conf. Record. of 1980 Biennial Display Research Conf., IEEE, p.107 (1980).
2) K. Sakai, H. Matsuda, H. Kawada, K. Eguchi, and T. Nakagiri, Appl. Phys. Lett., 53, 1274 (1988).
3) C. A. Hogarth and M. Zor, Phys. Status Solidi A, 98, 611 (1986).
4) T. Osaka, K. Ueyama, and K. Ouchi, Chem. Lett., 1989, 1543.
5) Y. Ohnuki, H. Matsuda, T. Ohsaka, and N. Oyama, J. Electroanal. Chem., 158, 55 (1983).
6) T. Ohsaka, Y. Ohnuki, and N. Oyama, J. Electroanal. Chem., 161, 399 (1984).
7) A. S. N. Murthy, S. Pal, and K. S. Reddy, J. Mater. Sci. Lett., 3, 745 (1984).
8) Y. Li and R. Qian, Synth. Met., 26, 139 (1988).
9) F. beck, P. Braun, and M. Oberst, Ber. Bunsenges. Phys. Chem., 91, 967 (1987).

(Received June 5, 1990)

Proceedings Report
RP2415-22
November 1990

WORKSHOP PROCEEDINGS

RECHARGEABLE
LITHIUM POLYMER BATTERIES

SPONSORED BY

THE ELECTRIC POWER RESEARCH INSTITUTE

AND

THE U.S. DEPARTMENT OF ENERGY

OCTOBER 11-13, 1990

THE WOODMARK HOTEL

KIRKLAND, WASHINGTON

RECHARGEABLE LITHIUM/POLYMER BATTERIES
- APPLICATION OF ELECTROPOLYMERIZED POLYMER FILMS TO LITHIUM BATTERIES -

Tetsuya OSAKA

Department of Applied Chemistry,
School of Science and Engineering,
Waseda University,
Okubo, Shinjuku-ku, Tokyo 169, Japan

INTRODUCTION

Electropolymerized conductive polymer films have been extensively investigated in recent years(1). Among these polymers, polyaniline(PAn), polypyrrole(PPy) and polyazulene(PAz) can be utilized as one of the promising candidates for cathode materials in future rechargeable lithium cell systems(2). The model of new secondary batteries utilizing electrochemically conductive PPy is recently examined to gain a better understanding of such new batteries(3), and possibility and limit of the cell performance of polymer cathode systems are theoretically indicated(4). Many researchers have paid an attention to polyaniline as a cathode material of lithium batteries, because of its high energy density, chemical stability, and high reversibility of doping-undoping process. The Bridgestone Corp. and the Seiko Instrument Inc. group realized the coin type battery utilizing an electropolymerized PAn as the cathode material(5) although the cell capacity is small.

In this paper, I will overview the electropolymerized polymers as a cathode material for rechargeable lithium batteries.

LITHIUM/POLYMER BATTERIES

The battery systems using polymers are schematically given in Fig. 1. Li/p-type polymer cell is the most common system because there are a lot of p-type conducting polymers. The system has a demerit to need larger electrolyte volume because of decrease in dopant concentration during charge process. The system of Li/n-type polymer, however, can avoid this disadvantage because only Li^+ ion moves as dopant during charge-discharge process. Unfortunately, there are very little kinds of n-type polymer, but another combination such as p-type polymer with polymer anion works as the same behavior as shown in Fig. 1d). For example, the composite membrane of PPy with PSS(polystyrenesulfonate) is examined, where only Li^+ is the moving ion in appearance(6).

The candidates of cathode materials for rechargeable Li batteries at ambient temperature are inorganic intercalation compounds as well as organic

conductive polymers. Figure 2 shows representative battery capacities of rechargeable Li batteries, where the possibility of Li/polymer battery is indicated. The capacity using polymer is inferior to that using inorganic compounds, however, the energy density becomes relatively higher because of its higher output voltage. Also, the polymer has higher power density because of its rapid kinetics of doping-undoping reaction. The most advantage of polymer batteries is that Li/polymer batteries have flexible form-free feature, as shown in Table 1, as well as higher voltage. Some demerits are also listed in Table 1.

Some samples of prototype or more advanced type batteries are shown in Fig. 3, where the coin type with PAn cathode is commercially available. The prototype of cylinder type has ca. 50 Wh kg^{-1} energy density per cell. The most possible candidates of polymer cathode materials are listed in Fig. 4, and the feature of PAn and PPy films as the most possible materials, which are used in Fig. 3, is shown in Table 2. PAn film has high doping level to keep larger capacity, while the PPy film has stronger mechanical strength.

PPy(POLYPYRROLE) CATHODES

[1] ANION EFFECT OF PPy PREPARATION

Film properties of PPy are strongly dependent on the species of electrolyte anions in the polymerization solution, and they can be controlled by varying the anions at PPy polymerization(7). Figure 5 shows the relationship between the doping charge of ClO_4^- dopant and the polymerization potential for PPy films formed with ClO_4^-, $CF_3SO_3^-$ or PF_6^- anions as a function of deposition charge. When polymerizing with PF_6^- or $CF_3SO_3^-$ anion, the PPy films become to give higher doping charge of ClO_4^- anion at the conditions of $LiClO_4$-PC(propylene carbonate) solution as is seen in Fig. 5. Battery performance of Li/$LiClO_4$-PC/PPy is given in Fig. 6. The battery assembled with the PPy cathode formed with PF_6^- keeps 100% coulombic yield up to the current density of 2.5 mA cm^{-2} at 20% doping charge level.

[2] PPy MORPHOLOGY MODIFICATION WITH NBR(NITRILE BUTADIENE RUBBER)

PPy preparation with the host polymer of NBR insulating film can make the structure rougher for accelerating anion diffusion in the film(8). A schematic image for the preparation procedure of NBR-aided grown PPy electrode (Pt/NBR/PPy) is illustrated in Fig. 7. A Pt substrate was first coated with a commercially available NBR prepolymer and dried completely. The NBR precoated Pt electrode was then immersed in the same polymerization solution used for the preparation of the Pt/PPy electrode. Thereafter, also on the Pt/NBR electrode, PPy was grown at 0.8V *vs.* Ag/Ag^+. After PPy was formed by passing 1 C cm^{-2}, the host polymer of NBR film was totally washed away with MEK (methylethylketone) and subsequently dried. By the SEM observation of

the films, the NBR-aided grown PPy film becomes more porous and rougher conditions than those of PPy film directly grown on Pt electrode. The battery performance of Li/$LiClO_4$-PC/PPy grown with NBR is shown in Fig. 8. The battery performance is observed to be very much enhanced with regard to both charge-discharge current density and charge capacity, especially the current density becomes three times larger at low doping level(9).

PAn(POLYANILINE) CATHODES

An electroactive PAn film was successfully obtained by electropolymerization from non-aqueous solution of propylene carbonate(PC) containing CF_3COOH and $LiClO_4$(10). The battery performance of lithium battery using PAn film deposited from PC solution was similar to that of the cell using PAn cathode deposited from aqueous solution, as is seen in Fig. 9. The most important factor to form electroactive PAn film is proton from an organic acid and its acidity strongly affects the activity and reversibility of anion doping-undoping process. The effect of acid content at the polymerization was clearly given and the PAn film formed with the conditions of 4:1 ratio (acid:aniline) finally gave the excellent battery performance as seen in Fig. 10(11).

CONCLUSION

The most advantage of Li/polymer batteries is form-free feature, moreover, the some disadvantages can be overcome by morphology control or development morphology for preparation method as is discussed in the text. The control of morphology gives the higher current density and also an increase of energy density per cathode materials.

As for future targets, the following three are the most attractive items to be developed in future in the field of Li/polymer batteries.

*R&D for solid polymer electrolyte with higher conductivity.
*R&D for p-type polymer with polymer anion.
(high voltage, constant volume)
*R&D for new material of n-type polymer.

REFERENCES

1. T.Osaka, T.Nakajima, K.Shiota and B.B.Owens, *Ext. Abst. of the 176th ECS Meeting (Hollywood, florida)*, 89-2, Abst. No.61 (1989); *Proc. of Symp. on Rechargeable Lithium Batteries*, S.Subbarao, V.R.Koch, B.B.Owens and W.H.Smyrl, ed by, p.170, Electrochem. Soc. Inc., NJ (1990).
2. T.Osaka and K.Ueyama, *Kagaku-Kogyo(Chemical Industry)*, March Issue, p.31 (1989).
3. T.Yeu and R.E.White, *J. Electrochem. Soc.*, 137, 1327 (1990).
4. K.Naoi, B.B.Owens and W.H.Smyrl, *Ext. Abst. of the 176th ECS Meeting (Hollywood, Florida)*, 89-2, Abst. No.63 (1989); *Proc. of Symp. on Rechargeable Lithium Batteries*, S.Subbarao, V.R.Koch, B.B.Owens and W.H.Smyrl, ed by, p.170, Electrochem. Soc. Inc., NJ (1990).
5. M.Ogawa, T.Fuse, T.Kida, T.Kawagoe and T.Matsunaga, *Proc. of Battery Meeting of Jpn.*, p.197 (1986).
6. T.Iyoda, A.Ohtani, T.Shimizu and K.Honda, *Synthetic Metals*, 18, 747 (1987).
7. T.Osaka, K.Naoi and S.Ogano, *J. Electrochem. Soc.*, 135, 1071 (1988).
8. K.Naoi and T.Osaka, *J. Electrochem. Soc.*, 134, 2479 (1987).
9. T.Osaka and K.Ueyama, *"Practical Lithium Batteries"*, p.114, JES Press, Ohio (1987).
10. T.Osaka, S.Ogano, K.Naoi and N.Oyama, *J. Electrochem. Soc.*, 136, 306 (1989).
11. T.Osaka, T.Nakajima, K.Naoi and B.B.Owens, *J. Electrochem. Soc.*, 137, 2139 (1990).

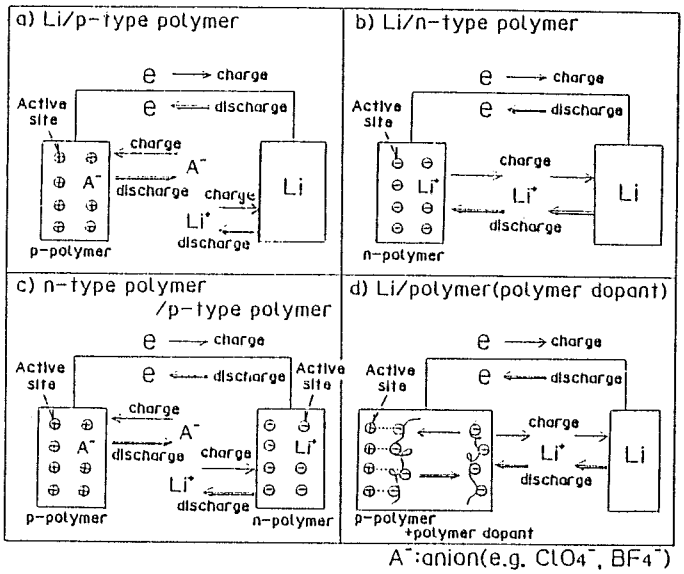

Fig.1 Various types of lithium/polymer batteries.

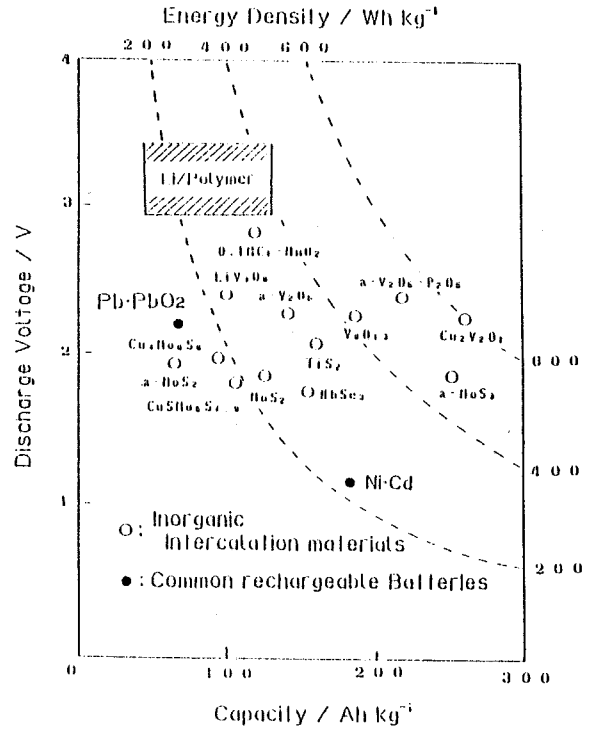

Fig.2 Performances of various rechargeable lithium batteries.

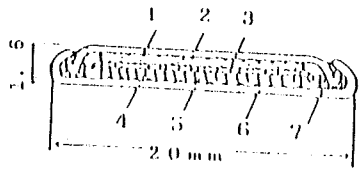

1. Anode Case 2. Current collector
3. Anode 4.Separator
5. Cathode 6. Cathode Case
7. Gasket

a) Coin type Li/PAn battery
(Bridgestone Corp., Seiko I)

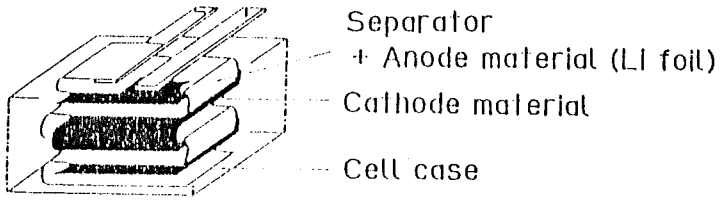

b) Li/PPy multilayer
type battery (BASF/BARTA)

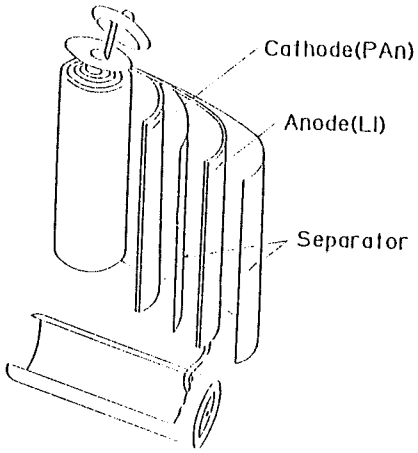

c) Cylinder type Li/PAn battery
(Furukawa Electric, Tokyo Electric Power)

Fig.3 Prototype and more advanced type lithium/polymer batteries using conductive polymers.

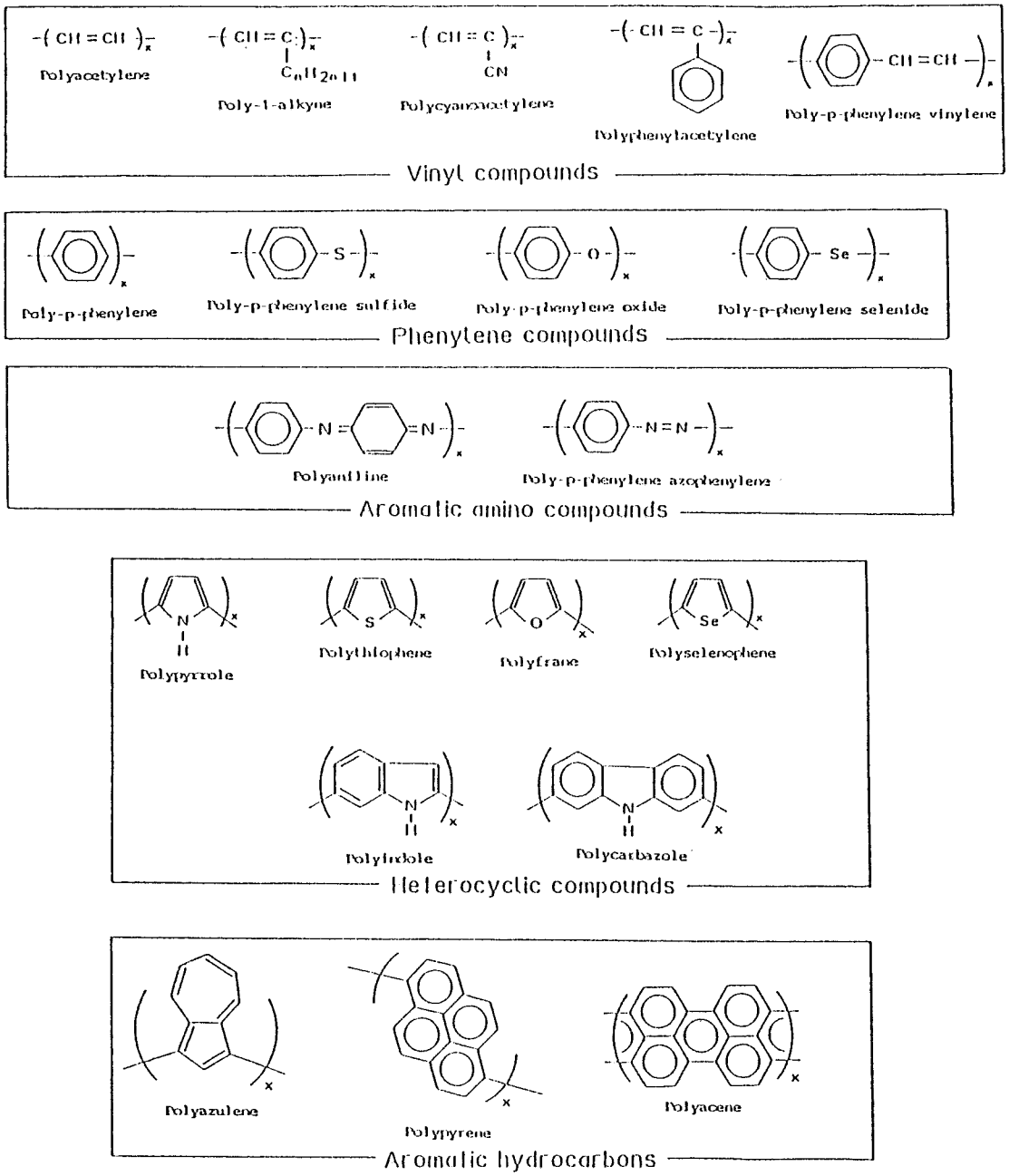

Fig.4 Classification of organic conductive polymers in terms of the chemical structure.

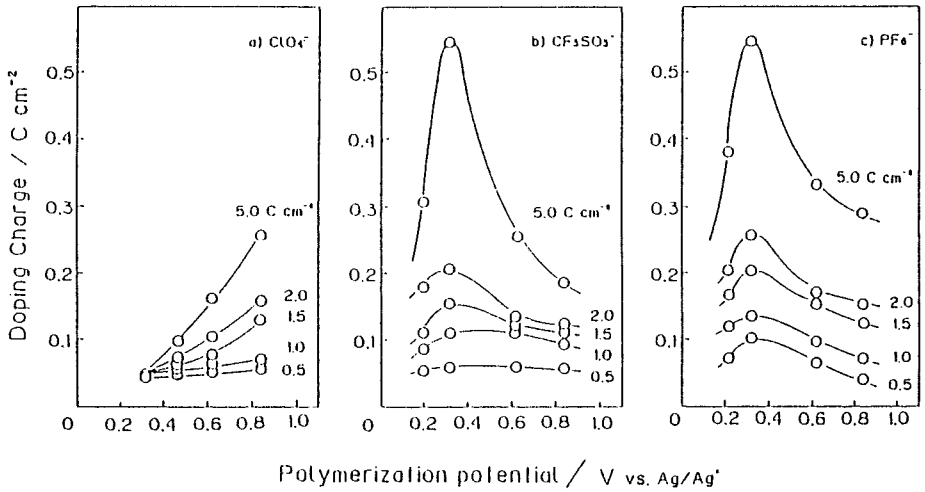

Fig.5 Dependence of polymerization potential on the dopoing charge of PPy films deposited with various supporting anions of a)ClO_4^-, b)$CF_3SO_3^-$ and c)PF_6^- as a function of the film thickness.

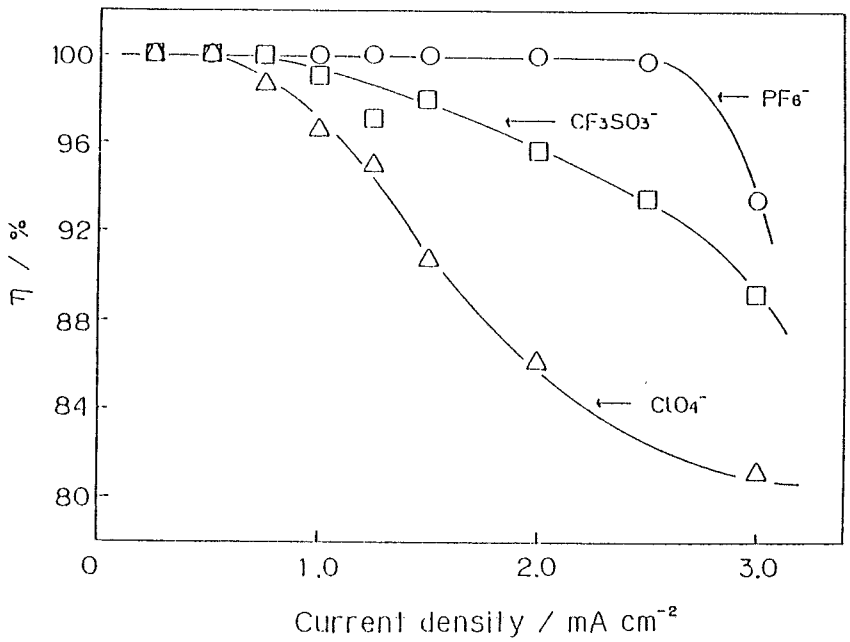

Fig.6 Dependence of current density on the coulombic efficiency of Li/$LiClO_4$-PC/PPy(5 C cm^{-2}) batteries; charge depth=20% of doping level.

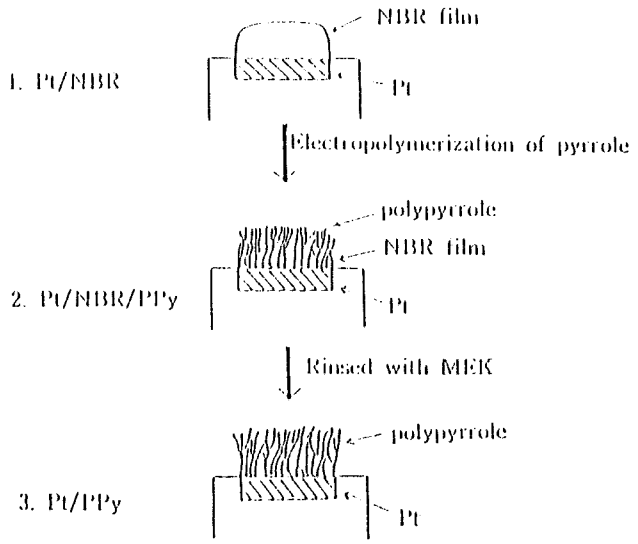

Fig.7 Preparation procedure of NBR/PPy(NBR-guided grown PPy) film.

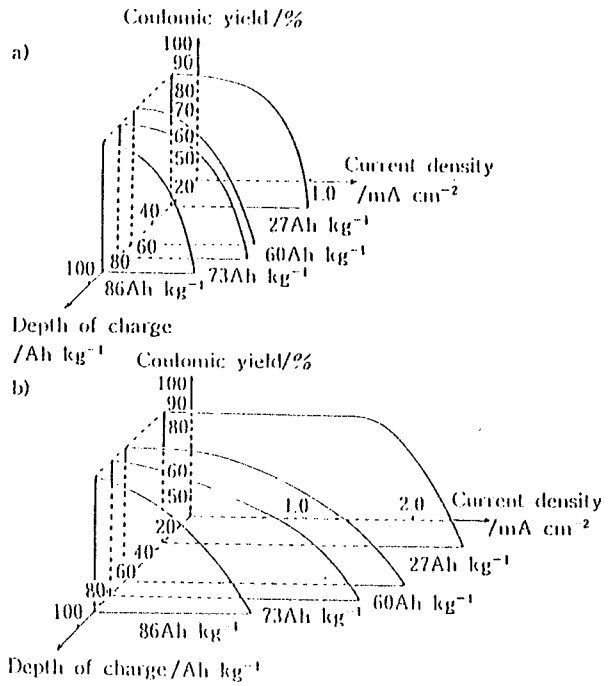

Fig.8 Comparison of charge-discharge performance of a)Li/$LiClO_4$-PC/(Pt/PPy) and b)Li/$LiClO_4$-PC/(Pt/NBR/PPy) batteries.

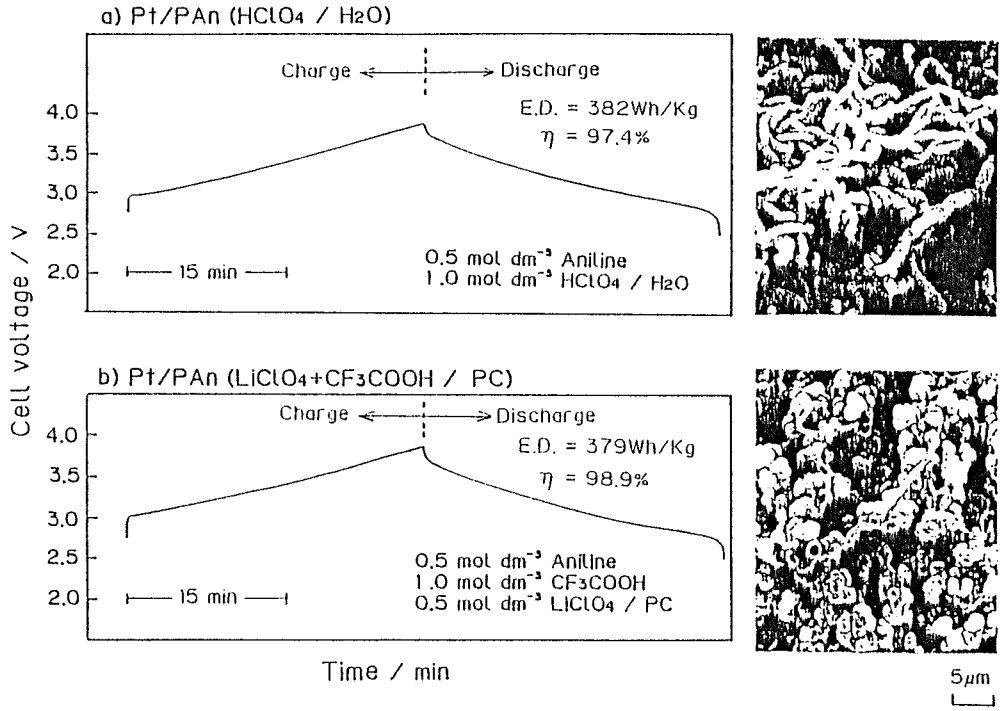

Fig.9 Charge-discharge curves of Li/$LiClO_4$-PC/PAn batteries at a constant current density of 2.0 mA cm^{-2} and SEM micrographs of PAn films deposited from a)aqueous solution containing $HClO_4$ and b)PC solution containing $LiClO_4$ and CF_3COOH.

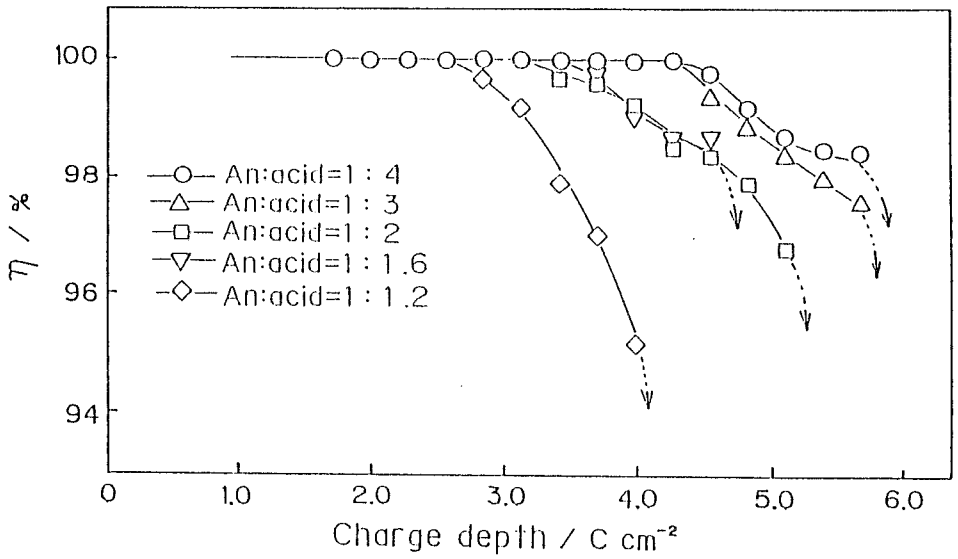

Fig.10 Dependence of charge depth on the coulombic efficiency for Li/$LiClO_4$-PC/PAn batteries as a function of aniline:acid ratio in polymerization solution.

Table 1. Merits and demerits of Li/Polymer batteries.

Merit

1. Form-free
2. High Energy Density and Capacity / Weight
   (~ 400 Wh/kg, 100 ~ 150 Ah/kg)
3. High Power Density / Weight

Demerit

1. Chemical and Physical Stability of Polymer Cathodes
2. Stablity of Non-aqueous Electrolyte due to higher voltage
3. Self-dischargeability of Li/Polymer Batteries

Common problem for Li batteries
Li anode cycleability and safety

Table 2. Comparison between PPy and PAn.

ITEMS	PPy	PAn
Structure	π-conjugated polymer	ionic polymer
Mechanical strength	Strong	Low
Conductivity	High (max. 10^{3} S cm^{-1})	Relatively high (max. 5S cm^{-1})
Doping level	- 45%	50 - 60%
Voltage	2.8 - 3.2V	3.0 - 3.2V
Preparation method	many variation	low variation